

DEVELOPMENT OF A CONCEPTUAL DESIGN TOOL AND CALCULATION
OF STABILITY AND CONTROL DERIVATIVES FOR MINI UAV SYSTEMS

A THESIS SUBMITTED TO
THE GRADUATE SCHOOL OF NATURAL AND APPLIED SCIENCES
OF
MIDDLE EAST TECHNICAL UNIVERSITY

BY

SENA YAZIRLI

IN PARTIAL FULFILLMENT OF THE REQUIREMENTS
FOR
THE DEGREE OF MASTER OF SCIENCE
IN
AEROSPACE ENGINEERING

DECEMBER 2015

Approval of the thesis:

**DEVELOPMENT OF A CONCEPTUAL DESIGN TOOL AND CALCULATION
OF STABILITY AND CONTROL DERIVATIVES FOR MINI UAV SYSTEMS**

submitted by **SENA YAZIRLI** in partial fulfillment of the requirements for the degree of **Master of Science in Aerospace Engineering Department, Middle East Technical University** by,

Prof. Dr. Gülbin Dural Ünver
Dean, Graduate School of **Natural and Applied Sciences**

Prof. Dr. Ozan Tekinalp
Head of Department, **Aerospace Engineering**

Prof. Dr. Nafiz Alemdaroğlu
Supervisor, **Aerospace Engineering Department, METU**

Examining Committee Members:

Prof. Dr. Serkan Özgen
Aerospace Engineering Department, METU

Prof. Dr. Nafiz Alemdaroğlu
Aerospace Engineering Department, METU

Prof. Dr. Altan Kayran
Aerospace Engineering Department, METU

Assist. Prof. Dr. Ali Türker Kutay
Aerospace Engineering Department, METU

Assist. Prof. Dr. Levent Ünlüsoy
Aeronautical Engineering, UTAA

Date:

I hereby declare that all information in this document has been obtained and presented in accordance with academic rules and ethical conduct. I also declare that, as required by these rules and conduct, I have fully cited and referenced all material and results that are not original to this work.

Name, Last Name: SENA YAZIRLI

Signature :

ABSTRACT

DEVELOPMENT OF A CONCEPTUAL DESIGN TOOL AND CALCULATION OF STABILITY AND CONTROL DERIVATIVES FOR MINI UAV SYSTEMS

YAZIRLI, Sena

M.S., Department of Aerospace Engineering

Supervisor : Prof. Dr. Nafiz Alemdaroğlu

December 2015, 115 pages

The main objective of this thesis is to write a design tool that will perform the conceptual design phase of an aircraft and achieve the desired specifications of the design. For this purpose, a code is written in MATLAB so that the designer does not have to change or check parameter values when a modification on the mission altitude, cruise conditions, airfoil type, propulsion system units, weight or general geometry of the aircraft. Most of the available design tools are created for large aircraft and not for uninhabited air vehicles. Besides they are mostly focused on a single branch of the aircraft design such as airfoil design, wing design, structural design, performance analysis etc. Whereas in this thesis, it is aimed to combine all these branches of the aircraft design and come up with a conceptual design tool for mini class uninhabited air vehicles manufactured from composite materials and powered by electrical motor. The code calculates the parameters for the general geometry, lift and drag forces, pitching moment, performance characteristics, composite structure weight, stability and control derivatives, state space matrices with their eigenvalues of longitudinal and lateral dimensions. In principle, the user enters the input parameters needed and rest of the computations are done automatically. Five critical input parameters are determined by the user according to the design features. These parameters are computed by the tool and in return the user gets the optimum values for the determined objective parameters of the aircraft within the given intervals and constraints. As a results, a user-friendly conceptual design tool that generates the whole information about the

aircraft from its geometry to its stability and control derivatives is devised. The thesis gives an example of the conceptual design of a mini UAV system performed using the design tool given in the thesis to verify the design tool.

Keywords: mini UAV, mini UAV design, conceptual design, design toolbox, lift, drag, moment, composite weight estimation, UAV performance, UAV design optimization, stability and control derivatives, state space matrix

ÖZ

MİNİ İNSANSIZ HAVA ARACI SİSTEMLERİ İÇİN KAVRAMSAL TASARIM ARACI GELİŞTİRİLMESİ VE KARARLILIK İLE KONTROL TÜREVLERİNİN HESAPLANMASI

YAZIRLI, Sena

Yüksek Lisans, Havacılık ve Uzay Mühendisliği Bölümü

Tez Yöneticisi : Prof. Dr. Nafiz Alemdaroğlu

Aralık 2015 , 115 sayfa

Bu tezin asıl hedefi bir hava aracının kavramsal tasarım fazını gerçekleştirecek ve tasarımı istenilen özelliklere eriştirecek bir tasarım aracı yazmaktır. Bu amaçla, MATLAB programında bir kod yazılmıştır ki böylelikle kullanıcı, tasarlanan uçağın görev irtifasında, seyir koşullarında, kanat profil türlerinde, itki sistemi elemanlarında, ağırlığında veya genel formunda bir değişiklik yaparsa, diğer parametre değerlerini tekrar kontrol etmek veya değiştirmek zorunda kalmayacaktır. Birçok tasarım aracı daha büyük türdeki ve insansız olmayan uçaklar için yaratılmıştır. Bunun yanında, onlar genel olarak uçak tasarımının profil tasarımı, kanat tasarımı, performans analizi veya yapısal tasarım gibi tek bir dalına odaklanmıştır. Bu tezde, tüm bu alanları birleştirmek ve elektrik motorlu, kompozit malzemelerden yapılmış ve mini sınıfında olan insansız hava araçları tasarımı için bir kavramsal tasarım aracı oluşturulması amaçlanmıştır. Bu kod genel geometri, kaldırma ve sürüklenme kuvvetleri, yunuslama momenti, performans karakteristiği, kompozit yapı ağırlığı, kararlılık ve kontrol türevleri, yanal ve boylamsal yönlerde ait durumsal uzay matriksi ve özgün değer parametrelerini hesaplamaktadır. Prensipite, kullanıcı girdi parametrelerini koda girer ve geri kalan hesaplamalar otomatik olarak yapılır. Beş tane kritik girdi parametresi kullanıcı tarafından tasarım özelliklerine göre belirlenir. Bu parametre değerleri kod tarafınan hesaplanır ve bunun karşılığında kullanıcı belirlenen aralıklarda ve kısıtlamalarda belirlenen

hedef parametresi için optimum deęerleri elde eder. Sonu olarak, kullanıcı dostu, hava aracı ile ilgili geometrisinden kararlılık türevlerine kadar tüm bilgileri üreten bir kavramsal tasarım aracı düzenlenmiştir. Bu tez, tasarım aracı kullanılarak ve tasarım aracını doğrulamak için gerçekleştirilen bir mini UAV sistem tasarımı örneğini içermektedir.

Anahtar Kelimeler: mini İHA, mini İHA tasarımı, kavramsal tasarım, tasarım araç kutusu, kaldırma kuvveti, sürüklenme kuvveti, moment, kompozit aęırlık tahmini, İHA performansı, İHA tasarım optimizasyonu, kararlılık ve kontrol türevleri, duraęan uzay matrisi

*To my extended family, my Güçlü and the designers who will find this design tool
helpful*

ACKNOWLEDGMENTS

I would like to thank my supervisor Professor Nafiz ALEMDAROĞLU for his constant support, guidance and friendship. It was a great honor to work with him for the last five years and our cooperation influenced my academical and world view highly.

There are a lot of people that were with me in these seven years. They defined me, they made me who I am, they are true owners of this work. It is not possible to write down why each of them is important to me and this work, because it will take more space than the work itself. I am very grateful to all people I know during my being undergraduate and doing master degree in METU-AEE, they changed me deeply: my vision towards life, happiness and friendship. I am very lucky to have them all. So I'll just give name of our group; "Havacı Tayfa" or "Anatolian Craft" or "KUŞKAŞ". I would also like to thank you my fiance Güçlü ÖZCAN for always listening, supporting, tolerating, leading and loving me deeply from the start of my masters.

Lastly and most deeply, sincerest thanks to each of my family members, my mother Nuran YAZIRLI, my father Özcan YAZIRLI and my little brother Eray YAZIRLI for supporting in every way and believing in me all the way through my university life.

TABLE OF CONTENTS

ABSTRACT	v
ÖZ	vii
ACKNOWLEDGMENTS	x
TABLE OF CONTENTS	xi
LIST OF TABLES	xiv
LIST OF FIGURES	xvi
LIST OF ABBREVIATIONS	xviii
CHAPTERS	
1 INTRODUCTION	1
1.1 MOTIVATION	3
1.2 CONTENT OF THE THESIS	6
1.3 LITERATURE SURVEY	9
1.3.1 LITERATURE OF THE AIRCRAFT DESIGN TOOLS	9
1.3.2 UAV SPECIFICATIONS FROM COMPETITORS	11
2 CODE GENERATION	15
2.1 GENERAL CODE STRUCTURE	15

2.2	LIFT, DRAG and MOMENT COMPUTATIONS	17
2.2.1	General Specifications of Flight Conditions and Aircraft Geometry	17
2.2.2	Flap Properties and Methods of Constitution of Graph Equation	20
2.2.3	Lift Calculation	26
2.2.4	Drag Calculation	31
2.2.5	Pitching Moment Calculation	33
2.3	PERFORMANCE CALCULATIONS	38
2.4	STABILITY AND CONTROL DERIVATIVES DETERMINATION	44
2.5	DESIGN TOOL STABILITY and CONTROL DERIVATIVE CALCULATIONS VERIFICATION	55
2.6	SYSTEM MATRIX CONSTITUTION	57
3	SELECTION OF OPTIMUM PARAMETER VALUES	63
3.1	Optimization Elements	64
3.1.1	Objectives	64
3.1.2	Constraints	64
3.1.3	Moving Variables	65
3.2	Optimization Part of Code Creation	65
4	MINI UAV DESIGN USING THE DESIGN TOOL	69
4.1	MISSION PLAN and USAGE CONCEPT	69
4.2	CONFIGURATION SELECTION	70

4.3	AIRFOIL SELECTION	71
4.4	PROPULSION SYSTEM SELECTION	73
4.5	AVIONIC SYSTEM and PAYLOAD SELECTION	75
4.6	WEIGHT ESTIMATION	75
4.7	OPTIMIZATION INPUT and RESULTS	76
4.7.1	Optimization Parameters Selection	76
4.8	DESIGN TOOL RESULTS	82
4.9	COMPARISON OPTIMIZED DESIGN with OTHER POSSIBLE DESIGNS	86
4.9.1	ADDITIONAL STUDY with SMALLER INCREMENT VALUES of MOVING VARIABLES	91
5	CONCLUSION	97
	REFERENCES	101
APPENDICES		
A	3D VIEWS AND DIMENSIONS OF UAV	103
B	OPERATING MANUAL OF DESIGN TOOL	107

LIST OF TABLES

TABLES

Table 1.1	Literature survey results [14]	12
Table 1.2	Photos of competitor UAVs [14]	13
Table 2.1	Validation of equation by using $\pm 7\%$ of real data	24
Table 2.2	Comparison of CFD results and code results for control derivatives	56
Table 2.3	Comparison of CFD results and code results for stability derivatives	56
Table 2.4	Concise longitudinal aerodynamic stability derivatives [8]	60
Table 2.5	Concise lateral aerodynamic stability derivatives [8]	61
Table 4.1	MotoCalc results for different configurations	74
Table 4.2	Force and moment values of the designed UAV	83
Table 4.3	Some performance characteristic values	83
Table 4.4	Stability derivatives of the designed UAV	84
Table 4.5	Control derivatives of designed UAV	84
Table 4.6	Objective function and constraint parameters variation with span	86
Table 4.7	Objective function and constraint parameters variation with angle of attack	87
Table 4.8	Objective function and constraint parameters variation with aspect ratio	88
Table 4.9	Objective function and constraint parameters variation with fuselage diameter	89
Table 4.10	Objective function and constraint parameters variation with horizontal tail volume ratio	91

Table 4.11 Objective function and constraint parameters variation with span by smaller increment	92
Table 4.12 Objective function and constraint parameters variation with angle of attack by smaller increment	93
Table 4.13 Objective function and constraint parameters variation with aspect ratio by smaller increment	94
Table 4.14 Objective function and constraint parameters variation with fuselage diameter by smaller increment	95
Table 4.15 Objective function and constraint parameters variation with horizontal tail volume ratio by smaller increment	96

LIST OF FIGURES

FIGURES

Figure 2.1	The general structure of the design tool code	16
Figure 2.2	Correction factor for nonlinear lift behaviour of plain flaps [18] . . .	21
Figure 2.3	Obtaining graph data by GetData Graph Digitizer program	22
Figure 2.4	Comparison of real graph (black curves) and graph obtained by code (red curves)	24
Figure 2.5	Correction factor for plain flap lift [18]	25
Figure 2.6	Procedure to calculate parameter K_b [18]	29
Figure 2.7	Effect of taper ratio and flap span on K_b [18]	29
Figure 2.8	Effect of aspect and flap-chord ratios on the 3D flap effectiveness [18]	30
Figure 4.1	Mission plan of the designed UAV	70
Figure 4.2	Comparison of possible wing airfoils [23]	72
Figure 4.3	Objective function change with angle of attack and wing span . . .	79
Figure 4.4	Objective function change with angle of attack and fuselage diameter	79
Figure 4.5	Objective function change with aspect ratio and fuselage diameter .	80
Figure 4.6	Objective function change with aspect ratio and wing span	80
Figure 4.7	Objective function change with fuselage diameter and wing span .	81
Figure 4.8	Graph of objective function variation with span and verification of constraints	87
Figure 4.9	Graph of objective function variation with angle of attack and verification of constraints	88

Figure 4.10 Graph of objective function variation with aspect ratio and verification of constraints	89
Figure 4.11 Graph of objective function variation with fuselage diameter and verification of constrains	90
Figure 4.12 Graph of objective function variation with horizontal tail volume ratio and verification of constraints	90
Figure 4.13 Graph of objective function variation with span and verification of constraints by smaller increment	92
Figure 4.14 Graph of objective function variation with angle of attack and verification of constraints by smaller increment	93
Figure 4.15 Graph of objective function variation with aspect ratio and verification of constraints by smaller increment	94
Figure 4.16 Graph of objective function variation with fuselage diameter and verification of constraints by smaller increment	95
Figure 4.17 Graph of objective function variation with horizontal tail volume ratio and verification of constraints by smaller increment	96
Figure A.1 Isometric 3D view of the UAV	103
Figure A.2 Top 3D view of the UAV	103
Figure A.3 Side 3D view of the UAV	104
Figure A.4 Front 3D view of the UAV	104
Figure A.5 Dimensions of the UAV	104
Figure A.6 Equipments of the UAV	105
Figure A.7 Placement of equipments in the UAV	105
Figure A.8 Centre of gravity location of the UAV from the top view	105
Figure A.9 Centre of gravity location of the UAV from the side view	106

LIST OF ABBREVIATIONS

UAV	Uninhabited Air Vehicle
CFD	Computational Fluid Dynamics
GPS	Global Positioning System
IMU	Inertial Measurement Unit
IMU	Inertial Measurement Unit
AGL	Above Ground Level
MSL	Mean Sea Level
AVL	Athena Vortex Lattice
ADS	Aircraft Design Software

CHAPTER 1

INTRODUCTION

Uninhabited Air Vehicles (UAVs) are aircraft in which the crew is replaced with an intelligent computer system and a radio link. They are controlled by human personnel through a ground control station. These aircraft also have avionic systems onboard. The types and properties of these avionic systems are chosen according to the mission of the aircraft. UAVs have advantages for several missions compared to manned aircraft. This is the reason why they exist in the aviation sector.

The use for UAVs can be categorized [3] in two parts: civilian and military. Civilian purposes are listed below:

- Aerial Photography : Film, video, still, etc.
- Agriculture : Crop monitoring and spraying
- Coastguard : Search and rescue
- Conservation : Pollution and land monitoring
- Customs and Excise : Surveillance for illegal imports
- Electricity Companies : Powerline inspection
- Fire Services and Forestry : Fire detection, incident control
- Fisheries : Fisheries protection
- Gas and Oil Supply Companies : Land survey and pipeline security
- Information Services : News information and pictures, feature pictured

- Lifeboat Institutions : Incident investigation, guidance and control
- Local Authorities : Survey, disaster control
- Meteorological Services : Sampling and analysis of atmosphere for forecasting etc.
- Traffic Agencies : Monitoring and control of road traffic
- Oil Companies : Pipeline security
- Ordnance Survey : Aerial photography for mapping
- Police Authorities : Search for missing persons, security and incident surveillance
- Rivers Authorities : Water course and level monitoring, flood and pollution control
- Survey Organizations : Geographical, geological and archaeological survey
- Water Boards : Reservoir and pipeline monitoring

Second category of UAV usage area is for military purposes [3]. In this type of purpose, there are three major topic: navy, army and air force.

- *NAVY* : Shadowing enemy fleets, Decoying missiles by the emission of artificial signatures, Electronic intelligence, Relaying radio signals, Protection of port from offshore attack, Placement of sonar buoys and possibly other forms of anti-submarine warfare, Monitoring of sonar buoys and possibly other forms of anti-submarine warfare;
- *ARMY* : Reconnaissance, Surveillance of enemy activity, Monitoring of nuclear, biological or chemical contamination, Electronic intelligence, Target designation and monitoring, Location and destruction of land mines;
- *AIR FORCE* : Long-range, high-altitude surveillance, Radar system jamming and destruction, Electronic intelligence, Airfield base security, Airfield damage assessment, Elimination of unexploded bombs.

1.1 MOTIVATION

Initial motivation of this study comes from the desire to write an aerodynamic design code complete with the calculation of stability derivatives. Usually automated design packages are prepared considering only the aerodynamic aspects of the design and leaving aside the stability and control aspects of the design. Therefore this study is aimed at filling this gap of the design and tries to make a more complete design package including the determination of stability and control analysis of the air craft design and include the effects of these dynamic effects in the full picture of the aerodynamic design. Therefore in this respect this thesis brings a novel approach to the concept of the design and include these dynamic effects right at the conception phase of the design instead of dealing with them after the whole aerodynamic design is completed. The calculation of the stability derivatives and therefore include the controllability aspect of the aircraft into the full picture of the design is intended to be the contribution of this thesis.

Usually the calculation of the stability derivatives are performed after the design phase is completed and the calculation of the stability derivatives are not considered at all in the design cycle. It is considered as a separate package by itself and these computations are performed outside the design cycle. Therefore this is a totally new and integrated approach to the aerodynamic design where these important affects are taken into consideration as a whole and the stability and control parameters of the aircraft are determined within the same package.

However making up this "integrated approach to design" is not an easy task to undertake. To realize this new undertaking of the design the famous work of Roskam [19] is extensively used as a guide and within this context most of the graphical representations in his book are re-interpreted as equations in order to able to be integrate them into the automated design procedure.

In the process of developing the code, several parameters should be entered as input. Therefore, in addition to stability and control derivatives, it is decided that the aerodynamic and performance parameter calculations should be included in the code. In this manner, a conceptual design tool is created that will not require any additional calculations. Furthermore, it is thought that some of the input parameters are to be selected by the code itself as the most proper parameters and are used in the code for

further design calculations. In this way, the user will not need to determine every and each input parameter. These explanations are the starting points of this thesis. Such a design tool will be very useful for UAV designers.

UAV design is one of the major fields of aeronautics due to their extensive use, relatively low cost and their very fast developing technologies. Therefore, many researchers ranging from university students to large aerospace companies work on design and manufacturing of UAVs and UAV systems. The design of UAV has similar phases with the design of manned aircraft. These are conceptual design, preliminary design and detailed design. Initial step is to start with the requirements coming from a customer, for a design competition or for a research and development study. During the conceptual design phase, the general form of the design is shaped. In this manner, the interaction between each requirement and limitations such as aerodynamical, structural and propulsive limitations are found. Moreover, approximate weight and cost values are determined. The technologies which should be used are found and the feasibility of these technologies are done. In the content of the conceptual design, it is important to observe that these requirements generate a practicable and commercial aircraft. In the preliminary design phase, configuration of these components are kept constant. Test results and analytical calculations are collected. Major items are designed. In this step a mockup may be constructed physically or by using computer aided drawing programs. Since preliminary design is a more detailed level of design, detailed cost analysis can be done and actual cost can be determined. Detailed design is the last phase before manufacturing. Thus, all pieces must be designed to be built. In addition, tools which are used in the manufacturing should be designed. Each component must be tested in structural manner. Performance characteristics and weight estimation is finalized.

When these phases are analysed, it can be seen that the conceptual design phase has high impact on the decision of the requirements which make an aircraft design feasible. In addition to that, it is vital for the companies to determine that the given UAV project is executable or not. In substantial point of view, a successful conceptual design supports a successful budget allocation. Labor force and logistic sufficiencies are determined and necessities are satisfied. In background information point of view, conceptual design figures out convenience of knowledge and experience of the people who will work on this job. According to the results, required lectures and

consultancies from experts are arranged. In the planning point of view, by the help of the conceptual design phase, the time needed for each process of the aircraft design and manufacturing, namely the time that will pass until release of product can be determined. In UAV point of view, conceptual design leads improvements and optimizations in the design since it constituted in general shape of the air vehicle.

Regarding all of these profits of the conceptual design phase, it can be seen how important it is. If conceptual design phase can be processed quickly, practically and safely, all these advantages increase dramatically. In company point of view, fast time planning and cost analysis supports bidding with right values. In addition to that, fast adjustments related to labor force and logistic help making up a shortage quickly. Therefore, they can get ahead of the other companies in a short time. When requirements given by customer are analysed quickly, the company can reply to the customer by correct comments and possible improvements. This situation improves the reliability of the company on the customer's point of view. Lastly, when general look of the aircraft is created, customer can see what the required aircraft will look like and reorganise or change the requirements according to the new thoughts and ideas. At the end, project can be finalized in time and without problems since customer requests and structured outcomes by company are suitable with each other.

In addition to this, when the student projects and competitions are focused on, same advantages can be achieved by quick conceptual designs. Financial supports, school opportunities, number of team members and their fields are determined quickly. Therefore, the team can apply the competition or submit the project before deadline so that they can get good points and have a higher chance of success. Moreover, if learning process is the point of view, the students can see how requirements shape the aircraft and limit the performance. Effects of any changed parameter on the other can be learned. They understand which component configurations bring which aerodynamic advantages. The relation between propulsion system selection and efficient flights can be seen. The students can observe at what rate structural elements change weight and cost. Quick conceptual design in research projects have advantage of focusing on the real research subject and develop the main points instead of losing time in doing whole design features.

In this chapter, the importance of the conceptual design is mentioned. Moreover, limitless benefits of a quick conceptual design phase are emphasised. As conceptual

design is a flowing process and the design layout is constantly changing, design tools are generated to prevent time loss. These design tools are used by universities and in every level of the aviation sector. They offer learning with results and speaking with values obtained promptly from each different possible design properties. Design programs have several distinguished properties. While some of them have only aerodynamic or performance calculations, others include stability analysis. In addition, their base sources can also be changed. For example, they can run with another program or they use some books' design methodology, formulations or experimental/historical data bases. Regardless of these properties, the reliability of the obtained results and calculated values of parameters are the most important aspects of a design tool program.

1.2 CONTENT OF THE THESIS

In this thesis, a design tool is developed. The tool is created in MATLAB programming environment. Initially, several input must be determined. In particular, atmospheric condition and flight conditions must be clarified for the code. Information related to the chosen airfoil and propulsion system must be entered in the code. Additionally, several geometrical properties and variables are needed to be optimized in the code. These are included in the code manually. In this manner, when the user runs the code, input parameters are asked to be entered one by one. Firstly, these input are used to compute lift [18], drag [17] and moment parameters [18]. The main parameters listed are the lift, drag and moment coefficients of individual aircraft components and the values for total aircraft, as well as the change of these coefficients with angle of attack and the effect of flap deflection on them.

Secondly, weight is estimated for each component separately. This code is prepared for composite structures. Therefore, initially, surface weights of each part of the aircraft should be estimated. In this way, the composite fabrics that are laid on each layer are determined. By using fabrics' weights per unit square area, components' surface area and approximate resin weight, the total weight of each layer are estimated. After that computation is completed, rib and spar numbers are determined. According to the necessary stiffness of the components, the structure and dimensions

of the spar and ribs are decided. Lastly, avionics, payload, landing equipments and propulsion system weights are added to the skin weight of the aircraft. There is an important point in determining the take-off weight. The value of the weight cannot be much less or much greater than the lift force for the level flight. This must be taken into account and if such a situation occurs, some parameters such as angle of attack, wing span, airfoil type or structural elements must be changed. In the code, there is a control loop that protects the design against the occurrence of these inequalities in the vertical aerodynamic forces. However, this is only a warning mechanism in the main logic of the design cycle; the code does not fix this inequality situation automatically, therefore, this should be done manually by the intervention of the designer. Namely, code does not fix inequality automatically, the user must correct it manually.

Thirdly, the performance parameters [2], [17] are calculated. According to the mission plan, these are constituted of take-off, climb, cruise, loiter and landing phases. The code considers that the take off the UAV is by hand launch. Therefore, take-off calculations are done by taking this fact into consideration. After take-off segment of the mission plan, climb until cruise altitude, cruise to mission and then loiter and cruise back to home situations are analysed. In this manner, several performance characteristics such as power consuming from battery, passing time, velocities, rate of climbs and required powers are also computed. Another limitation of this code is its landing procedure. The code is valid for aircraft that makes parachute, airbag, deep stall or belly landing after unpowered gliding. Therefore, in the code, landing part does not exist. Last calculations related to performance are done for the loiter segment. During loiter, the aim of the mission is realized. Since this segment includes rotational movement, performance characteristics such as turn rate, minimum turn radius are also computed. At the end of the performance computation part of the code, one of the most important parameters, mission time, is found by adding the take-off, climb, cruise and loitering times.

In the fourth part of the code, stability derivatives, longitudinal and lateral control derivatives are computed using principally the stability book of Roskam [19]. At the end following stability derivatives are obtained.

- Lift coefficient variation with velocity, pitch rate, angle of attack and rate of angle of attack ($c_{L_u}, c_{L_q}, c_{L_\alpha}, c_{L_{\dot{\alpha}}}$)

- Drag coefficient variation with velocity and angle of attack (c_{D_u}, c_{D_α})
- Side force coefficient variation with sideslip angle, roll rate and yaw rate ($c_{y_\beta}, c_{y_p}, c_{y_r}$)
- Pitching moment coefficient variation with velocity, pitch rate, angle of attack and rate of angle of attack ($c_{m_u}, c_{m_q}, c_{m_\alpha}, c_{m_{\dot{\alpha}}}$)
- Rolling moment coefficient variation with sideslip angle, roll rate and yaw rate ($c_{l_\beta}, c_{l_p}, c_{l_r}$)
- Yawing moment coefficient variation with sideslip angle, roll rate and yaw rate ($c_{n_\beta}, c_{n_p}, c_{n_r}$)

In addition to them, following longitudinal, lateral and directional control derivatives are computed.

- Lift coefficient variation with flap deflection, stabilizer incidence and elevator angle ($c_{L_{\delta_F}}, c_{L_{i_H}}, c_{L_{\delta_E}}$)
- Drag coefficient variation with flap deflection and elevator angle ($c_{D_{\delta_F}}, c_{D_{\delta_E}}$)
- Pitching moment coefficient with stabilizer incidence and elevator angle ($c_{m_{\delta_F}}, c_{m_{i_H}}, c_{m_{\delta_E}}$)
- Drag, side force, rolling moment and yawing moment coefficients variation with aileron deflection ($c_{D_{\delta_A}}, c_{y_{\delta_A}}, c_{l_{\delta_A}}, c_{n_{\delta_A}}$)
- Side force, rolling moment and yawing moment coefficients variation with rudder deflection ($c_{y_{\delta_R}}, c_{l_{\delta_R}}, c_{n_{\delta_R}}$)

Last part of the code includes system matrix generation of designed UAV. In this manner, the equations in [8] are used and below matrices of longitudinal and lateral parameters are obtained.

$$A_{longitudinal} = \begin{bmatrix} X_u & X_w & X_q & X_\theta \\ Z_u & Z_w & Z_q & Z_\theta \\ M_u & M_w & M_q & M_\theta \\ 0 & 0 & 1 & 0 \end{bmatrix} \quad A_{lateral} = \begin{bmatrix} Y_v & Y_p & Y_r & Y_\phi & Y_\psi \\ L_v & L_p & L_r & L_\phi & L_\psi \\ N_v & N_p & N_r & N_\phi & N_\psi \\ 0 & 1 & 0 & 0 & 0 \\ 0 & 0 & 1 & 0 & 0 \end{bmatrix}$$

When this design tool is examined in detail by its parts, it can be observed that the most valuable and important part of the code is the section where the automatic calculations and the optimizations are performed. When the calculations of the required parameters are performed, equations that are needed to perform the computations are obtained from various related reference books (i.e, [17], [2], [18], [19], [8]). There are also several parameters that are read from various graphs. In this thesis, automatic calculation is aimed. To achieve this aim, graphical approach should be surpassed, so that the user does not have to read any data from the graphs. In the light of this idea, the equations of the particular graphs are determined. Some of the data from the graphs are taken manually. The intervals of x and y axis are divided into sections to make the equation as accurate as possible. These data are written in the code and the equation of the graph is obtained. Some of the graphs' data are taken from the GRAPHDATA program. The next task of the code is optimization. In this section of the code, values for several geometrical parameters are chosen such that maximum mission time and minimum wing loading can be achieved.

When the coding of the design tool is finalized, it is validated by values of the mini uninhabited air vehicle which is the product of a Turkish company. At the end of the thesis work, a sample design of a mini UAV is done by using this tool.

1.3 LITERATURE SURVEY

1.3.1 LITERATURE OF THE AIRCRAFT DESIGN TOOLS

Design tools supply several opportunities therefore, some companies and some individuals produced design tools that have different properties. They are for aerodynamic, structure, propulsion and stability calculations. While some of them are

specific for one of these branches, others are combinations of two or more. In addition to that, some programs are created to design a specific component of the aircraft such as wing, tail or empennage. Examples of some of these design tools are listed below:

- XFOIL offers the design and analysis of the subsonic airfoils. ([13])
- XFLR5 is an aerodynamic analysis and design tool for airfoils, wing and planes at low Reynolds Numbers by using XFOIL. ([24])
- Tornado Vortex Lattice Method is a MATLAB code to design a linear aerodynamic wing. ([21])
- Athena Vortex Lattice Method (AVL) supports aerodynamic and flight dynamic analysis. ([12])
- MIAReX is the program that calculates the 2.5D wing properties. ([20])
- CEASIOM supply higher representation fidelity in a quick way than the recognised handbook methods. ([9])
- Project Falcon is a wind tunnel simulation program. ([7])
- ADS (Aircraft Design Software) is design tool that gives the best solutions of aircraft configuration. ([15])
- AVID Software are created for combining and optimizing parts of an aircraft. ([11])

When these softwares are analysed in detail, their usage areas, modules and properties can be seen. The XFOIL programme includes viscous analysis of an existing airfoil, performs new airfoil design from the beginning and by modifying an existing airfoil, blending of airfoils, writing and reading of airfoil coordinates and polar save files and plotting geometry, pressure distributions and multiple polar. XFLR5 includes wing design and analysis based on the Lifting Line Theory, Vortex Lattice Method and 3D Panel Method. Tornado program supplies linear aerodynamic wing design in conceptual design. In addition to that, by using Tornado, most of the aerodynamic derivatives can be solved. MIAReX is similar to XFLR5. It also

uses the XFOIL. MIAReX computes lift distribution, induced and airfoil drag and airfoil moment locally and globally by using Lifting Line Theory. These programs generally study on lifting surfaces and airfoils and they are based on only aerodynamic calculations and only one component. CEASIOM software includes geometry module to define the geometry of an aircraft, aerodynamic module to replace digital DATCOM methods with new fidelity modules, stability and control module to simulate test flights with six degree of freedom and to predict performance, flight control system design module to give control design system philosophy and architecture and aeroelastic module for structural analysis. AVID is a program that give optimum solutions for given requirements. It includes geometry definition, fixed wing and ducted-fan aircraft design, optimization and performance analysis. Lastly, ADS has analysis module to analyse existing key stages, statistical analysis module to analyse an existing aircraft, design tool to determine geometry, weight, propulsion, performances and balance, optimisation module, 3D module to make visual analysis, balance and stability module to locate centre of gravity, digitizer module to make measurements on the designed aircraft, airfoil, airplane and engine databases. This last software is very comprehensive. In this thesis, a similar code to this software content was tried to be developed. However, it can not be so detailed and the study area of the thesis is small UAVs with electric engine which is different from other design tools. Therefore, although the work in this thesis is very specific, it will probably fill a blank in the design tool market.

1.3.2 UAV SPECIFICATIONS FROM COMPETITORS

Before starting the design, requirements must be clarified. In this manner, similar UAV specifications are examined by a literature survey (Table 1.1 and Table 1.2) [14].

UAV	MTOW (kg)	W.Span (Cm)	Length (Cm)	Mission Time (min)	Range (km)	Cruise Speed (km/h)	Operating Ceiling (m)	Max. Ceiling (m)	Recovery
NIGHT HAWK	0.73	66	61	60	10	64	3353		
PRIORIA ROBOTICS MAVERIC	1.16	75	67	45-60	10-15	48	91-244 AGL	7620	
LA LM SERIES LEHMANN AVIATION	0.95	92		40	5				Parachute
BIRD EYE 100	1.30	85	80	60	5				
CARCARA		160		60-95		40			Deep Stall
ZALA 421-08	1.70	80	41		15	65-150		3600	Parachute
RAVEN RQ-11	1.90	138	915	60-90	10	56			Deep Stall
WASP III	0.43	72	38	45	5	40-65			Horizontal
PUMA AE		280	140	120	15	37-83			Deep Stall
MICRO B	1.50			60	10	55-93		3000	Parachute
GOLDEN EAGLE	0.85	66	77	60			198		Deep Stall
E 100 MICRO	1.00	120	80		5	50			Belly

Table 1.1: Literature survey results [14]



Table 1.2: Photos of competitor UAVs [14]

The values in this table is analysed. The requirements are determined according to the average or maximum/minimum of given parameters. In this manner, following list is formed for limitations of the UAV.

- Maximum take-off weight is limited to 2 kg,
- Wing span interval is decided to be between 0.9 m and 1.4 m,
- Fuselage diameter is chosen to be in the interval of 0.04-0.12 m,
- Minimum mission time is determined as 60 minutes,
- Range is specified as 5 km,
- Cruise speed is restricted between 8 m/s and 16 m/s and
- Operating ceiling preference to be concluded in the 1000-2000 m interval.

To sum up, the aim of the thesis is to generate a design tool which computes lift, drag and moment parameters, performance characteristics, stability and control derivatives. The tool produced in the thesis allows a fast and an optimized conceptual design for uninhabited air vehicles. By using this design tool, a mini UAV design is realized to see its usage and benefits more clearly. All the items mentioned in this chapter, which form scope of this thesis, are investigated in detail in the following chapters.

CHAPTER 2

CODE GENERATION

2.1 GENERAL CODE STRUCTURE

The present design tool calculates, the lift and drag forces and the pitching moment, as well as the stability and control derivatives, performance specifications, state space matrix constitution and the eigenvalues. As the initial step, the user of this design tool must enter the input parameters that are necessary for doing these computations. The input parameters can be categorized in six groups.

1. The first group are the optimization input which determine the moving variables, their lower and upper limits and increments, objective function and constraint parameters with their limits (the parameter definitions related to optimization are done in the Chapter 3).
2. Second group are the altitude and atmospheric conditions during mission.
3. The third group are the propulsion system specifications such as battery capacity, propeller diameter.
4. Fourth group are the airfoil information such as thickness ratios of both wing and tail airfoils.
5. Fifth group are general geometry properties which are used to calculate the geometry of whole aircraft.
6. Sixth and last group are the parameters which are used in weight estimation such as composite densities.

After entering all these input parameters, all calculations except state space matrices are done for each configuration of the selected moving variable values. At the end, desired optimum values are found and the same calculations of lift, drag, pitching moment, stability and control derivatives and performance of the aircraft are repeated by using the optimized values. Lastly, state space representation and eigenvalue foundation are done. The flow chart of the design procedure and the general structure of the design tool can be seen in Figure 2.1.

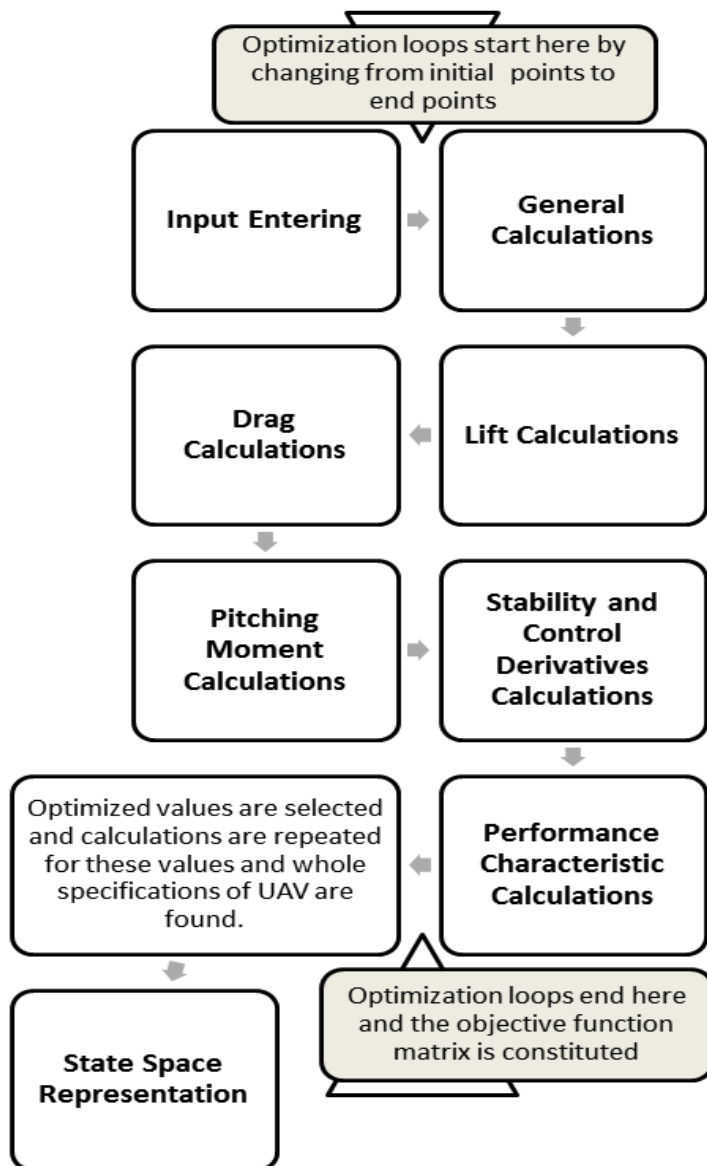


Figure 2.1: The general structure of the design tool code

2.2 LIFT, DRAG and MOMENT COMPUTATIONS

2.2.1 General Specifications of Flight Conditions and Aircraft Geometry

Initial step for the design tool generation is to determine some flight and air conditions; propulsion system, airfoil and some geometrical specifications. Atmospheric conditions must be determined before starting any kind of air vehicle design. Therefore, in the code the user enters mission altitude, launch altitude and, according to these altitudes, dynamic viscosity and temperature. In this part of the code, gravitational acceleration and air density at sea level are placed as default values. Air density at cruise altitude (Eqn. 2.1) and speed of sound are calculated from the given information automatically. Cruise speed and angle of attack are user defined flight conditions. Mach number and dynamic pressure are calculated by the code.

$$\rho = \left(-\frac{(altitude/1000 - 44.3308)}{42.2665} \right)^{1/0.234969} \quad (2.1)$$

While propulsion system parameters are being entered, the code design limitations should not be forgotten. This design tool is valid for the aircraft that use electrical propulsion systems. Therefore, propeller efficiency, motor efficiency, battery capacity, motor power, battery voltage, propeller diameter and propeller pitch are the input parameters for the propulsion system. In the code, available power at sea level and at cruise altitude (Eqn. 2.2) and current drawn by the motor at full throttle (Eqn. 2.3) are calculated.

$$P_a = P_{a@sl} \left(\frac{\rho}{\rho_{sl}} \right)^{0.7} \quad (2.2)$$

$$Amper_{full} = \frac{P}{volt_{battery}} \quad (2.3)$$

Airfoil is chosen according to the design requirements. After that, important parameters related to the airfoil are entered to the code for wing and tail separately. In this step of the design, the user should be aware that the code does calculations for the aircraft that use same airfoil type for both the horizontal and vertical tails. Slope of

the lift curve at zero Mach, thickness ratio, maximum thickness chord wise location, maximum 2D lift coefficient, zero lift angle of attack and trailing edge angle are entered to the code according to the chosen airfoil specifications. Stall angle of attack (Eqn. 2.4), lift curve slope at cruise Mach (Eqn. 2.5) and airfoil lift coefficient (Eqn. 2.6) are calculated by using formulations. Airfoil aerodynamic center is determined from the graph [18]. The equation of the curve is obtained for different thickness ratios. It gives the percentage of the aerodynamic center for any value of trailing edge.

$$\alpha_{st} = \frac{c_{l_{max}}}{c_{l_{\alpha}} \pi / 180} - 4 \quad (2.4)$$

$$c_{l_{\alpha}} = \frac{c_{l_{\alpha sl}}}{\sqrt{(1 - Mach^2)}} \quad (2.5)$$

$$c_l = c_{l_{\alpha}} |(\alpha - \alpha_{l=0}) \pi / 180| \quad (2.6)$$

Next, geometric parameters must be entered. Necessary input parameters for wings are aspect ratio, span, dihedral angle, taper ratio, thickness difference of airfoil at 6% and 0.15% of chord, quarter chord and semi-chord line sweep angles, incidence angle and vertical distance from fuselage centerline to wing root quarter chord point. In addition to wing parameters, horizontal and vertical tail input are angle of attack, taper ratio, quarter chord and maximum thickness line sweep angles, volume ratio, distance between wing aerodynamic center and tail (vertical or horizontal) aerodynamic center, distance between wing and (horizontal and vertical) tail in vertical direction, distance between wing root chord and horizontal tail root chord, submerged (horizontal and vertical) tail area in the propeller airstream and incidence angle. The arranged parameters are put into the code separately for vertical and horizontal tails. The other geometrical specifications are calculated from the aerodynamic formulations [17] (from Eqn. 2.7 to Eqn. 2.22). As it can be seen from the equations, sub "f" refers to fuselage parameters, sub "ht" refers to horizontal tail and sub "vt" refers to vertical tail. If there is no sub letter, this means that the parameter is related to wing. Calculations belonging to vertical tail are not included here as they are the same with

that of horizontal tail. In addition to that, semi-chord and leading edge sweep angle equations (Eqn. 2.14 and Eqn. 2.15) are formed from geometrical relations. There are two wetted wing area equations (Eqn. 2.17) which are chosen according to the thickness ratio in the code. Moreover, for both of horizontal and vertical tails, aspect ratio, volume ratio and distance between aerodynamic centres are chosen as input parameters. By using these parameters, area (Eqn. 2.18), span (Eqn. 2.19) and chord (Eqn. 2.20 and Eqn. 2.21) values are calculated by the code. Lastly, the tail area affected by the flow coming from the motor propeller is calculated, (Eqn. 2.22). In this manner, the ratio of total area to slipstream area is taken as equal the ratio of half of the propeller diameter to span. The reason to take half of the propeller diameter is reducing area by increased air flow speed at the outflow of the propeller when it is compared to the inflow of the propeller.

$$S_{wet_f} = 3.4(S_{f_{side}} + S_{f_{top}})/2 \quad (2.7)$$

$$S = \frac{b^2}{AR} \quad (2.8)$$

$$S_{flap} = \frac{flapspan}{wingspan} S \quad (2.9)$$

$$S_{unflap} = S - S_{flap} \quad (2.10)$$

$$c_{rt} = \frac{2S}{b(1 + \lambda)} \quad (2.11)$$

$$c_t = c_{rt}\lambda \quad (2.12)$$

$$c = \frac{c_{rt} + c_t}{2} \quad (2.13)$$

$$\Lambda_{le} = atan(\tan(\Lambda_{c/4}) + \frac{1 - \lambda}{AR(1 + \lambda)})180/\pi \quad (2.14)$$

$$\Lambda_{c/2} = atan(\tan(\Lambda_{le}) - \frac{2}{AR} \frac{1 - \lambda}{1 + \lambda})180/\pi \quad (2.15)$$

$$S_{exp} = S - (\pi(\frac{f_{use\ dia}}{2})^2 c_{rt}) \quad (2.16)$$

$$S_{wet} = 2.003S_{exp} S_{wet} = S_{exp}(1.977 + 0.52\frac{t}{c}) \quad (2.17)$$

$$S_{ht} = \frac{Vr_{ht}cS}{l_{ht}} \quad (2.18)$$

$$b_{ht} = \sqrt{S_{ht}AR_{ht}} \quad (2.19)$$

$$c_{rt_{ht}} = \frac{S_{ht}}{(b_{ht}/2)(\lambda_{ht} + 1)} \quad (2.20)$$

$$c_{t_{ht}} = c_{rt_{ht}} tpr_{ht} \quad (2.21)$$

$$S_{ht_{slip}} = S_{ht} \frac{prop_{dia}0.3048/2}{b_{ht}} \quad (2.22)$$

2.2.2 Flap Properties and Methods of Constitution of Graph Equation

Lastly, user clarifies flap deflection values. Flap deflection, percent of flap chord to chord and percent of flap span to span are entered for both wing and horizontal tail. These values and following graphs are used to calculate the 2D lift coefficient increment under the effect of the flap. Therefore, in this subsection, constitution of equations from graphs [18] is mentioned. The methods applied to gather these equations are used several times in the code. When equation of the given graph (Figure

2.2) [18] is obtained, it is required to select the correct curve and respective equation according to the ratio between flap chord to chord. From the graph (Figure 2.2), it can be seen that between chord ratio values of 0.1 and 0.3, the ratio increases by 0.05. Therefore, in this interval, if the calculated ratio falls in between an increment step, it is rounded down or up to its closest value (i.e. 1.2 is rounded down to 1, whereas 1.4 is rounded up to 1.5). Moreover, between 0.3 and 0.5, same logic is applied but rounding is done according to step of 0.1. Regarding the situation that the chord ratio is less than 0.1 or greater than 0.5, two more condition loops are added to the code. As a result, following part of the code is constituted.

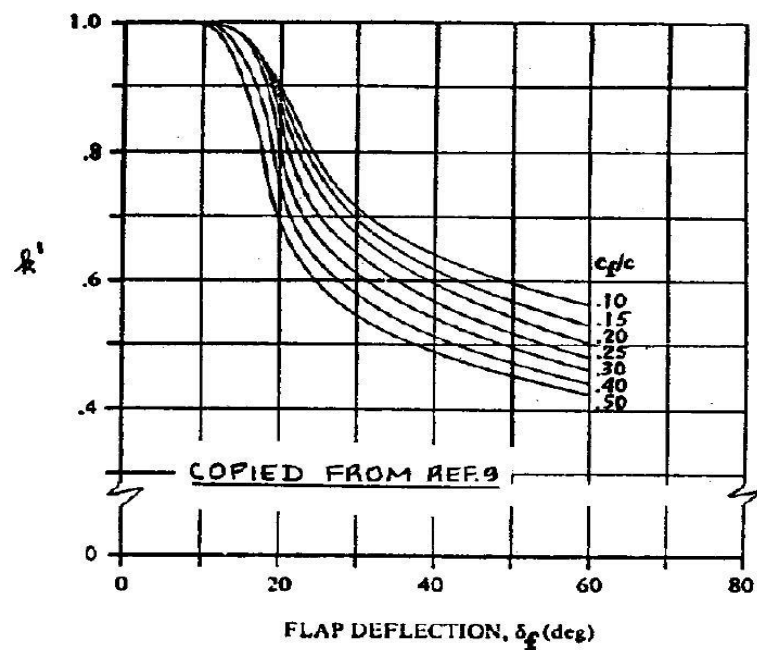


Figure 2.2: Correction factor for nonlinear lift behaviour of plain flaps [18]

```

1  if cfc <= 0.1
2  cfc1 = 0.1
3  else if cfc > 0.1 & cfc < 0.3
4      cfc1 = round(cfc*20)/20
5  else if cfc >= 0.3 & cfc < 0.5
6      cfc1 = round(cfc*10)/10
7  else if cfc >= 0.5
8      cfc1 = 0.5
9  end

```

```

10         end
11     end
12 end

```

In the graph (Figure 2.2) [18], there are seven curves. Several data that belong to each curve are collected. The number of chosen points is determined according to the change in the first and second derivatives. If the curve has many different slope values and concavity/convexity, the number of selected data is increased. In addition to that, degree of the polynomial can be increased. x and y values of the point selected on curve are obtained from the program "GetData Graph Digitizer", (Figure 2.3). Initially, it is important to introduce the maximum and minimum x and y axes places and values on the graph to the program.

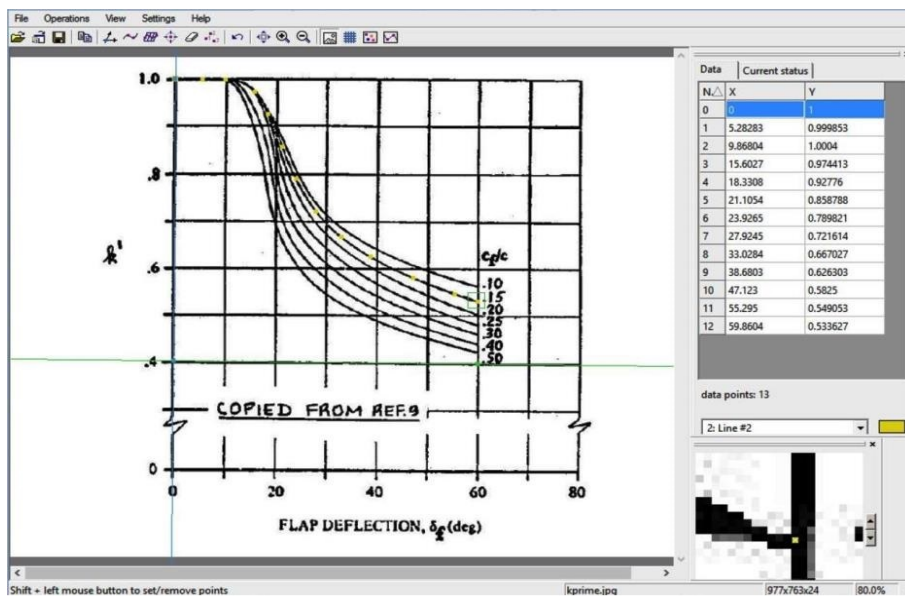


Figure 2.3: Obtaining graph data by GetData Graph Digitizer program

After the gathered x and y values are entered to the code, the fitting curve equation is obtained with the desired degree of polynomial. It can be seen in the following part of the code.

```

2  if cfc1 == 0.5
3  % delta_f = [0 5 10 15 20 25 30 35 40 45 50 55 60]
4  % kprime = [1 1 1 0.9 0.8 0.61 0.55 0.51 0.49 0.47

```

```

0.45 0.44 0.43]
5 % plot(delta_f,kprime)
6 % [p7,S,mu] = polyfit(delta_f,kprime,5)

```

By running this part of the code, p7 and mu values which are the coefficients of polynomial and coefficients of indices are obtained. By using these numbers, the equation is formed.

```

p7 =
0.0272 -0.0979 0.0158 0.2579 -0.3265 0.5913
mu =
26.5579
18.8532

```

```

1 kprime = 0.0089*((delta_f-30)/19.4722).^5
-0.0682*((delta_f-30)/19.4722).^4+0.026*
((delta_f-30)/19.4722).^3+0.2206*
((delta_f-30)/19.4722).^2-0.2945*
((delta_f-30)/19.4722)+0.5654

```

Lastly, these new obtained curves and formed equations should be checked. Gathered data are plotted to check that obtained curve is similar to the real graph, Figure 2.4. In addition to that, random values are put into the equation and results are compared with the real graph. If the obtained value is close to the real value in an interval of $\pm 7\%$, the equation is designated as valid, Table 2.1. If it is not, the number of selected points and/or degree of fitting curve polynomial are increased. After that previous checking procedure is repeated. The check percentage, 7 percent value, is chosen according to the graph values. Generally, the graph results have increments in the range of $\pm 10\%$. Therefore, the check percentage is chosen to be less than $\pm 10\%$ so that the result should not be compared to the upper or lower real graph value. In addition to this, for several graphs, it is observed that choosing the accuracy greater than 8 percent causes the obtained curves not to follow real curves as required. Therefore, the most proper percentage is decided to be as $\pm 7\%$.

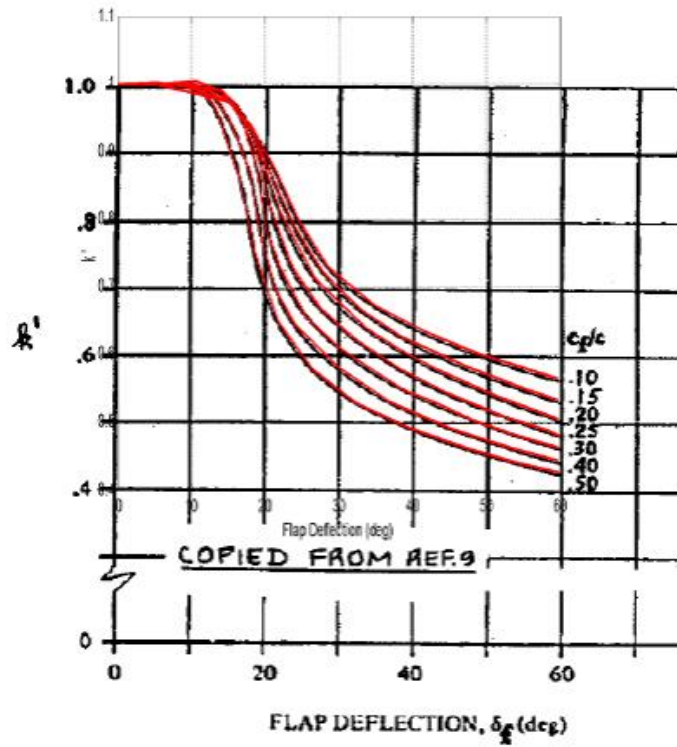


Figure 2.4: Comparison of real graph (black curves) and graph obtained by code (red curves)

Table 2.1: Validation of equation by using $\pm 7\%$ of real data

k'	1.00000	0.99877	0.99754	0.96513	0.85810	0.75012
k'_{upper_limit}	1.07000	1.06869	1.06737	1.03269	0.91816	0.80263
k'_{lower_limit}	0.94000	0.93885	0.93769	0.90722	0.80661	0.70511
$k'_{calculated}$	0.98250	1.05680	0.98080	0.91800	0.82470	0.77060
k'	0.57926	0.52869	0.49167	0.46205	0.44207	0.42557
k'_{upper_limit}	0.61980	0.56570	0.52609	0.49439	0.47301	0.45536
k'_{lower_limit}	0.54450	0.49697	0.46217	0.43433	0.41554	0.40003
$k'_{calculated}$	0.59490	0.51520	0.47620	0.46580	0.44970	0.42080

The graph below has several curves, (Figure 2.5) [18]. These curves give close results for the same flap chord to chord ratio. They also have similar curve slopes. They are also like shifted curves for different ratios of c_{l_a} to $c_{l_{a_{theory}}}$ (taken as 2π). Therefore, a relation between this ratio and shifting value is established. The shifting value, changing with each curve according to the value of the ratios of c_{l_a} to $c_{l_{a_{theory}}}$, is

added to the equations of the ratio of $c_{l\delta}$ to $c_{l\delta_{theory}}$. Obtaining the curve equations by shifting them is used only for this graph in the entire code.

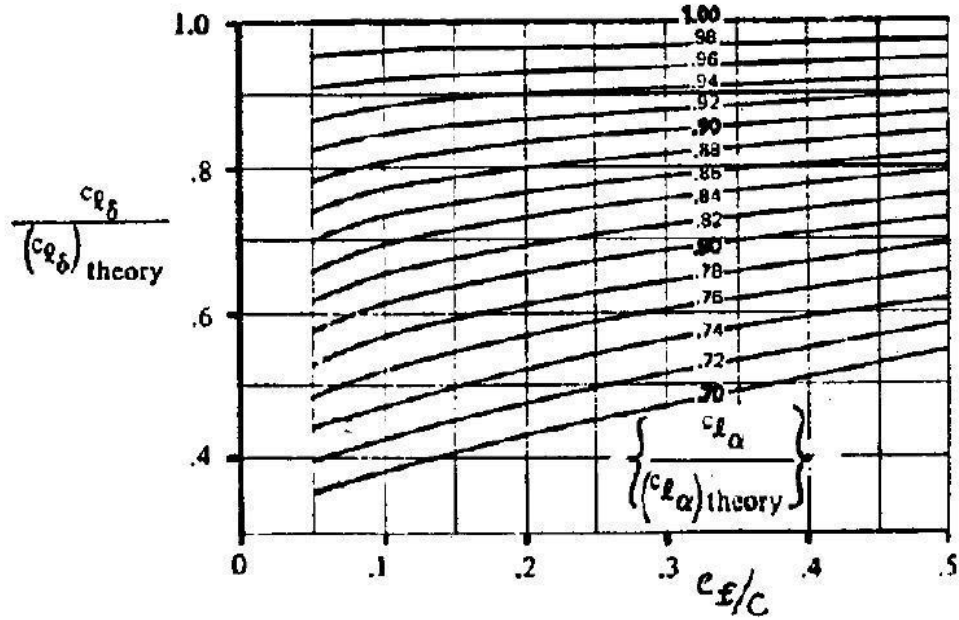


Figure 2.5: Correction factor for plain flap lift [18]

The values obtained from the formed equations belong to the wing since the wing airfoil thickness ratio and wing flap chord ratio are used. Therefore, to obtain same parameters for horizontal tail, the same procedure is applied by using horizontal tail data instead of wing data. At the end, lift coefficient changes with flap and elevator deflection are calculated in 2D, Eqn. 2.23. In addition, base of the maximum lift coefficient of airfoil and some coefficients are obtained from other formed equations. These parameters help finding maximum lift coefficient change with flap in 2D, Eqn. 2.24.

$$\Delta c_l = \delta f \pi / 180 \frac{c_{l\delta}}{c_{l\delta_{theory}}} c_{l\delta_{theory}} k' \quad (2.23)$$

$$\Delta c_{l_{max}} = k_1 k_2 k_3 \Delta c_{l_{max_{base}}} \quad (2.24)$$

2.2.3 Lift Calculation

Lift calculations are done separately for each component of the aircraft. All graphs and several equations (not all of them) are taken from the book by Roskam [18]. As general method, firstly, lift coefficients changing with different angles of attack are calculated for three-dimensional wing and horizontal tail. Wing c_{l_α} (Eqn. 2.25 to Eqn. 2.27) is combined with the fuselage and $c_{l_{\alpha_{wf}}}$ (Eqn. 2.28 and Eqn. 2.29) is obtained. In these calculations, β parameter is not very important since the thesis study is related to incompressible flows and β is for compressible flows. It is still added to the code so that the usage area of the code can be extended.

$$\beta = \sqrt{1 - Mach^2} \quad (2.25)$$

$$\nu = \frac{cl_\alpha}{2 \times \pi \times \beta} \quad (2.26)$$

$$c_{L_{\alpha w}} = \frac{2\pi AR}{2 + \sqrt{4 + (AR\beta/\nu)^2(1 + (\tan(\Lambda_{c/2})/\beta)^2)}} S_{exp}/S \quad (2.27)$$

$$F = 1.07 \times (1 + fuse_{dia}/b)^2 \quad (2.28)$$

$$c_{L_{\alpha_{wf}}} = c_{L_{\alpha w}} F \quad (2.29)$$

In addition to alpha derivatives, zero-angle-of-attack lift coefficients of wing-fuselage combination and horizontal tail are found. The slip stream effect coming from the motor propeller is added to the horizontal tail c_{L_0} value, Eqn. 2.30. This addition of the accelerated flow on the tail is very important, since the velocity of airflow on the tail is increased, thus lift is increased.

$$c_{L_{0h}} = (-inc_{ht} - \epsilon_{0ht})\pi/180 c_{L_{\alpha_{ht}}} n_{uh} \frac{S_{ht}}{S} \quad (2.30)$$

On the other hand, $c_{L_{0w}}$ is calculated without the addition of the slip stream effect, Eqn. 2.31.

$$c_{L_{0w}} = (inc_w - \alpha_{L=0w})\pi/180c_{L_{\alpha w}} \quad (2.31)$$

If the propeller and motor is placed in front of the aircraft, wing will also experience the slip stream effect. For such a situation, an additional term (Eqn. 2.33) and wing lift coefficient (Eqn. 2.32), which is used to calculate this additional term, are added to the code so that lift increase caused by the slip stream effect can be reflected on the total lift force. The wing and horizontal tail areas which are exposed to slipstream must be determined correctly.

$$c_{L_w} = (c_{L_{0w}} + c_{L_{\alpha w}}(\alpha - \alpha_{L=0w})\pi/180) + \sigma_w(2sign(\alpha)(sin(\alpha))^2cos(\alpha)) \quad (2.32)$$

$$\Delta c_{L_{wslip}} = \frac{S_{slip}}{S} c_{L_w} \frac{2200P_{av}0.001341}{qV_c\pi(propdia)^2} \quad (2.33)$$

After the two lift coefficient values are calculated, sigmoid function [16] is constituted separately for wing and horizontal tail, (Eqn. 2.34 and Eqn. 2.35). This function is added to the lift coefficient calculation so that the angle of attack corrections can be done for all values of angle of attack. Sigmoid function helps to create an aerodynamic model which gives more realistic lift coefficient values, especially for deep stall landing. It provides more reliable lift calculations at higher angle of attacks.

$$\sigma_w = \frac{1 + e^{-Mach(\alpha - \alpha_{st})} + e^{Mach(\alpha + \alpha_{st})}}{1 + e^{-Mach(\alpha - \alpha_{st})}} (1 + e^{Mach(\alpha + \alpha_{st})}) \quad (2.34)$$

$$\sigma_h = \frac{1 + e^{-Mach(\alpha + inc_{ht} - \alpha_{st_t})} + e^{Mach(\alpha + inc_{ht} + \alpha_{st_t})}}{1 + e^{-Mach(\alpha + inc_{ht} - \alpha_{st_t})}} (1 + e^{Mach(\alpha + inc_{ht} + \alpha_{st_t})}) \quad (2.35)$$

As a result, total lift coefficient (Eqn. 2.36) is calculated by adding wing and fuselage combined lift coefficient (Eqn. 2.37), horizontal tail lift coefficient (from Eqn. 2.38

to Eqn. 2.43) and the increment coming from the slipstream effect (Eqn. 2.33). To obtain these coefficients, zero-angle-of-attack lift coefficients and lift coefficient angle of attack derivatives are used with the addition of sigmoid functions. Total lift coefficient is multiplied with wing area and dynamic pressure so that lift force can be obtained.

$$c_L = c_{L_{wf}} + c_{L_{ht}} + \Delta c_{L_{wslip}} \quad (2.36)$$

$$c_{L_{wf}} = (c_{L_{0wf}} + c_{L_{\alpha wf}}(\alpha - \alpha_{L=0_w})\pi/180) + \sigma_w(2\text{sign}(\alpha)(\sin(\alpha))^2\cos(\alpha)) \quad (2.37)$$

$$n_{u_h} = 1 + \frac{S_{hslip}}{S_{ht}} \frac{2200P_{av}0.001341}{qV_c\pi(\text{propdia})^2} \quad (2.38)$$

$$K_A = \frac{1}{AR} - \frac{1}{1 + AR^{1.7}} \quad (2.39)$$

$$K_\Lambda = \frac{10 - 3\Lambda}{7} \quad (2.40)$$

$$K_h = \frac{\frac{1-z_{ht}}{b}}{\sqrt[3]{\frac{2l_{ht}}{b}}} \quad (2.41)$$

$$\frac{\delta\varepsilon}{\delta\alpha} = 4.44 \frac{(K_A K_\Lambda K_h \sqrt{\cos(\Lambda_c/4)})^{1.19} c_{L_{\alpha w}}}{c_{L_{\alpha w0}}} \quad (2.42)$$

$$c_{L_{ht}} = (c_{L_{0h}} + c_{L_{\alpha ht}} n_{u_h} \frac{S_{ht}}{S} (1 - \frac{\delta\varepsilon}{\delta\alpha})(\alpha - \alpha_{L=0_t})\pi/180) + \sigma_h(2\text{sign}(\alpha)(\sin(\alpha))^2\cos(\alpha)) \quad (2.43)$$

Additional calculations for the parameters related to the lift are done. Initially, flap-deflected lift coefficient is calculated, (from Eqn. 2.44 to Eqn. 2.47). In this manner, four empirical data are used. This results in four different graph analysis. One of them

is flap-span factor, K_b , Figure 2.7. This is found by taking the difference between two points on the graph, Figure 2.6. Namely, the flap span factor is calculated from the same equation by changing the variables and subtracting the obtained values. Two variables are determined according to inner and outer limits of the flap span, measured from the aircraft center line. Such parameter finding procedures are applied throughout the code.

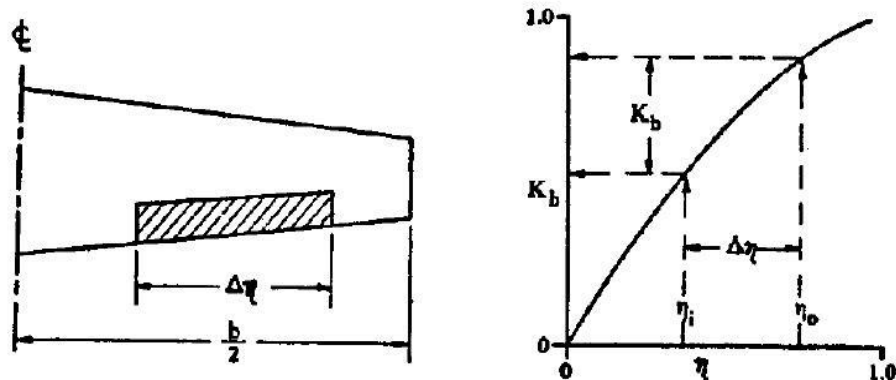


Figure 2.6: Procedure to calculate parameter K_b [18]

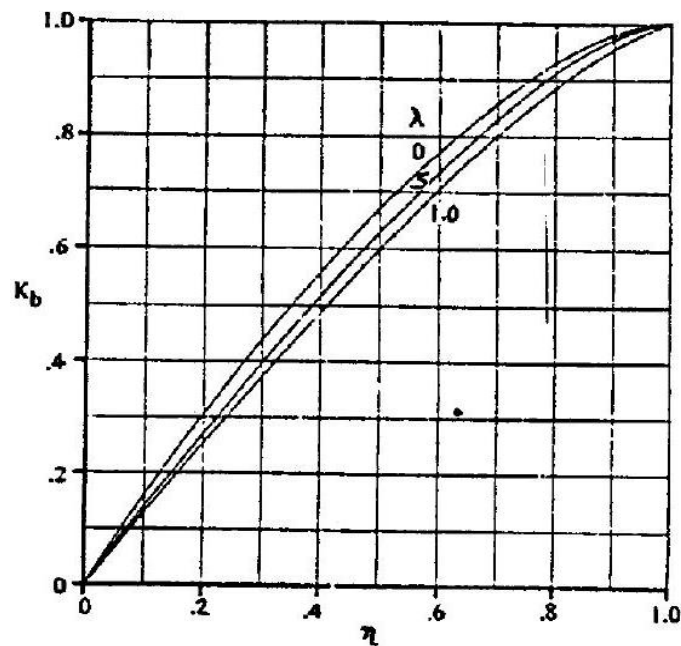


Figure 2.7: Effect of taper ratio and flap span on K_b [18]

The second and third graphs are studied together, (Figure 2.8). Although these graphs have different independent and dependent variables, the parameter read from one of

the graphs becomes curve selection variable for the other. After both of the curve equations are obtained, the value taken from the initial equation must be rounded. Thus, the curve to be chosen on the other graph is determined according to this rounded value. The fourth equation is composed from one curve on the graph following the general procedure mentioned in the beginning.

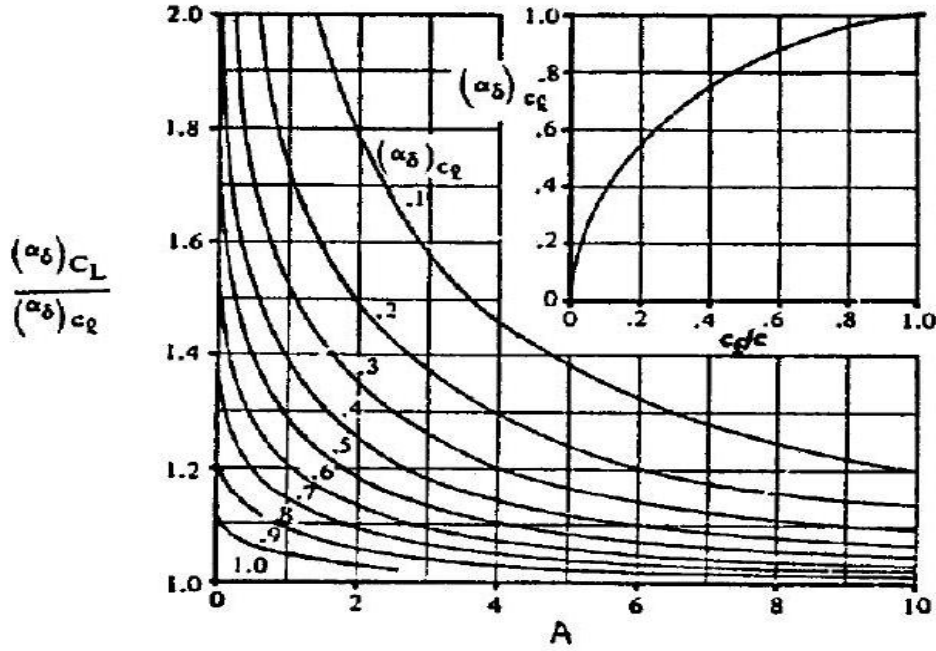


Figure 2.8: Effect of aspect and flap-chord ratios on the 3D flap effectiveness [18]

After all of the equations are formed, necessary parameters are calculated for wing and horizontal tail separately. In this manner, horizontal tail and wing specifications are entered as independent variables and the parameters related to them are obtained. At the end, by combining all necessary parameters, lift coefficient when the flaps are deflected is obtained.

$$\Delta C_{L_w} = K_b \Delta c_l \frac{C_{L_{\alpha w}}}{C_{l_{\alpha}}} \frac{\alpha_{\delta c_L}}{\alpha_{\delta c_l}} \quad (2.44)$$

$$\Delta \varepsilon_f = Inc_{downwash} \frac{\Delta C_{L_w}}{AR b_f / b} \quad (2.45)$$

$$\Delta C_L = \Delta C_{L_w} + k_{wh} \frac{S_{ht}}{S} \Delta C_{L_h} - C_{L_{\alpha ht}} n_{uh} \frac{S_{ht}}{S} \Delta \varepsilon_f \pi / 180 \quad (2.46)$$

$$c_{L_{flap}} = c_L + \Delta c_L \delta f \pi / 180 \quad (2.47)$$

2.2.4 Drag Calculation

Drag coefficient is calculated by separating it to its components and using several equations (not all of them) from the book by Raymer [17]. Initially, parasite drag is obtained. In this manner, component build-up method, which computes parasite drags for each component of the aircraft separately, is used. This method is based upon skin-friction drag in addition to a small separation pressure drag. The general formulation is shown in Eqn. 2.48.

$$c_{D_0} = \frac{\sum(C_{fc} F F_c Q_c S_{wet_c})}{S_{ref}} \quad (2.48)$$

Flat plate skin friction coefficient, C_{fc} , is expressed in the code for turbulent flow since wetted area of most aircrafts is under turbulent flow, (Eqn. 2.49). Reynolds Number is included in this coefficient formulation. However, it is important to decide whether actual Reynolds Number (Eqn. 2.51) or cutoff Reynolds Number (Eqn. 2.50) will be used. Lower Reynolds Number is selected and it is implemented to code as in the following example of wing component.

$$c_f = \frac{0.455}{(\log_{10} R)^{2.58} (1 + 0.144(Mach)^2)^{0.65}} \quad (2.49)$$

$$R_{cutoff} = 38.21(l/k)^{1.053} \quad (2.50)$$

$$Reynolds = \frac{\rho V l}{\mu} \quad (2.51)$$

```

1 R1_w = ro*Vc*c/mu
2 R_cutoff_w = 38.21*(c/k)^1.053
3 if R1_w < R_cutoff_w
4 R_w = R1_w
```

```

5  else Rl_w > R_cutoff_w
6  R_w = R_cutoff_w
7  end

```

The reason of this situation is surface roughness. If the surface is relatively rough, the friction coefficient will be higher. This is can be explained by the use of cutoff Reynolds Number, which includes skin roughness value, k . This parameter is chosen as 0.052×10^{-5} since the code is valid for the aircraft that have structure of smooth molded composite. Form factor that estimates the pressure drag due to viscous separation, FF_c , is found by different formulations, according to components of aircraft (Eqn. 2.52 is for wing and tail, Eqn. 2.53 is for fuselage). Interference factor, Q_c , takes additional drag caused by mutual interference between components into account. All the gained data is used in the above equation and total parasite drag is obtained.

$$FF_{w,t} = \left[1 + \frac{0.6}{(x/c)_m} \frac{t}{c} + 100 \left(\frac{t}{c}\right)^4\right] [1.34 Mach^{0.18} (\cos(\Lambda_m))^{0.28}] \quad (2.52)$$

$$FF_f = \left[1 + \frac{60}{(f)^3} \frac{f}{400}\right] \quad (2.53)$$

After that, drag due to lift is calculated for horizontal tail and wing combined with fuselage. These values are added to the parasite drag. In this manner, sigmoid function is used as in the lift calculation, (from Eqn. 2.54 to Eqn. 2.57).

$$K = \frac{1}{\pi e AR} \quad (2.54)$$

$$c_{D_{wf}} = (c_{D_{0w}} + c_{D_{0f}}) / S + (1 - \sigma_w) K (c_{L_{0w}} + c_{L_{\alpha wf}} (\alpha - \alpha_{L=0_w}) \pi / 180)^2 + \sigma_w (2 \text{sign}(\alpha) (\sin(\alpha))^3) \quad (2.55)$$

$$c_{D_{ht}} = (c_{D_{0ht}})/S + (1 - \sigma_h)K(c_{L_{0h}} + c_{L_{\alpha ht}}n_{u_h} \frac{S_{ht}}{S} (1 - \frac{\delta\varepsilon}{\delta\alpha})(\alpha - \alpha_{L=0_t})\pi/180)^2 + \sigma_h(2\text{sign}(\alpha)(\sin(\alpha))^3) \quad (2.56)$$

$$c_{D_{vt}} = (c_{D_{0vt}})/S \quad (2.57)$$

At the end, total drag is calculated for all components and drag types (Eqn. 2.58).

$$c_D = c_{D_{wf}} + c_{D_{ht}} + c_{D_{vt}} \quad (2.58)$$

2.2.5 Pitching Moment Calculation

Moment coefficient prediction is included in the code by using several equations (not all of them) and all graphs from the book by Roskam [18]. The method is based on the calculation of pitching moment coefficient changing with lift coefficient. At the end, this variable is multiplied by lift coefficient so that pitching moment can be obtained. When the steps are followed from final to initial, to create pitching moment coefficient and hence pitching moment, wing zero lift coefficient must be calculated. This parameter is the base. Therefore, increment due to lift is added to the zero-lift moment coefficient. In this manner, pitching moment change with lift coefficient is added to the base by multiplying lift coefficient. Moreover, aircraft pitching moment coefficient increment due to flaps is included in computation. Firstly, zero-lift pitching moment coefficient for combined wing and fuselage and horizontal tail is required so that the total zero-lift moment coefficient can be obtained. Horizontal tail part is calculated just like the moment calculation from the force and moment arm. Namely, zero-angle-of-attack lift coefficient and horizontal tail moment arm, which is found from the difference between aircraft centre of gravity and horizontal tail aerodynamic centre, are used. In addition, zero-lift moment coefficient of combined wing and fuselage is calculated from summation of the zero-lift moment coefficients of only wing and only fuselage. In this manner, zero-lift moment coefficient for fuselage is multiplied with a parameter that declines zero Mach Number to cruise Mach Number, $\frac{(c_{m_0})_M}{(c_{m_0})_{M=0}}$. When the zero-lift pitching moment of the fuselage computed, the fuselage

is separated to segments. For each segment, average width and length of the segment and incidence angle of the fuselage camber line relative to the fuselage reference plane at the centre of each fuselage increment are calculated iteratively according to the formulation, Eqn. 2.59.

$$c_{m_{0f}} = \frac{k_2 - k_1}{36.5Sc} \left[\sum_{i=1}^1 3(w_{f_i})^2 (-inc_w + \alpha_{0L_w} + inc_f) \Delta x_i \right] \quad (2.59)$$

1/13 of total length, which is the length of each fuselage segment, is added to the code so that each of them have the same length. Average width values are entered in two parts. For the first seven segments, the fuselage diameter increases linearly and for the last six segments it decreases linearly. This part of the code given below can be modified regarding to the fuselage shape.

```

1  cM01_f(1) = 0
2  for i=1:13
3  delx(i) = fuse_leng/13
4  if i <= 6
5  wf(i) = 0.1+i*(fuse_dia-0.1)/6
6  end
7  if i > 6
8  wf(i) = fuse_dia-(i-6)*(fuse_dia-0.1)/7
9  end
10 inc_f(i) = 0
11 cM01_f(i+1) = ((k2_k1)/36.5*S*c)*(((wf(i))^2*
    (inc_w+a0L_w+inc_f(i))*delx(i)))+cM01_f(i)
12 end
13 cM0_f = cM01_f(14)

```

Change in the pitching moment coefficient with lift coefficient is calculated from the difference between pitching moment reference centre and aircraft aerodynamic centre, Eqn. 2.60. As a reference location, aircraft centre of gravity is used in the

code, Eqn. 2.61.

$$dc_m/dc_L = x/c \quad (2.60)$$

$$x = -x_{ac_A} + x_{cg_A} \quad (2.61)$$

Aircraft total aerodynamic centre is calculated as summation of aerodynamic centres of fuselage-wing combination and horizontal tail by multiplying them with their lift curve slopes. This method is often applied in the code. The parameter, Eqn. 2.62, is obtained by dividing mentioned equation with total lift curve slope. Wing-fuselage combined aerodynamic centre is obtained from addition of wing aerodynamic centre and the increment due to fuselage aerodynamic centre, Eqn. 2.63.

$$x_{ac_A} = \frac{x_{ac_{wf}} c_{L_{\alpha wf}} + c_{L_{\alpha ht}} n_{wh} \frac{S_{ht}}{S} (1 - \frac{\delta \bar{\epsilon}}{\delta \alpha}) x_{ac_h} / c}{c_{L_{\alpha \text{total}}}} \quad (2.62)$$

$$x_{ac_{wf}} = x_{ac_w} / c + \Delta x_{ac_f} / c \quad (2.63)$$

The parameter which represents the additional aerodynamic centre shift due to fuselage includes derivative of moment with respect to angle of attack, Eqn. 2.64. $dM/d\alpha$ is computed for each segment and added together to find the total value, Eqn. 2.65. Width and length of each fuselage segment are entered as obtained from calculations of zero-lift moment coefficient of fuselage. In addition, downwash gradient is obtained in three different ways in the code, according to the segment number, which can be seen in the following code part. Two methods can be used; finding from the graph equation or using the given equation.

$$\Delta x_{ac_f} = \frac{-(dM/d\alpha)}{q S c c_{L_{\alpha w}}} \quad (2.64)$$

$$(dM/d\alpha) = (q/36.5)(c_{L_{\alpha w}}/0.08) \left[\sum_{i=1}^1 3(w_{f_i})^2 (\delta \bar{\epsilon} / \delta \alpha)_i \Delta x_i \right] \quad (2.65)$$

```

1     if i <= 4
2     % xicf(i) = [0.2 0.4 0.6 0.8 1 1.2 1.4 1.6 1.8 2]
3     % deda1 = [1.7 1.5 1.4 1.34 1.27 1.18 1.1 1.05
4     1.02 1.01]
5     % plot(xicf(i),deda1)
6     % [p82,S,mu] = polyfit(xicf(i),deda1,5)
7     deda_mean(i) = -0.031*((xicf(i)-1.1)/0.6055).^5
8     +0.0381*((xicf(i)-1.1)/0.6055).^4
9     +0.0793*((xicf(i)-1.1)/0.6055).^3
10    -0.0251*((xicf(i)-1.1)/0.6055).^2
11    -0.2563*((xicf(i)-1.1)/0.6055)+1.2248
12    end
13    if i == 5
14    % xicf(i) = [0.2 0.4 0.6 0.8 1]
15    % deda1 = [3.5 2.6 2.2 1.9 1.8]
16    % plot(xicf(i),deda1)
17    % [p83,S,mu] = polyfit(xicf(i),deda1,5)
18    deda_mean(i) = -0.0494*((xicf(i)-0.6)/0.3162).^5
19    +0.1302*((xicf(i)-0.6)/0.3162).^4
20    +0.0729*((xicf(i)-0.6)/0.3162).^2
21    -0.5455*((xicf(i)-0.6)/0.3162)+2.2
22    end
23    xh = l_ht-3*xac_w
24    if i >= 6
25    deda_mean(i) = xi(i)/xh*(1-deda)
26    end
27    dMda(i+1) = q/36.5*cL_alpha_w/0.08*(wf(i))^2
28    *deda_mean(i)*delx(i)+dMda(i)
29    end
30    dMda = dMda(14)

```

As it is seen from the code, there is "xicf" parameter. This is found from the below

equation, Eqn. 2.66.

$$\frac{x_i}{c_f} = \frac{x_i}{13 - (bsegment + fsegment)\Delta x_i} \quad (2.66)$$

To find zero-lift moment coefficient and pitching moment coefficient derivative with respect to lift coefficient, airplane pitching moment coefficient increment due to flaps must be computed. The parameter is obtained by addition of the same parameters that belong to each of the aircraft components, Eqn. 2.67.

$$\Delta c_m = \Delta c_{mw} + c_{L\alpha ht} n_{uh} \frac{S_{ht}}{S} (x_{ac_h}/c - x_{cg_A}/c) \Delta \varepsilon_f \quad (2.67)$$

The parameter that represents pitching moment change due to wing flaps require a challenging computation, Eqn. 2.68.

$$\begin{aligned} \Delta c_{mw} = & (x_{cg_A} - 0.25)\Delta c_{L_w} + K_\Lambda \frac{AR}{1.5} \Delta c_{L_{refw}} \tan(\Lambda_{c/4}) \\ & + K_p \frac{\Delta c'_m}{\Delta c_{L_{refw}}} \left(\frac{c'}{c}\right)^2 - K_p 0.25 c_{L_w} \left(\left(\frac{c'}{c}\right)^2 - \left(\frac{c'}{c}\right)\right) + K_p c_{m_w} \left(\left(\frac{c'}{c}\right)^2 - 1\right) \end{aligned} \quad (2.68)$$

From this equation, flap span factor, which is mentioned as K_p , $\frac{\Delta c'_m}{\Delta c_{L_{refw}}}$, and conversion factor (K_Λ), which accounts for a partial-span flap on a swept wing, are found. In this level of calculations, K_p and K_Λ parameters are computed for two independent variables and they are subtracted from each other. In addition, c' value belongs to the chord length when the flaps are deflected. Its equation, Eqn. 2.69 is formed from geometrical specifications.

$$c' = c - c_f + \cos(\delta f)c_f \quad (2.69)$$

Lift increment due to flaps for a reference wing, $\Delta c_{L_{refw}}$, is found from the same equation of lift increment effect on wing due to flaps by inserting $AR = 6$ and $\Lambda_{c/4}$ geometrical values.

2.3 PERFORMANCE CALCULATIONS

Mission plan is constituted so that performance characteristics can be determined for each part of the flight. In this manner, flight is divided into five parts: take-off, climb, cruise, loiter and landing. Several equations (not all of them) are taken from the book by Anderson [2]. Firstly, calculations are done for the take-off part. It is important to know that the velocity in this part is not equal to the cruise velocity. Therefore, lift and drag values are required to be computed again according to the new designated speed. This code is designed for hand launched aircrafts. That's why initial velocity is entered as 7 m/s which is an average value for the aircraft speed at the instant of throwing by hand. In addition, the ending of the take-off phase is defined as the condition of reaching the stall velocity. If the aircraft is able to reach stall velocity, this means that it is flying and it can start to climb. When take-off calculations are done, velocity is taken as the average of the hand launch speed and stall speed. In addition to the velocity, altitude is different from the cruise altitude. Thus, air density is taken according to the take-off altitude. Lift and drag change due to flaps and zero-lift drag coefficient are computed again for take-off part by using take-off altitude and speed value. In this manner, to reduce the code running time, only the parameters which are affected from speed and density are determined again. The other parameters are used the same. Lift force is calculated from thrust and weight, Eqn. 2.70.

$$L_{to} = W \cos(\theta_{to} - \alpha_{to}) - T_{av_{to}} \sin(\theta_{to} - \alpha_{to}) \quad (2.70)$$

After that, the code computes drag coefficient by using lift coefficient, Eqn. 2.71 and Eqn. 2.72.

$$c_{L_{to}} = \frac{L_{to}}{q_{to} S} \quad (2.71)$$

$$c_{D_{to}} = c_{D_{0_{to}}} + K(c_{L_{to}})^2 + \sigma_{w_{to}} 2(\sin(\alpha_{to}))^3 \quad (2.72)$$

Accelerations in x and z directions are computed Eqn. 2.73, Eqn. 2.74, to find total

acceleration by their resultant value, Eqn. 2.75.

$$acc_{to_x} = \frac{T_{av_{to}} \cos(\theta_{to} + \phi_{to}) - ((c_{D_{0_{to}}} + c_{D_{flap}} \delta f_{to} \pi / 180) q_{to} S) \cos(\theta_{to} - \alpha_{to})}{W/g \cos(\theta_{to} - \alpha_{to})} - \frac{((c_{L_{0_{to}}} + c_{L_{flap}} \delta f_{to} \pi / 180) q_{to} S) \sin(\theta_{to} - \alpha_{to})}{W/g \cos(\theta_{to} - \alpha_{to})} \quad (2.73)$$

$$acc_{to_z} = \frac{T_{av_{to}} \sin(\theta_{to} + \phi_{to}) - ((c_{D_{0_{to}}} + c_{D_{flap}} \delta f_{to} \pi / 180) q_{to} S) \sin(\theta_{to} - \alpha_{to})}{W/g \sin(\theta_{to} - \alpha_{to})} - \frac{((c_{L_{0_{to}}} + c_{L_{flap}} \delta f_{to} \pi / 180) q_{to} S) \cos(\theta_{to} - \alpha_{to})}{W/g \sin(\theta_{to} - \alpha_{to})} \quad (2.74)$$

$$acc_{to} = \sqrt{(acc_{to_x})^2 + (acc_{to_z})^2} \quad (2.75)$$

After this, time (Eqn. 2.77) and altitude (Eqn. 2.78) to complete the take-off are calculated. These values are important to know the total mission time and to determine the remaining altitude to climb.

$$RC_{to} = \frac{T_{av_{to}} V_{to} - c_{D_{to}} q_{to} S V_{to}}{W} \quad (2.76)$$

$$time_{to} = \frac{V_{to_{end}} - V_{to_{start}}}{acc_{to}} \quad (2.77)$$

$$h_{to} = RC_{to} time_{to} \quad (2.78)$$

During the take-off phase, current drawn from the battery is maximum since the throttle is 100%. Therefore, consumed capacity (mAh) of battery during take-off is calculated by the equation below, (Eqn. 2.79).

$$cap_{battery_{to}} = Amper_{to} 1000 time_{to} / 60 / 60 \quad (2.79)$$

After the take-off calculations are complete, performance calculations began for the other mission plan segment, climb. In this step, velocity and air density are obtained again. Climb starting speed is taken as the take-off ending speed, which is equal to the stall speed. The final speed of the climb part is calculated according to the altitude. Namely, aircraft speed increases by the amount of calculated climb acceleration until it reaches the cruise altitude. Within this period, velocity is increased by 0.01 at each loop in the code. In addition to this, different from take-off phase, in climb acceleration equations (Eqn. 2.80 and Eqn. 2.81), flap is not included since flaps are closed. Therefore, lift and drag increments are not needed to be calculated according to the climb velocity and altitude. Only necessary calculations are done for sigmoid function and zero-lift drag coefficient. Lift and drag coefficients are obtained just as in the take-off phase (Eqn. 2.70 to Eqn. 2.72) by using climb specifications instead of take-off specifications. Moreover, available thrust value (Eqn. 2.82) is important for the climb. In take-off phase, it is assumed that all available power is used since the throttle is full. However, for climb, it is assumed that 90% of the power available is used.

$$acc_{cl_x} = \frac{T_{av_{cl}} \cos(\theta_{cl} + \phi_{cl}) - (c_{D_{cl}} q_{cl} S) \cos(\theta_{cl} - \alpha_{cl}) - (c_{L_{cl}} q_{cl} S) \sin(\theta_{cl} - \alpha_{cl})}{W/g \cos(\theta_{cl} - \alpha_{cl})} \quad (2.80)$$

$$acc_{cl_z} = \frac{T_{av_{cl}} \sin(\theta_{cl} + \phi_{cl}) - (c_{D_{cl}} q_{cl} S) \sin(\theta_{cl} - \alpha_{cl}) - (c_{L_{cl}} q_{cl} S) \cos(\theta_{cl} - \alpha_{cl})}{W/g \sin(\theta_{cl} - \alpha_{cl})} \quad (2.81)$$

$$T_{av_{climb}} = \frac{P_{av} 0.9}{V_{to}} \quad (2.82)$$

Climb time, altitude and capacity of battery are calculated as take-off part. For the ampere taken from the battery during climb is computed from the given equation, 2.83.

$$Amper_{climb} = \frac{Power 0.9}{volt_{battery}} \quad (2.83)$$

For the climb part, several performance criteria are computed in the code so that some comments and observations can be done. These parameters are maximum theta angle (Eqn. 2.84), maximum lift to drag ratio (Eqn. 2.85), velocity that makes the rate of climb maximum (Eqn. 2.86), velocity that makes the climb angle θ maximum (Eqn. 2.87), required power for climb (Eqn. 2.88) and rate of climb that maximise θ , (Eqn. 2.89).

$$\theta_{climb_{max}} = \text{asin}\left(\frac{T_{av_{climb}}}{W} - \sqrt{4c_{D_{0_{cl}}}K}\right)180/\pi \quad (2.84)$$

$$(L/D)_{max_{climb}} = \sqrt{\frac{1}{4c_{D_{climb}}K}} \quad (2.85)$$

$$V_{RC_{max_{climb}}} = \sqrt{\frac{(T/W)(W/S)}{3\rho c_{D_0}} \left[1 + \sqrt{1 + \frac{3}{(L/D)_{max}^2 (T/W)^2}}\right]} \quad (2.86)$$

$$V_{\theta_{max_{climb}}} = \sqrt{\frac{2}{\rho} \sqrt{\frac{K}{c_{D_0}} \frac{W}{S}} \cos(\theta_{max})} \quad (2.87)$$

$$P_{req_{climb}} = \sqrt{\frac{2W^3 c_{D_{climb}}^2}{\rho S c_{L_{climb}}^3}} \quad (2.88)$$

$$RC_{\theta_{max_{climb}}} = V_{\theta_{max_{climb}}} \sin(\theta_{climb_{max}}) \quad (2.89)$$

After climb, the cruise phase comes in. First step for this phase is to determine the range. By using the range and cruise velocity, cruise time is calculated. Power required for cruise, current drawn and consumed battery capacity are all computed in the same way as in climb phase. At the end, to check if the determined range value is meaningful or not, the following formulation is used, Eqn. 2.90.

$$Range_{check} = \frac{2}{c} \sqrt{\frac{2}{\rho S}} \frac{c_L^0}{c_D} \cdot 5 \quad (2.90)$$

The computations on the code proceed with loiter phase. All lift, drag and other parameters calculated similar to that of cruise. Lift and drag coefficients are calculated from the load factor since turning maneuver is involved, (Eqn. 2.91 to Eqn. 2.93).

$$n = (L/W) \quad (2.91)$$

$$c_{L_{loiter}} = n c_L \quad (2.92)$$

$$c_{D_{loiter}} = c_{D_0} + K c_{L_{loiter}}^2 \quad (2.93)$$

The power required and current drawn in loiter phase are calculated, (Eqn. 2.94 to Eqn. 2.95).

$$P_{req_{loiter}} = \sqrt{\frac{2W^3 c_{D_{loiter}}^2}{\rho S c_{L_{loiter}}^3}} \quad (2.94)$$

$$Power_{loiter} = \frac{P_{req_{loiter}}}{\eta_{motor} \eta_{prop}} \quad (2.95)$$

In this part of the mission, different from the other parts, battery capacity is not found from the current drawn and time. Firstly, remaining battery capacity (Eqn. 2.96) is calculated by subtracting consumed capacity in take-off, climb and cruise from 90% of total capacity. The reason of this method is that aircraft executes its mission during loitering and needs more time in this phase. Moreover, 90% of total capacity is entered to the code instead of full battery capacity for the possible case of an emergency. It is also not good to deplete battery fully for each flight in terms of battery efficiency and lifetime.

$$cap_{battery_{loiter}} = cap_{battery} 0.9 - cap_{battery_{to}} - cap_{battery_{climb}} - cap_{battery_{cruise}} \quad (2.96)$$

The time passing during loiter is found from current drawn during loiter and battery capacity for loiter, Eqn. 2.97.

$$time_{loiter} = \frac{cap_{battery}}{Amp_{loiter}1000} \times 60 \times 60 \quad (2.97)$$

At the end, some performance parameters related to the turning maneuver are added to the code to clearly observe the limits of aircraft. These parameters are maximum load factor(Eqn. 2.98), minimum turn radius (Eqn. ??), maximum turn rate velocity (Eqn. 2.100), load factor (Eqn. 2.101) and maximum turn rate (Eqn. 2.102).

$$n_{max} = \frac{0.5\rho V_c^2 c_{L_{max}}}{W/S} \quad (2.98)$$

$$R_{turn_{min}} = \frac{2}{\rho g c_{L_{max}}} \frac{W}{S} \quad (2.99)$$

$$V_{\omega_{max}} = \sqrt{\frac{2(W/S)}{\rho} \left(\frac{K}{c_{D_0}}\right)^{1/4}} \quad (2.100)$$

$$n_{\omega_{max}} = \sqrt{\frac{T/W}{\sqrt{K c_{D_0}}} - 1} \quad (2.101)$$

$$\omega_{max} = q \sqrt{\frac{\rho}{W/S} \left[\frac{(T/W)}{2K} - \sqrt{\frac{c_{D_0}}{K}} \right]} \quad (2.102)$$

Performance characteristic designation ends with mission time calculation in the code (Eqn. 2.103). Mission time is found by addition of each time value of every phase of flight. This parameter is very important for small aircrafts, as in UAV sector, small aircrafts compete especially in terms of their flight time.

$$MISSIONTIME = [time_{loiter} + time_{climb} + time_{cruise} + time_{to}]/60 \quad (2.103)$$

2.4 STABILITY AND CONTROL DERIVATIVES DETERMINATION

The created code includes the stability and control derivative calculations. In this manner, user can see the entire table related to the stability characteristic of the UAV. This aspect of the code supplies general information of stability without using any detailed computer programs and thus without losing much time. The equations in this part of the code are taken from [19]. In addition to that, same necessary information related to the stability and control derivatives, their physical meanings, the properties or components that affect them and their intervals for a successful design are learned and added from several sources ([6], [4], [10] and [1]).

As the initial computations, angle of attack derivatives of lift, drag and pitching moment coefficients are determined. Drag coefficient derivative with respect to angle of attack is neglected since it is very small. However, for the low subsonic flight such as mini UAVs, this assumption is not meaningful. Therefore, it is calculated from the below equation (Eqn. 2.104).

$$c_{D_\alpha} = \frac{\partial c_{D_0}}{\partial \alpha} + \frac{2c_L c_{L_\alpha}}{\pi A R e} \quad (2.104)$$

3D lift curve slope is determined (from Eqn. 2.105 to Eqn. 2.112). It gives information related to the turbulence changes. In addition to that, this parameter has significance on aircraft manoeuvrability and pitching motion damping. This parameter increases with Mach number below the critical Mach number due to the compressibility effects.

$$c_{L_\alpha} = c_{L_{\alpha_{wf}}} + c_{L_{\alpha_{ht}}} \eta h t \frac{S_{ht}}{S} \left(1 - \frac{d\varepsilon}{d\alpha}\right) \quad (2.105)$$

$$c_{L_{\alpha_{wf}}} = K_{wf} c_{L_{\alpha_w}} \quad (2.106)$$

$$K_{wf} = 1 - 0.25 \left(\frac{d}{b}\right)^2 + 0.025 * \left(\frac{d}{b}\right) \quad (2.107)$$

$$\frac{d\varepsilon}{d\alpha} \Big|_M = \frac{d\varepsilon}{d\alpha} \Big|_{M=0} \frac{c_{L_{\alpha_w}|M}}{c_{L_{\alpha_w}|M=0}} \quad (2.108)$$

$$\frac{d\varepsilon}{d\alpha}|_{M=0} = 4.44[K_A K_\lambda K_H \sqrt{\cos(\Lambda_{c/4})}]^{1.19} \quad (2.109)$$

$$K_A = \frac{1}{A} - \frac{1}{1 + A^{1.7}} \quad (2.110)$$

$$K_\lambda = \frac{10 - 3\lambda}{7} \quad (2.111)$$

$$K_H = \frac{1 - h_H/b}{\sqrt[3]{\frac{2l_h}{b}}} \quad (2.112)$$

Derivative of moment coefficient with respect to angle of attack (Eqn. 2.113) is computed by using static margin ($\frac{dc_m}{dc_L}$), which is an essential parameter for the stability. This variable is found from the difference between aircraft total aerodynamic centre and aircraft total centre of gravity (Eqn. 2.114). Aircraft centre of gravity location must be known or must be estimated properly. Additionally, calculation of aerodynamic centre of aircraft is mentioned in previous sub section. This parameter is also called as pitch stiffness and plays an important role in pitching motion. This parameter is in the interval of -3 and +1 rad^{-1} .

$$c_{m_\alpha} = \frac{dc_m}{dc_L} c_{L_\alpha} \quad (2.113)$$

$$\frac{dc_m}{dc_L} = x_{cg} - x_{acA} \quad (2.114)$$

Second derivatives are found for velocity variation. Change of drag coefficient with respect to speed is computed (Eqn. 2.115). In addition to that, the dependency of lift coefficient to the speed is calculated. This is occurred due to compressibility and aeroelastic effects. However, aeroelastic effects are neglected in this formulation (Eqn. 2.116). Same situation is valid for the variation of pitching moment with speed

(Eqn. 2.117).

$$c_{D_u} = Mach \frac{\partial c_D}{\partial Mach} \quad (2.115)$$

$$c_{L_u} = c_L \frac{Mach^2}{1 - Mach^2} \quad (2.116)$$

$$c_{m_u} = -c_L \frac{\partial x_{ac_w}}{\partial M} \quad (2.117)$$

Third part is related to the pitch rate derivatives. For subsonic flights, the drag coefficient derivative with respect to the pitch rate is negligible (Eqn. 2.118).

$$c_{D_q} = 0 \quad (2.118)$$

The derivative c_{L_q} is resultant both of the wing and horizontal tail (Eqn. 2.119). Same situation is valid for the pitching moment derivative (Eqn. 2.123). This derivative is called as pitch damping derivative. It should be negative since the derivative is a counteracting to any pitch rate.

$$c_{L_q} = c_{L_{q_w}} + c_{L_{q_{ht}}} \quad (2.119)$$

$$c_{L_{q_w}|M} = \frac{AR + 2\cos(\lambda_{c/4})}{ARB + 2\cos(\lambda_{c/4})} c_{L_{q_w}|M=0} \quad (2.120)$$

$$c_{L_{q_w}|M=0} = (1/2 + \frac{2x_w}{c}) c_{L_{\alpha_w}|M=0} \quad (2.121)$$

$$c_{L_{q_{ht}|M}} = 2c_{L_{\alpha_{ht}|M}} \eta_{ht} V r_{ht} \quad (2.122)$$

$$c_{m_q} = c_{m_{q_w}} + c_{m_{q_{ht}}} \quad (2.123)$$

$$c_{m_{q_w|M}} = \left[\frac{\frac{AR^3(\tan(\Lambda_{c/4}))^2}{ARB+6\cos(\Lambda_{c/4})} + \frac{3}{B}}{\frac{AR^3(\tan(\Lambda_{c/4}))^2}{AR+6\cos(\Lambda_{c/4})+3}} \right] c_{m_{q_w|M=0}} \quad (2.124)$$

$$c_{m_{q_w|M=0}} = -K c_{l_{\alpha_w}} \cos(\Lambda_{c/4}) \left[\frac{AR[2(\frac{x_w}{c})^2 + 0.5(\frac{x_w}{c})]}{AR + 2\cos(\Lambda_{c/4})} + \frac{1/24 \frac{AR^3(\tan(\Lambda_{c/4}))^2}{AR + 6\cos(\Lambda_{c/4}) + 1/8}}{AR + 6\cos(\Lambda_{c/4}) + 1/8} \right] \quad (2.125)$$

$$c_{m_{q_{ht}}} = -2c_{L_{\alpha_{ht}}} \eta_{ht} V r_{ht} \frac{x_{ht}}{c} \quad (2.126)$$

Fourth derivative set is done for the angle of attack rate derivatives. These derivatives are caused by the wing downwash which affects the horizontal tail. The lift force of the horizontal tail and pitching moment are affected from this situation. Drag coefficient derivative with respect to angle of attack rate is also assumed as zero just like the derivative with respect to pitch rate. Lift coefficient variation by angle of attack rate is found from below formulations (from Eqn. 2.127 to Eqn. 2.129).

$$c_{L_{\dot{\alpha}}} = c_{L_{\dot{\alpha}_w}} + c_{L_{\dot{\alpha}_{ht}}} \quad (2.127)$$

$$c_{L_{\dot{\alpha}_w}} = 1.5 \left(\frac{x_{ac_w}}{c_r} \right) c_{L_{\alpha_w}} + 3c_L \quad (2.128)$$

$$c_{L_{\dot{\alpha}_{ht}}} = 2c_{L_{\alpha_{ht}}} \eta_{ht} V r_{ht} \frac{d\varepsilon}{d\alpha} \quad (2.129)$$

Pitching moment coefficient derivative with respect to angle of attack rate is found from the given formulation (Eqn. 2.130). Although wing contribution is seen in the formulation, there is no explicit method to estimate $c_{m_{\dot{\alpha}_w}}$. In addition to that, for conventional aircrafts this parameter is generally small. Because of all these reasons, pitching moment derivative is found directly from the horizontal tail contribution (Eqn. 2.131).

$$c_{m_{\dot{\alpha}}} = c_{m_{\dot{\alpha}_w}} + c_{m_{\dot{\alpha}_{ht}}} \quad (2.130)$$

$$c_{m\dot{\alpha}_{ht}} = -2c_{L\alpha_{ht}}\eta_{ht}Vr_{ht}\frac{x_{ht}}{c}\frac{d\varepsilon}{d\alpha} \quad (2.131)$$

The next derivative calculations are done for the variations with sideslip angle. Initially, side force derivative is determined. Wing contribution of this parameter (Eqn. 2.133) has importance only when the aircraft has dihedral angle. The effects of the fuselage and vertical tail components (Eqn. 2.134 and Eqn. 2.135) are determined so that entire side force derivative can be found (Eqn. 2.132).

$$c_{y\beta} = c_{y\beta_w} + c_{y\beta_f} + c_{y\beta_{vt}} \quad (2.132)$$

$$c_{y\beta_w} = -0.0001|\Gamma|57.3 \quad (2.133)$$

$$c_{y\beta_f} = -2K_i\left(\frac{S_0}{S}\right) \quad (2.134)$$

$$c_{y\beta_{vt}} = -kc_{L\alpha_{vt}}\left(1 + \frac{d\sigma}{d\beta}\right)\eta_{vt}\frac{S_{vt}}{S} \quad (2.135)$$

$$\left(1 + \frac{d\sigma}{d\beta}\right)\eta_{vt} = 0.724 + 3.06\frac{S_{vt}/S}{1 + \cos(\Lambda_{c/4})} + 0.4\frac{z_w}{d} + 0.009AR \quad (2.136)$$

Variation of rolling moment coefficient (Eqn. 2.137 to Eqn. 2.143) is found by adding the contributions of horizontal (Eqn. 2.142) and vertical tail (Eqn. 2.143) and wing fuselage interaction (Eqn. 2.138). This derivative is a result of a dihedral effect. A stable aircraft is inclined to roll away from the side slip. In this way, lift force is not decreased. The situation brings a negative $c_{l\beta}$ for lateral stability.

$$c_{l\beta} = c_{l\beta_{wf}} + c_{l\beta_{ht}} + c_{l\beta_{vt}} \quad (2.137)$$

$$c_{l_{\beta_{wf}}} = 57.3 \left[c_{L_{wf}} \left(\frac{c_{l_{\beta}}}{c_L} \right)_{\Lambda_{c/2}} K_{M_{\Lambda}} K_f + \left(\frac{c_{l_{\beta}}}{c_L} \right)_A \right. \\ \left. \Gamma \frac{c_{l_{\beta}}}{\Gamma} K_{M_{\Gamma}} + \frac{\Delta c_{l_{\beta}}}{\Gamma} + (\Delta c_{l_{\beta}})_{z_w} + \right. \\ \left. \theta \tan(\Lambda_{c/4}) \left(\frac{\Delta c_{l_{\beta}}}{\theta \tan(\Lambda_{c/4})} \right) \right] \quad (2.138)$$

$$\frac{\Delta c_{l_{\beta}}}{\Gamma} = -0.0005 \sqrt{AR} \left(\frac{d}{b} \right)^2 \quad (2.139)$$

$$d = \sqrt{\frac{\text{average fuselage cross sectional area}}{0.7854}} \quad (2.140)$$

$$(\Delta c_{l_{\beta}})_{z_w} = -\frac{1.2 \sqrt{AR}}{57.3} \left(\frac{z_w}{b} \right) \left(\frac{2d}{b} \right) \quad (2.141)$$

$$c_{l_{\beta_{ht}}} = c_{l_{\beta_{htf}}} \frac{S_{ht} b_{ht}}{S b} \quad (2.142)$$

$$c_{l_{\beta_{vt}}} = c_{y_{\beta_{vt}}} \frac{z_v \cos(\alpha) - l_v \sin(\alpha)}{b} \quad (2.143)$$

Yawing moment derivative with respect to sideslip angle (Eqn. 2.144) is another parameter to be computed. This is static directional stability. Positive values of this parameter means that the aircraft is stable in terms of yawing motions. Although fuselage (Eqn. 2.145) has decreasing effect on the derivative, vertical tail (Eqn. 2.146) and wing have dominating positive effects on the yawing moment change with sideslip angle.

$$c_{n_{\beta}} = c_{n_{\beta_w}} + c_{n_{\beta_f}} + c_{n_{\beta_{vt}}} \quad (2.144)$$

$$c_{n_{\beta_f}} = -57.3 K_N K_{R_l} \frac{S_{f_{side}} l_f}{S b} \quad (2.145)$$

$$c_{n\beta_{vt}} = -c_{y\beta_{vt}} \frac{l_v \cos(\alpha) + z_v \sin(\alpha)}{b} \quad (2.146)$$

Following derivatives are calculated with respect to roll rate. Side force derivative (Eqn. 2.147) is constituted by vertical tail. During the rolling motion, vertical tail moves in horizontal direction. This causes change in angle of attack and thus change in horizontal force. Roll rate and horizontal force are inversely proportional. Therefore, variation of side force coefficient with roll rate should be negative.

$$c_{y_p} = c_{y_{p_{vt}}} = 2 \frac{z_v \cos(\alpha) - l_v \sin(\alpha)}{b} c_{y\beta_{vt}} \quad (2.147)$$

Change of rolling moment coefficient with roll rate (Eqn. 2.148) is found by the contributions of wing fuselage interaction (Eqn. 2.149), vertical (Eqn. 2.151) and horizontal tail (Eqn. 2.150). During the rolling motion, the lift forces on left and right the wings are different from each other due to changing angle of attack. This fact causes an opposite motion to rolling. Therefore, it is obvious that the rolling moment coefficient derivative with respect to the rolling is negative.

$$c_{l_p} = c_{l_{p_{wf}}} + c_{l_{p_{ht}}} + c_{l_{p_{vt}}} \quad (2.148)$$

$$c_{l_{p_{wf}}} = c_{l_{pw}} = \frac{\beta c_{l_p} \kappa}{\kappa \beta} \quad (2.149)$$

$$c_{l_{p_{ht}}} = 0.5(c_{l_p})_{ht} \frac{S_{ht}}{S} \left(\frac{b_{ht}}{b}\right)^2 \quad (2.150)$$

$$c_{l_{p_{vt}}} = 2\left(\frac{z_v}{b}\right)^2 c_{y\beta_{vt}} \quad (2.151)$$

Variation of yawing moment coefficient with roll rate is computed from the given formulations (from Eqn. 2.152 to Eqn. 2.157). Rolling motion creates additional values to drag and thrust forces. This brings a yawing moment opposite to the rolling. On the contrary, for the vertical tail, the situation is different. Positive rolling motion

causes positive yawing motion. For high angle of attacks, wing is more dominant than vertical tail. Therefore, c_{n_p} should be less than zero. For the normal flight conditions which have less angle of attack, the situation is the reverse.

$$c_{n_p} = c_{n_{pw}} + c_{n_{pvt}} \quad (2.152)$$

$$c_{n_{pw}} = -c_{l_{pw}} \tan(\alpha) - [-c_{l_p} \tan(\alpha) - \left(\frac{c_{n_p}}{c_L}\right)_{c_L=0|M} c_L] + \left(\frac{\Delta c_{n_p}}{\theta}\right) \theta + \left(\frac{\Delta c_{n_p}}{\alpha_{\delta_f} \delta_f}\right) \alpha_{\delta_f} \delta_f \quad (2.153)$$

$$\left(\frac{c_{n_p}}{c_L}\right)_{c_L=0|M} = \frac{AR + 4\cos(\Lambda_{c/4})}{ARB + 4\cos(\Lambda_{c/4})} \quad (2.154)$$

$$\frac{ARB + 0.5(ARB + \cos(\Lambda_{c/4}))(\tan(\Lambda_{c/4}))^2}{AR + 0.5(AR + \cos(\Lambda_{c/4}))(\tan(\Lambda_{c/4}))^2} \left(\frac{c_{n_p}}{c_L}\right)_{c_L=0|M=0}$$

$$B = \sqrt{1 - Mach^2(\cos(\Lambda_{c/4}))^2} \quad (2.155)$$

$$\left(\frac{c_{n_p}}{c_L}\right)_{c_L=0|M=0} = -\frac{1}{6} \frac{AR + 6(AR + \cos(\Lambda_{c/4}))}{AR + 4\cos(\Lambda_{c/4})} \frac{\frac{x}{c} \tan(\Lambda_{c/4}) + \frac{(\tan(\Lambda_{c/4}))^2}{12}}{AR + 4\cos(\Lambda_{c/4})} \quad (2.156)$$

$$c_{n_{pv}} = -\frac{2}{b} (l_v \cos(\alpha) + z_v \sin(\alpha)) \frac{z_v \cos(\alpha) - l_v \sin(\alpha)}{b} c_{y_{\beta_{vt}}} \quad (2.157)$$

Another set of computations are done for the yaw rate derivatives. The least important derivative is the side force coefficient derivative with respect to the yaw rate (Eqn. 2.158) and its value comes from the vertical tail (Eqn. 2.159).

$$c_{y_r} = c_{y_{rvt}} \quad (2.158)$$

$$c_{y_{rvt}} = -\frac{2}{b} (l_v \cos(\alpha) + z_v \sin(\alpha)) c_{y_{\beta_{vt}}} \quad (2.159)$$

Rolling moment variation with yaw rate is found from the given formulation (Eqn. 2.160). As it can be seen from the formulation, it is constituted from the vertical tail (Eqn. 2.164) and wing affects (from Eqn. 2.161 to Eqn. 2.163). Since yawing motion and moment are proportional, rolling moment derivative with respect to the yaw rate should be positive.

$$c_{l_r} = c_{l_{r_{vt}}} + c_{l_{r_w}} \quad (2.160)$$

$$c_{l_{r_w}} = c_L \left(\frac{c_{l_r}}{c_L} \right)_{c_L=0|M} + \left(\frac{\Delta c_{l_r}}{\Gamma} \right) \Gamma + \left(\frac{\Delta c_{l_r}}{\theta} \right) \theta + \left(\frac{\Delta c_{l_r}}{\alpha_{\delta_f} \delta_f} \right) \alpha_{\delta_f} \delta_f \quad (2.161)$$

$$\begin{aligned} \left(\frac{c_{l_r}}{c_L} \right)_{c_L=0|M} &= \frac{1 + \frac{AR(1-B^2)}{2B(ARB+2\cos(\Lambda_{c/4}))}}{1 + \frac{AR+2\cos(\Lambda_{c/4}) (\tan(\Lambda_{c/4}))^2}{AR+4\cos(\Lambda_{c/4})} \frac{1}{8}} \\ &\quad \frac{\frac{ARB+2\cos(\Lambda_{c/4}) (\tan(\Lambda_{c/4}))^2}{AR+4\cos(\Lambda_{c/4})} \frac{1}{8}}{1 + \frac{AR+2\cos(\Lambda_{c/4}) (\tan(\Lambda_{c/4}))^2}{AR+4\cos(\Lambda_{c/4})} \frac{1}{8}} \left(\frac{c_{l_r}}{c_L} \right)_{c_L=0|M=0} \end{aligned} \quad (2.162)$$

$$\frac{\Delta c_{l_r}}{\Gamma} = \frac{1}{12} \frac{\pi AR \sin(\Lambda_{c/4})}{AR + 4\cos(\Lambda_{c/4})} \quad (2.163)$$

$$c_{l_{r_{vt}}} = -\frac{2}{b^2} (l_v \cos(\alpha) + z_v \sin(\alpha)) (z_v \cos(\alpha) - l_v \sin(\alpha)) c_{y\beta_{vt}} \quad (2.164)$$

Yawing moment coefficient due to the yaw rate (Eqn. 2.165) is computed by the sum of two affecting components, wing (Eqn. 2.166) and vertical tail (Eqn. 2.167). Vertical tail effect is caused by the side force on the moment arm. Moreover, wing contribution is caused by the moment created by the changing drag force along span-wise direction.

$$c_{n_r} = c_{n_{r_{vt}}} + c_{n_{r_w}} \quad (2.165)$$

$$c_{n_{r_w}} = c_L^2 \left(\frac{c_{n_r}}{c_L^2} \right) + c_{D_0} \left(\frac{c_{n_r}}{c_{D_0}} \right) \quad (2.166)$$

$$c_{n_{r_{vt}}} = \frac{2}{b^2} (l_v \cos(\alpha) + z_v \sin(\alpha))^2 c_{y_{\beta_{vt}}} \quad (2.167)$$

In the code, longitudinal control derivatives are also focused on. In this manner, variation of lift coefficient (Eqn. 2.168) with flap deflection is computed. Reference book ([19]) is used for all the calculations assuming that the flaps and trailing edges are plain type. Therefore, code is limited to the plain flaps. To determine the effect of the flap deflection on lift coefficient, airfoil lift curve slope at cruise Mach (Eqn. 2.169) and variation of flap deflection with airfoil lift coefficient (Eqn. 2.170) are required.

$$c_{L_{\delta_F}} = c_{l_{\delta_F}} \frac{c_{L_{\alpha|M}}}{c_{l_{\alpha|M}}} \left[\frac{(\alpha_{\delta})_{c_L}}{(\alpha_{\delta})_{c_l}} \right] K_b \quad (2.168)$$

$$c_{l_{\alpha|M}} = \frac{c_{l_{\alpha}}}{\sqrt{1 - Mach^2}} \quad (2.169)$$

$$c_{l_{\delta_F}} = \frac{c_{l_{\delta}}}{c_{l_{\delta_{Theory}}}} c_{l_{\delta_{Theory}}} K' \quad (2.170)$$

Lift coefficient derivative and moment coefficient derivative with respect to the stabilizer incidence are calculated from the given formulas (Eqn. 2.171 and Eqn. 2.172).

$$c_{L_{i_{ht}}} = c_{L_{\alpha_{ht}}} \frac{S_{ht}}{S} \quad (2.171)$$

$$c_{m_{i_{ht}}} = -c_{L_{\alpha_{ht}}} V r_{ht} \quad (2.172)$$

As the last longitudinal control derivative, lift (Eqn. 2.173) and moment coefficient (Eqn. 2.174) changes with elevator deflection are calculated.

$$c_{L_{\delta_E}} = c_{L_{\delta_F}} \frac{S_{ht}}{S} \quad (2.173)$$

$$c_{m_{\delta_E}} = -c_{L_{\delta_E}} V r_{ht} \quad (2.174)$$

Lateral control derivatives are computed. In this manner, aileron deflections are analysed. Initially, rolling moment coefficient derivative with respect to aileron deflection is computed. In the determination process, parameters for left and right wings are summed and several additional parameters are found (from Eqn. 2.175 to Eqn. 2.181).

$$c_{l_{\delta_A}} = [c_{l_{\delta_L}} + c_{l_{\delta_R}}] \quad (2.175)$$

$$c_{l_{\delta}} = \frac{c_{l_{\delta}}}{c_{l_{\delta_{Theory}}}} c_{l_{\delta_{Theory}}} K' \quad (2.176)$$

$$|\alpha_{\delta}| = \frac{c_{l_{\delta}}}{c_{l_{\alpha}}} \quad (2.177)$$

$$c_{l_{\delta}} = |\alpha_{\delta}| c'_{l_{\delta}} \quad (2.178)$$

$$c'_{l_{\delta}} = \frac{\kappa}{\beta} \left(\frac{\beta c'_{l_{\delta}}}{\kappa} \right) \quad (2.179)$$

$$c_l = \left[\left(\frac{c_{l_{\delta}}}{2} \right)_L + \left(\frac{c_{l_{\delta}}}{2} \right)_R \right] (\delta_L - \delta_R) \quad (2.180)$$

$$\delta_A = \frac{1}{2} (\delta_L - \delta_R) \quad (2.181)$$

Yawing moment variation with aileron is also discussed and found from bellow formulation (Eqn. 2.182). This derivative is also called adverse yaw. It causes a nose left motion when the aircraft rolls to the right. Therefore, it should be negative.

$$c_{n_{\delta_A}} = K c_L c_{l_{\delta_{aileron}}} \quad (2.182)$$

Next step is discussion of the directional control derivatives. Rudder deflections are discussed. In the code, side force, rolling moment and yawing moment coefficients derivatives with respect to the rudder deflection are computed respectively (Eqn. 2.183, Eqn. 2.184 and Eqn. 2.185).

$$c_{y\delta_R} = c_{L\alpha_{vt}} \frac{(\alpha_\delta)_{c_L}}{(\alpha_\delta)_{c_l}} (\alpha_\delta)_{c_l} K' K_b \frac{S_{vt}}{S} \quad (2.183)$$

$$c_{l\delta_R} = c_{y\delta_R} \left(\frac{z_v \cos(\alpha) - l_v \sin(\alpha)}{b} \right) \quad (2.184)$$

$$c_{n\delta_R} = -c_{y\delta_R} \left(\frac{l_v \cos(\alpha) + z_v \sin(\alpha)}{b} \right) \quad (2.185)$$

2.5 DESIGN TOOL STABILITY and CONTROL DERIVATIVE CALCULATIONS VERIFICATION

For the code that is generated up to this point, the methods, formulations and computations are needed to be checked. In this manner, the UAV system that is designed and manufactured by my company is used. Its flight tests related to the aerodynamic and structural design are finished and it is placed in the product list of the company. In addition to that, stability and control derivative values taken from DATCOM and CFD results of this UAV properties are compared with each other and with the flight test results. Therefore, the parameters belonging to this aircraft are used so that the input values can be entered to the code and it can be checked. At the result of the running code, following stability and control derivative results which are compared with the CFD results are obtained (Table 2.3 and Table 2.2). As it can be seen, the results are very close to each other. Therefore, the design tool code can be qualified as valid, confidential and accurate.

Table 2.2: Comparison of CFD results and code results for control derivatives

Control Derivatives	Results from CFD	Results from Generated Code
$C_{L\delta_F}$	1.690	1.160
$C_{D\delta_F}$	0.051	0.046
$C_{m_{\delta_F}}$	-0.100	-0.092
$C_{L\delta_E}$	0.147	0.118
$C_{m_{\delta_E}}$	-0.475	-0.407
$C_{D\delta_E}$	0.003	0.005
$C_{l_{\delta_A}}$	-0.115	-0.268
$C_{n_{\delta_A}}$	0.010	0.018
$C_{D\delta_A}$	0.014	0.023
$C_{y_{\delta_R}}$	0.062	0.035
$C_{l_{\delta_R}}$	0.001	0.001
$C_{n_{\delta_R}}$	-0.014	-0.009

Table 2.3: Comparison of CFD results and code results for stability derivatives

Stability Derivatives	Results from CFD	Results from Generated Code
$C_{D_{\alpha}}$	0.16	0.17
$C_{L_{\alpha}}$	5.40	5.36
$C_{m_{\alpha}}$	-0.26	-0.29
C_{L_q}	4.07	4.19
C_{m_q}	-8.50	-8.97
$C_{L_{\dot{\alpha}}}$	0.48	0.51
$C_{m_{\dot{\alpha}}}$	-1.70	-1.88
$C_{y_{\beta}}$	-0.25	-0.24
$C_{l_{\beta}}$	-0.0041	-0.0041
$C_{n_{\beta}}$	0.0190	0.0290
C_{y_p}	-0.0012	-0.0014
C_{l_p}	-0.60	-0.47
C_{n_p}	-0.046	-0.074
C_{y_r}	0.048	0.066
C_{n_r}	-0.02	-0.01
C_{l_r}	0.108	0.166

2.6 SYSTEM MATRIX CONSTITUTION

In the created design tool, last step is formed as system matrix constitution. In this manner, "A" matrix is obtained by using the equations in the book, [8]. As it can be seen from the reference book, some assumptions are done to simplify the calculations. Initially, the derivatives are calculated in dimensionless form.

The force in X direction derivative with respect to the velocity is obtained from Eqn. 2.186. This is a simplified equation by assuming that θ is a small angle. This assumption is meaningful for level flight.

$$X_u = -2c_D - V_0 \frac{\partial c_D}{\partial V} + \frac{1}{0.5\rho V_0 S} \frac{\partial \tau}{\partial V} \quad (2.186)$$

Normal force due to axial velocity is computed from the below equation (2.187).

$$Z_u = -2c_L - V_0 \frac{\partial c_L}{\partial V} \quad (2.187)$$

Axial force due to normal velocity is obtained from 2.188.

$$X_w = c_L - \frac{\partial c_D}{\partial \alpha} \quad (2.188)$$

Last force derivative due to velocity perturbations of longitudinal forces is normal force due to normal velocity, (2.189).

$$Z_w = -\left(\frac{\partial c_L}{\partial \alpha} + c_D\right) \quad (2.189)$$

Moment derivatives due to velocity perturbations are computed by the given order; pitching moment due to axial velocity and due to normal velocity (Eqn. 2.190 and Eqn. 2.191).

$$M_u = V_0 \frac{\partial c_m}{\partial V} \quad (2.190)$$

$$M_w = \frac{\partial c_m}{\partial \alpha} \quad (2.191)$$

Another set of derivative calculations are done for due to pitch velocity perturbations. They are obtained in given order Eqn. 2.192, Eqn. 2.193 and Eqn. 2.194. These equations are applied by the assumption that the pitch rate perturbations are dominated by tailplane.

$$X_q = -V r_{ht} \frac{\partial c_{D_{ht}}}{\partial \alpha} \quad (2.192)$$

$$Z_q = -Vr_{ht}c_{l_\alpha} \quad (2.193)$$

$$M_q = \frac{l_{ht}}{c_{ht}} Z_q \quad (2.194)$$

The derivatives due to the acceleration perturbations are computed as the next step. Axial force, normal force and pitching moment due to rate of change of normal velocity parameters are computed according to the following equations (Eqn. 2.195, Eqn. 2.196 and Eqn. 2.197).

$$X_{\dot{w}} = X_q \frac{d\varepsilon}{d\alpha} \quad (2.195)$$

$$Z_{\dot{w}} = Z_q \frac{d\varepsilon}{d\alpha} \quad (2.196)$$

$$M_{\dot{w}} = M_q \frac{d\varepsilon}{d\alpha} \quad (2.197)$$

All of the above equations belong to the longitudinal directional derivatives. Following calculations are done for longitudinal-directional aerodynamic stability derivatives. They are more difficult to estimate when compared to the longitudinal ones. This is due to asymmetric flow conditions on mutual aerodynamic interference between the aircraft components. Initially, derivatives due to sideslip (side force, rolling moment, yawing moment due to sideslip) are computed in the given order, (from Eqn. 2.198 to Eqn. 2.204).

$$Y_v = \frac{S_{f_{side}}}{S} y_f - \frac{S_{vt}}{S} c_{l_{\alpha vt}} \quad (2.198)$$

$$L_v = L_{v_{dihedral}} + L_{v_{fin}} + L_{v_{sweep}} \quad (2.199)$$

$$L_{v_{dihedral}} = -\frac{1}{Sb/2} c_{l_\alpha} c_\Gamma \frac{(b/2)^2}{2} \quad (2.200)$$

$$L_{v_{sweep}} = -\frac{2c_L \tan(\Lambda_{c/4})}{Sb/2} (c_{rt} * \frac{(b/2)^2}{2} + (b/2)^{2/3} * (tpr - 1) * c_{rt}) \quad (2.201)$$

$$L_{v_{fin}} = -Vr_{vt} * \frac{b_{vt}}{l_{vt}} * c_{l_{\alpha t}} \quad (2.202)$$

$$N_v = N_{v_{fin}} \quad (2.203)$$

$$N_{v_{fin}} = Vr_{vt} * c_{l_{\alpha_t}} \quad (2.204)$$

Following calculations are done for the derivatives due to rate of roll. In this manner, side force due to rate of roll is determined by using given formulation Eqn. 2.205. Additionally, rolling moment and yawing moment coefficients due to rate of roll are computed in the previous sub section, which includes stability and control derivatives calculations.

$$Y_p = Y_{p_{fin}} = -\frac{1}{S * b} * c_{l_{\alpha_t}} * (c_{r_{vt}} * \frac{b_{vt}^2}{2} + \frac{b_{vt}^2}{1.5} * (\lambda - 1) * c_{r_{vt}}) \quad (2.205)$$

Calculation of derivatives due to rate of yaw is another part of this sub section. Therefore, by applying the following equations, calculations related to the side force (Eqn. 2.206), rolling moment (Eqn. 2.207) and yawing moment (Eqn. 2.209) due to yaw rate are done. When rolling moment is calculated, wing and fin components are calculated separately. Wing yawing moment derivative coefficient has already been computed in the previous sub section. Same situation is also valid for the yawing moment derivative coefficient.

$$Y_r = Vr_{vt} * c_{l_{\alpha_t}} \quad (2.206)$$

$$L_r = L_{r_{wing}} + L_{r_{fin}} \quad (2.207)$$

$$L_{r_{fin}} = -L_{v_{fin}} \frac{l_{vt}}{b} \quad (2.208)$$

$$N_r = N_{r_{wing}} + N_{r_{fin}} \quad (2.209)$$

$$N_{r_{fin}} = -N_{v_{fin}} \frac{l_{vt}}{b} \quad (2.210)$$

As mentioned before, all derivatives are calculated in dimensionless form. After that, by using them, concise longitudinal and lateral derivatives are determined in the code. In this step, the equations in the following tables are used for longitudinal and lateral derivatives.(Table 2.4 and Table 2.5).

<i>Concise derivative</i>	<i>Equivalent expressions in terms of dimensionless derivatives</i>
x_u	$\frac{X_u}{m'} + \frac{\frac{\bar{c}}{V_0} X_{\dot{w}} Z_u}{m' \left(m' - \frac{\bar{c}}{V_0} Z_{\dot{w}} \right)}$
z_u	$\frac{Z_u}{m' - \frac{\bar{c}}{V_0} Z_{\dot{w}}}$
m_u	$\frac{M_u}{I'_y} + \frac{\frac{\bar{c}}{V_0} M_{\dot{w}} Z_u}{I'_y \left(m' - \frac{\bar{c}}{V_0} Z_{\dot{w}} \right)}$
x_w	$\frac{X_w}{m'} + \frac{\frac{\bar{c}}{V_0} X_{\dot{w}} Z_w}{m' \left(m' - \frac{\bar{c}}{V_0} Z_{\dot{w}} \right)}$
z_w	$\frac{Z_w}{m' - \frac{\bar{c}}{V_0} Z_{\dot{w}}}$
m_w	$\frac{M_w}{I'_y} + \frac{\frac{\bar{c}}{V_0} M_{\dot{w}} Z_w}{I'_y \left(m' - \frac{\bar{c}}{V_0} Z_{\dot{w}} \right)}$
x_q	$\frac{\bar{c} X_q - m' W_e}{m'} + \frac{(\bar{c} Z_q + m' U_e) \frac{\bar{c}}{V_0} X_{\dot{w}}}{m' \left(m' - \frac{\bar{c}}{V_0} Z_{\dot{w}} \right)}$
z_q	$\frac{\bar{c} Z_q + m' U_e}{m' - \frac{\bar{c}}{V_0} Z_{\dot{w}}}$
m_q	$\frac{\bar{c} M_q}{I'_y} + \frac{(\bar{c} Z_q + m' U_e) \frac{\bar{c}}{V_0} M_{\dot{w}}}{I'_y \left(m' - \frac{\bar{c}}{V_0} Z_{\dot{w}} \right)}$
x_θ	$-g \cos \theta_e - \frac{\frac{\bar{c}}{V_0} X_{\dot{w}} g \sin \theta_e}{m' - \frac{\bar{c}}{V_0} Z_{\dot{w}}}$
z_θ	$-\frac{m' g \sin \theta_e}{m' - \frac{\bar{c}}{V_0} Z_{\dot{w}}}$
m_θ	$-\frac{\frac{\bar{c}}{V_0} M_{\dot{w}} m' g \sin \theta_e}{I'_y \left(m' - \frac{\bar{c}}{V_0} Z_{\dot{w}} \right)}$

Table 2.4: Concise longitudinal aerodynamic stability derivatives [8]

<i>Concise derivative</i>	<i>Equivalent expressions in terms of dimensionless derivatives</i>
y_v	$\frac{Y_v}{m'}$
y_p	$\frac{(bY_p + m'W_e)}{m'}$
y_r	$\frac{(bY_r - m'U_e)}{m'}$
y_ϕ	$g \cos \theta_e$
y_ψ	$g \sin \theta_e$
l_v	$\frac{(I'_z L_v + I'_{xz} N_v)}{(I'_x I'_z - I'^2_{xz})}$
l_p	$\frac{(I'_z L_p + I'_{xz} N_p)}{(I'_x I'_z - I'^2_{xz})}$
l_r	$\frac{(I'_z L_r + I'_{xz} N_r)}{(I'_x I'_z - I'^2_{xz})}$
l_ϕ	0
l_ψ	0
n_v	$\frac{(I'_x N_v + I'_{xz} L_v)}{(I'_x I'_z - I'^2_{xz})}$
n_p	$\frac{(I'_x N_p + I'_{xz} L_p)}{(I'_x I'_z - I'^2_{xz})}$
n_r	$\frac{(I'_x N_r + I'_{xz} L_r)}{(I'_x I'_z - I'^2_{xz})}$
n_ϕ	0
n_ψ	0

Table 2.5: Concise lateral aerodynamic stability derivatives [8]

In conclusion, longitudinal and lateral system matrices are obtained. By using these matrices, the stability characteristics related to each mode (short period mode, phugoid mode, roll subsidence mode, dutch roll mode and spiralling) can be analysed.

$$A_{longitudinal} = \begin{bmatrix} X_u & X_w & X_q & X_\theta \\ Z_u & Z_w & Z_q & Z_\theta \\ M_u & M_w & M_q & M_\theta \\ 0 & 0 & 1 & 0 \end{bmatrix}$$

$$A_{lateral} = \begin{bmatrix} Y_v & Y_p & Y_r & Y_\phi & Y_\psi \\ L_v & L_p & L_r & L_\phi & L_\psi \\ N_v & N_p & N_r & N_\phi & N_\psi \\ 0 & 1 & 0 & 0 & 0 \\ 0 & 0 & 1 & 0 & 0 \end{bmatrix}$$

CHAPTER 3

SELECTION OF OPTIMUM PARAMETER VALUES

In this thesis a conceptual design tool is created. The user of this tool must enter several input parameter values when the code starts to run. There are several critical input changing according to the mission of the designed UAV. In this input step, it is thought that this tool should be a guide for the user. Therefore, a selection of decided input parameters is added to the code so that these critical parameters can be optimum among their determined limits and can give maximum and minimum values of the UAV's desired properties. Thus, the user can be guided to have a more efficient conceptual designs. This kind of optimization part of the code is explained in the following sections. However, it should not be forgotten that this optimization is not a common optimization process. This is only a selection process so that the code can be more user-friendly.

For this design tool it is tried to equate the lift and weight forces which is the principal concept for the design. The selection of the optimum values depends on the establishment of the equality of the lift and weight forces to each other. Among these values, the selection of optimum ones are executed.

The word meaning of optimization [22] is finding an alternative with the most cost effective achievable performance under given constraints, by maximizing desired factors and minimizing undesired ones. Actually, optimization is a maximizing and minimizing process. However, in comparison, maximization means trying to attain the highest result or outcome without regarding the cost or expense. Therefore, it is very important to choose the correct parameters to be the highest or lowest so that a real optimization process can be constituted. In this manner, several determined variables affect the objective function in different ways. These variables do not have to be max-

imum or minimum to get the desired value of target function. On the contrary, they can be arbitrary values. Optimization supports to find these arbitrary variables to get ideal target value of objective function that makes a situation, in our case the flight, more efficient.

Aircraft design is a multi-disciplinary process. Therefore, selection of multiple parameters as optimum is applied. In addition to that, more than one objective parameters are chosen according to the mission and type of the aircraft. The type of aircraft, which assigns performance, aerodynamic, structural or control property is vital. Regarding these in the course of design, high performance and efficient flights can be done in the determined limits by an easy way for the user. As a result, the students, companies or people who are into UAV design will be able to get ahead of their competitors.

3.1 Optimization Elements

3.1.1 Objectives

Objectives are the parameters that should be maximized or minimized. When more than one parameter are selected for maximization and minimization, these properties of the aircraft can be optimized according to the objective of the design. For the optimization part of the code, an "optimization function" should be obtained. In this manner, the parameters which will be maximized are written to the denominator, the parameters which will be minimized are written to the numerator of the optimization function. After that, this function is maximized by the code according to the floating variables and limitations. By this way, maximization and minimization of several parameters can be done simultaneously.

3.1.2 Constraints

Constraints are the limits for the variables that are included in the optimization process. When the constraints are determined, optimized solutions are found such that the determined variables remain in their limitations. The code writes these results

into an array. In this manner, the results are selected according to the constraints by a condition loop. Therefore, the conditions which do not satisfy the constraints are not included in the maximization process.

3.1.3 Moving Variables

In the optimization process, selected variables are changed by determined increments in determined intervals. These variations cause the objective function to have different results. The combination of values which make the objective function maximum is constituted among these moving variables. In this manner, it is important to determine the intervals of each moving variable properly. If these intervals are selected properly, the optimization process can be faster. Among the input parameters, user enters initial and end points of the moving variables to determine these intervals. According to the desired precision, increments of moving variables are also entered to the code by user. While choosing these increment values for each parameter, user should compromise between the precision and calculation speed of the results. In addition to the interval and increment selection, it is important to decide which input parameters will be moving variables. In this manner, all the parameters that changes objective function's numerator or denominator can be selected. However, this situation causes the code to run for longer. Therefore, some of the selected moving variables are taken out of the optimization process. The variables which cause peaks and reverse peaks in the graphs of variation with objective function are preferred.

3.2 Optimization Part of Code Creation

In the code, first step is to determine the properties that will be maximized or minimized. After all of them are determined, the parameters which will be maximized are defined in the parameter "MaxOBJ" by multiplying with each other. On the other hand, the parameters which will be minimized are written into the parameter "MinOBJ" again by multiplying with each other (Eqn. 3.1).

$$OptimizationFunction = \frac{MaxOBJ}{MinOBJ} \quad (3.1)$$

Second step is to decide which parameter or parameters will be the moving variables. In this manner, the designer can select maximum 5 variables. After this, for each variable, initial value, last value and increment values are entered to the code as "mov#_start", "mov#_end" and "mov#_inc". In addition to that, constraints are determined and written into the "CONS#" parameters in the code. Their limits are entered to the code as "Cons#_lim" according to the upper or lower bound that is used.

Each moving variable step means one loop and the optimization part of the code is constituted of several loops. The results of the objective function for each loop or each combination of parameters are collected in a matrix. At the end, maximum element of the matrix is taken. The moving variable values which give this maximum result are the values of the optimized version of designed UAV. The code part related to these procedures can be seen in the following MATLAB script.

```

1  if L > (W) && L < (W+1) && CONS1 < Cons1_lim
&& CONS2 > Cons2_lim && CONS3 < Cons3_lim &&
CONS4 > Cons4_lim
2      j5 = j5+1
3  OPTIM1(j5,:) = [MaxOBJ/MinOBJ]
4  OPTIM(j5,:) = [mov1 mov2 mov3 mov4 mov5]
5  end
6
7  mov1 = mov1 + mov1_inc;
8  end
9  mov2 = mov2 + mov2_inc;
10 end
11 mov3 = mov3 + mov3_inc;
12 end
13 mov4 = mov4 + mov4_inc;
14 end
15 mov5 = mov5 + mov5_inc;
16 end
17

```

```
18 [DESIRED, I] = max(OPTIM1(:));
19
20 mov1_optim = OPTIM(I, 1);
21 mov2_optim = OPTIM(I, 2);
22 mov3_optim = OPTIM(I, 3);
23 mov4_optim = OPTIM(I, 4);
24 mov5_optim = OPTIM(I, 5);
```


CHAPTER 4

MINI UAV DESIGN USING THE DESIGN TOOL

In this section of the thesis, an example of the design is presented by demonstrating the applicability of the present design code to the conceptual design of a mini UAV system. In this way, the use of the design tool and its advantages can be observed and tested. The UAV general specifications are listed below and they will be explained during this chapter in detail.

- The UAV can practice autonomous flights with a camera as payload,
- Span is less than 2 m and it is in mini UAV class,
- Its propulsion system includes electric motor and propeller,
- The designed UAV system can be carried by one person in its bag,
- It has a parachute for landing, take-off is done by hand-launch.

4.1 MISSION PLAN and USAGE CONCEPT

The designed UAV will be used for reconnaissance purposes in both civil and military area. Therefore, it carries a camera as payload. Due to its low weight, it can be used by anyone and in any place by carrying it in a back-pack. Its dimensions are suitable to conduct its mission in smaller and narrower places than huge empty terrains. For example, this designed UAV can be used for real time video shoot in crowded places of like festivals, concerts and sports games. It can be very useful especially for observing over crowded areas among streets. In addition to this, the UAV can be

useful in these activities for the purpose of security. In military applications, search and rescue missions along critical and rough terrains can be executed regardless of the obstacles. Military convoys can be followed and the security of the road can be checked beforehand.

The mission planning of the designed UAV is started by hand launching the UAV. After the climb segment comes the cruise part of the flight. Until the UAV reaches to the target area where the mission is conducted, cruise flight continues. After that time, loiter segment starts. According to the endurance value, the loitering over the desired area is maintained and later the UAV cruises back to home. At home, it releases the parachute and lands. This mission plan is summarized in the Figure 4.1.

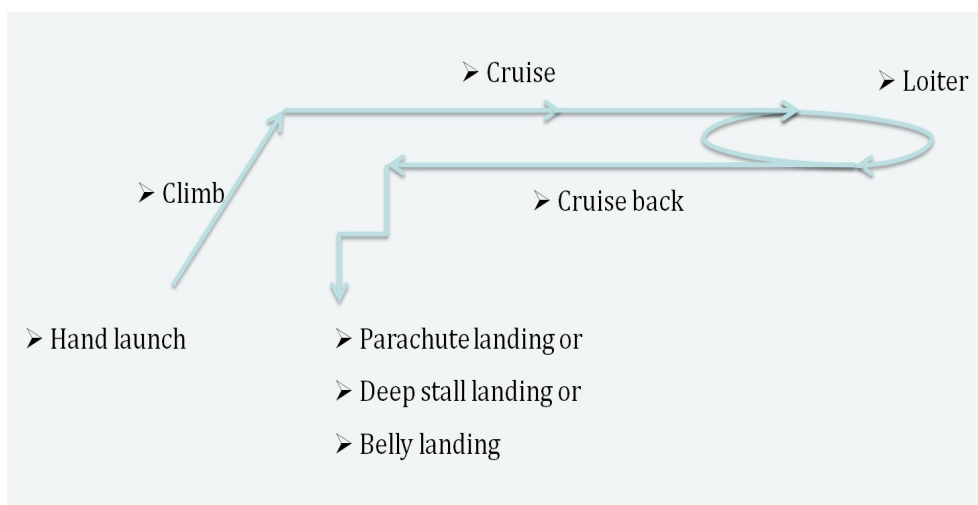


Figure 4.1: Mission plan of the designed UAV

In addition to the above considerations, some of the technical specifications of the designed UAV are mentioned in the design tool case study (Chapter 1). During this case study the applicability of the present design tool will be demonstrated and its limitations will be considered.

4.2 CONFIGURATION SELECTION

Configuration selection is done as simple as possible so that the UAV has to compete with minimum problems and the user can easily assemble-disassemble the UAV or repair it in a very quick way. In addition, by a conventional design, manufac-

turing can be less challenging, as well. Regarding these situations, initially wing is determined as high wing so that the aircraft can be more stable. In addition to that, conventional tail configuration is chosen. Since the UAV is a mini type, the engine is selected as electric motor with propeller. When the propeller is located in front of the fuselage, induced drag can be reduced since undisturbed air flow is effective on the wing. Therefore, tractor configuration is applied in the UAV.

Hand launch and parachute landing is thought to be most proper ways of landing and launch. This is because that the aircraft is in the class of the mini UAV and it is used in rough or narrow flight areas. Therefore, it is beneficial not to require long and straight runway.

4.3 AIRFOIL SELECTION

The first design phase is the airfoil selection. The design is done for the low Reynolds Number. Therefore, to choose a proper airfoil is very important. It is known that flying in subcritical Reynolds Numbers are very worthy of notice. When the aircraft passes from subcritical Reynolds Number to supercritical Reynolds Number, an important change is occurred in the aerodynamic properties. For example, according to [5], lift to drag ratio increases 50%. In addition to that information, paper says that for low speed flights, airfoil should have high camber and small thickness to increase lift to drag ratio as much as possible. Regarding of the gained information, some airfoils are compared. During the investigation, airfoil L/D losses found from computational experiment results are considered. Moreover, from lift versus angle of attack graphs, stall angles and maximum lift coefficients are studied.

Some low speed airfoils are chosen and following comparison is done [23]. As you can see from the Figure 4.2, in terms of lift to drag ratio, maximum lift coefficient value and maximum lift to drag ratio at given angle of attacks, Eppler 61 airfoil is the most proper one for the design. However, when the paper [5] is applied, amount of lift to drag ratio loss when the Reynolds Number transferring from subcritical to supercritical is very high. Therefore, it is thought that one of the secondary possible airfoils, GOE 495 and FX 60100, should be chosen. They have very similar properties but FX 60100 has more advantages since its loss of L/D is very low. Therefore,

FX 60100 is chosen as the wing airfoil.

Plot	Airfoil	Reynolds #	Ncrit	Max Cl/Cd	Description
<input checked="" type="checkbox"/>	e61-il	100,000	9	75.6 at $\alpha=6.25^\circ$	Mach=0 Ncrit=9
<input checked="" type="checkbox"/>	e193-il	100,000	9	58.7 at $\alpha=8^\circ$	Mach=0 Ncrit=9
<input checked="" type="checkbox"/>	fx60100sm-il	100,000	9	62.8 at $\alpha=5.5^\circ$	Mach=0 Ncrit=9
<input checked="" type="checkbox"/>	goe495-il	100,000	9	69.2 at $\alpha=5.75^\circ$	Mach=0 Ncrit=9
<input checked="" type="checkbox"/>	naca2412-il	100,000	9	50 at $\alpha=6.75^\circ$	Mach=0 Ncrit=9
<input checked="" type="checkbox"/>	goe532-il	100,000	9	53.3 at $\alpha=7.5^\circ$	Mach=0 Ncrit=9

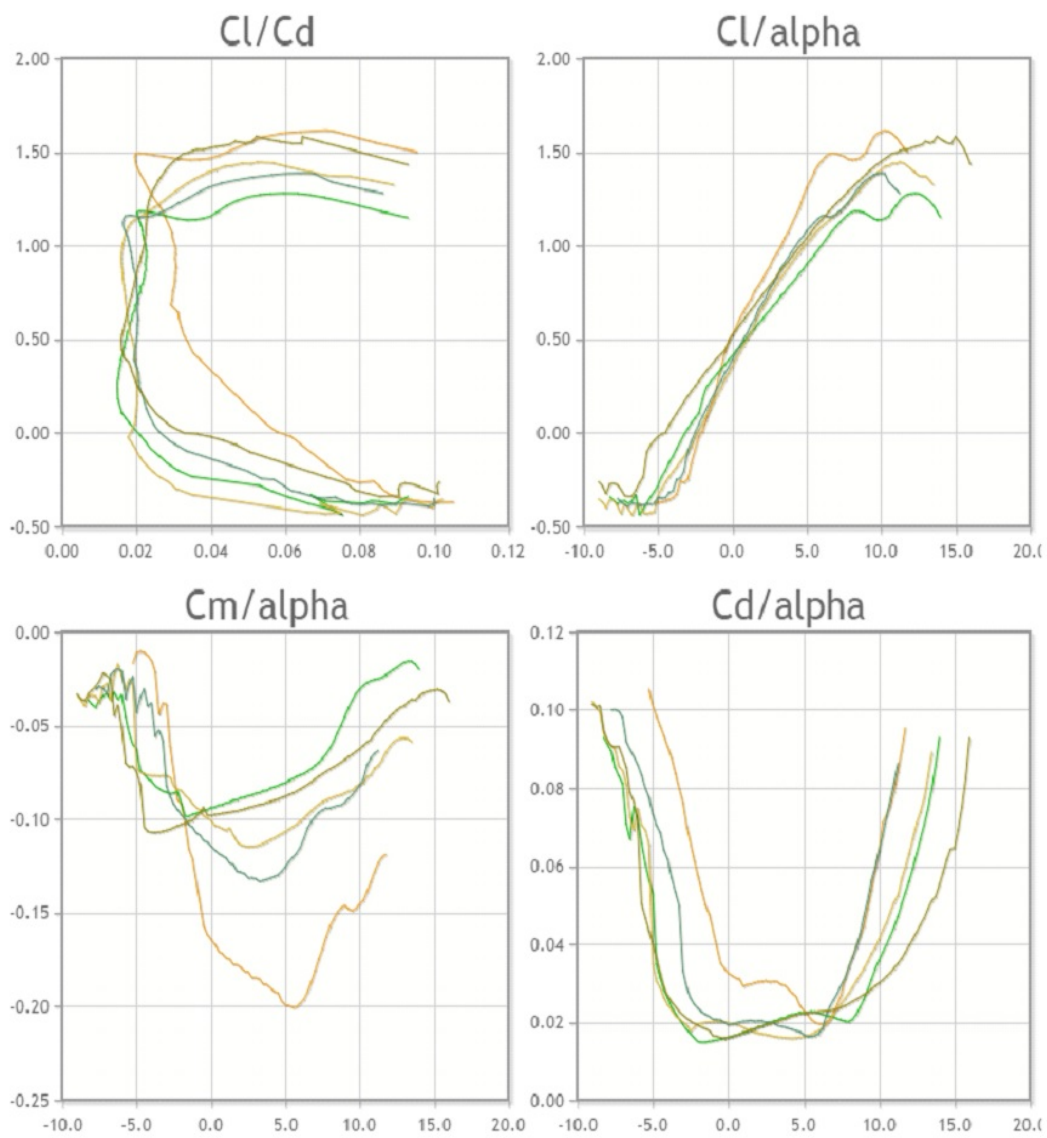


Figure 4.2: Comparison of possible wing airfoils [23]

The other airfoil selection is done for the vertical and horizontal tail. They are chosen as NACA0009 for its simplicity and for not applying negative lift at zero angle of attack.

4.4 PROPULSION SYSTEM SELECTION

In this part of the design, MotoCalc program is used. This program has huge databases for each propulsion system component especially for electrical motors, batteries. This property is very useful to see and compare several configurations. In addition to that, the program gives the user approximate mission time, thrust and the total weight of the chosen propulsive elements. When a probable set of motor, battery, ESC, gear ratio and propeller is chosen, it arrays the mission time and thrust values according to the cruise velocity. This arranged table is made colorful so that propeller stall, the supporting enough lift at cruise level flight situations can be seen clearly. On the other hand, thrust level can be set to different percentages. Beyond of whole these, MotoCalc gives reliable and accurate information and it supplies quick solutions. Therefore, for the conceptual design, it is a proper program. In the subsection of the thesis, the propulsion system, which provides the desired requirements is chosen by using mentioned properties of MotoCalc.

As the initial step, the electric motor is determined as NeuMotor due to its high efficiency and low weight for small-sized aircrafts. However, which type of this motor is proper for the purpose of the thesis is found by running the program for each one separately. In addition to that, Thunder Power batteries are commonly used and pleased with products. Therefore, the battery is chosen as Thunder Power in the interval of 3900 mAh and 4500 mAh, so that mission time can be around sixty seconds. In addition to that, ESC is chosen as 40 A. CAMCarbon propeller is determined. Diameter and pitch limits are entered from 6 to 12. Lastly, gear ratio is changed from 1:1 to 3:1. When the program is run with these values, several results are obtained. Among them, the data which has desired thrust and mission time values is selected. In this manner, mission time is desired to be one hour as mentioned before. On the other hand, thrust determination is done from weight. The total weight of the aircraft is assumed to be around 1.4 kg from literature survey. Therefore, thrust which is

approximately half of the weight is thought to be sufficient. The obtained probable elements that are screened a few times are listed in the below Table 4.1. Static thrust for all configurations is approximately 700 grams.

From the table (4.1), the propulsion system elements which have low weight, high thrust and long flight time properties are selected. The designated system elements can be listed as the below.

- NEU1105/1.5Y Electric Motor (66 grams) with 2:1 gear box (total 85 grams),
- Thunder Power 3900 mAh 1S3P Li-Po Battery (349 grams),
- Castle Creations 40 Amper ESC (54 grams) and
- 9x6 CAMCarbon Propeller (16 grams).

Table 4.1: MotoCalc results for different configurations

MOTOR (NEU)	B. CELL	W (g)	GEAR RATIO	PROP.	SPEED (m/s)	ENDUR.	THRUST LEVEL
1105/1.5Y	1S4P	1172	1.5:1	6X4	13.5	52:13	0.91
1105/1.5Y	1S3P	1078	1.5:1	5.5X4	12.5	57:17	0.86
1105/1.5Y	1S3P	1078	2:1	9X6	15	59:16	0.66
1105/2Y	1S3P	1078	2:1	9X6	15	62:21	0.85
1105/2Y	1S5P	1266	2:1	10X6	16.5	74:15	0.96
1105/2.5Y	1S3P	1078	2:1	10.5X7	15	59:46	0.97
1105/2.5Y	1S5P	1266	2:1	11.5X7.5	16.5	66:54	-
1105/2.5Y	1S5P	1266	2:2	10X7	16.5	91:02	1
1105/3.5Y	1S3P	1078	dd	11x7	15	61:11	0.78
1105/3.5Y	1S4P	1172	dd	9x6	16	61:25	0.96
1105/3.5Y	1S5P	1266	dd	10X7	16.5	51:28	1
1107/2Y	1S4P	1194	dd	8x5	16	43:16	0.99
1107/2Y	2S2P	1194	3:1	9X6	16	75:44	-
1107/6D	2S2P	1194	dd	7X4	16	63:58	0.95
1107/6D	4CELL	1194	2:1	7X4	16	62:08	0.91

According to MotoCalc, this propulsion system configuration gives flight time of 59 minutes and around 700 grams static thrust. These values are valid for 15 m/s cruise speed, which is level flight speed for optimum lift coefficient. Propeller stall is not seen for this flight.

Lastly, the weight of the total propulsion system is 507 grams.

4.5 AVIONIC SYSTEM and PAYLOAD SELECTION

Since the UAV flies in autonomous mode, an autopilot (including GPS and IMU), data modem, modem antenna and GPS antenna for communication with the ground control station are necessary. In addition to them, AGL sensor, to know the altitude at low altitudes; pitot tube, to calculate the true air speed; compass (magnetometer), to get accurate heading value even when GPS is lost; and servo board to control the servos on the UAV by autopilot are also necessary. Other than pitot tube, all avionic system elements are chosen from products of MicroPilot. In this way, avionic system and sensors will be small-sized, low-weighted and reliable. Total weight of these specified elements is calculated as 222 grams

UAV has reconnaissance mission, as the payload gimbal camera is chosen. Gimbal is placed under the aircraft since there is no place in front of the aircraft due to the tractor configuration. Moreover, UAV lands with parachute on its belly. Regarding all these situations, gimbal must be retracted into the fuselage so that it is not damaged in the landing process. In this manner, BTC-40 Micro Pan gimbal is chosen because of its retracting mechanism, being small sized to fit into the fuselage and being only 80 grams.

The designated equipments are proper for the designed UAV requirements, such as 5 km range, full autonomous flight and live video transmission in terms of their technical specifications.

4.6 WEIGHT ESTIMATION

Weight is estimated from separate composite elements as mentioned in Chapter 1. Initially, weights of wing, horizontal tail, vertical tail and fuselage surface compos-

ites and internal supportive elements are computed. In this manner, wing surface is decided to include 1 each layer of $25\text{gr}/\text{m}^2$ and $49\text{gr}/\text{m}^2$ fiberglass fabric and 1 layer, which is placed from root to middle of the wing, of $80\text{gr}/\text{m}^2$. As the core material, 1 mm of rohacell is used. Support elements are chosen as 10 ribs from balsa composite and 2 carbon tube spars. Horizontal tail surface composite structure is determined as the same with the wing except existence of the carbonfiber fabric layer. It also includes 5 ribs and 2 carbon pipes. Vertical tail is decided as the same with the horizontal tail in terms of both surface and internal structure. When it comes to the fuselage, its surface is formed by 1 layer of $80\text{gr}/\text{m}^2$ carbonfiber and 2 each layers of $25\text{gr}/\text{m}^2$ and $49\text{gr}/\text{m}^2$ fiberglass fabrics. As the core material 2mm-by-rohacell is used. Lastly, 2 bulkheads made from balsa composite are added to inside of the fuselage. Aircraft components are consisted of resin 67% of fabric weights and glue 50% of internal structure weights. Whole these weights are arranged so that they are updated according to the dimensions of the aircraft components. In conclusion, total weight is computed by adding weights of avionic system elements, payload, parachute and propulsion system elements to these component weights.

4.7 OPTIMIZATION INPUT and RESULTS

4.7.1 Optimization Parameters Selection

Before the optimization part, several decision should be made. These can be categorized as objectives, constraints and moving variables as mentioned in Chapter 3. Initially, objective function is constituted by selecting maximized and minimized parameters. It is important to meet the requirements of the UAV and to have a design which is able to practice its mission by the best way. Therefore, objective parameters are selected according to the desired properties and their corresponding technical meanings. In this manner, to increase the general performance of the UAV, in other words to decrease the consuming energy during flight and make the UAV more efficient, lift to drag ratio can be maximized. Thus, to maximize lift to drag ratio provides higher range property to the UAV since it will fly in an efficient way. In the same way, loiter endurance can be increased by selecting the proper wing loading to get higher

L/D. In addition, it is important to climb with a higher slope from the mission point of view. This UAV is designed to reconnoitre in a certain limited areas. Therefore, it should be climb in as short as possible projection distances so that it can reached the desired altitude to start visualisation in a short way. This property can also be supported by decreasing drag and weight. Therefore, L/D maximization and W/S minimization can give higher climb angles. Secondly, this UAV mission necessitates to fly at lower velocities since it will monitorize such as crowded people in small areas, slow moving people or a standing target in a measurable place. It will be like a multicopters but have more mission time. Therefore, it is very important to minimise the stall velocity. This can be done by wing loading. When the stall velocity equation is applied, it can be seen that wing loading and stall velocity is directly proper to each other. Therefore, to minimise the W/S decreases the stall velocity. When all these explanations are considered, objective function is decided to be consisted of lift to drag ratio as numerator and wing loading as denominator (Eqn. 4.1).

$$OptimizationFunction = \frac{L/D}{W/S} \quad (4.1)$$

As the second step, constraints should be determined. Initially, equality of the lift and weight is a necessary condition for the cruise segment. Therefore, to supply this equality, the code includes this statement as constraint. In addition to that, designer can choose two upper limit values for the two parameters and two lower limits for the two another or the same parameters. For the design, one constraint is determined to show the running of the optimisation part code. As the known fact, the aircraft is stable if the alpha derivative of the pitching moment is less than zero. Therefore, the code tries to find the maximum of the optimization function among the configurations which give the negative pitching moment variation with angle of attack. The other constraints are entered as so that the condition is always valid.

```
1  if L > (W) && L < (W+1) && cm_alpha < 0
&& 5 > 2 && 2 < 3 && 4 > 3
```

Thirdly, the parameters which their values will be given as the results of a optimization part are determined. These moving variables are selected among the input. Actu-

ally, all of the input can be moving variables. However, this makes the code running time much longer and the designer can lose time recklessly. Therefore, some parameters are decided to be taken out of the optimization process. Binary combinations of the parameter graphs with respect to the objective function are drawn. According to the results, the parameters which cause peaks and dips in the graphs of variation are preferred. In this manner, following 3D plots are obtained by taking the other input as constant. These constants belong to the base design. The graphs that have peak points which are not on the interval limits are shown below. When these graphs are analysed, it can be seen that these parameters can be selected as moving variables. In this way, the code can give optimized results which are not on the limits. Moreover, run times for the code will be significantly shortened by determining the proper limits for the variables and avoid the searching limits on moving variables regardless of the nature of the variables. For this purpose the following carpet plots are produced to represent the variations of the variable pairs two by two as;

- angle of attack and wing span (Figure 4.3),
- angle of attack and fuselage diameter (Figure 4.4),
- aspect ratio and fuselage diameter (Figure 4.5),
- wing span and aspect ratio (Figure 4.6),
- wing span and fuselage diameter (Figure 4.7) variations

In addition to that, one extra moving variable is thought to be determined even if it is not an obligation. This property is selected according to its relation to the constraint variable. Therefore, horizontal tail volume ratio is added to the moving variable list since it affects the pitching moment derivative with respect to α .

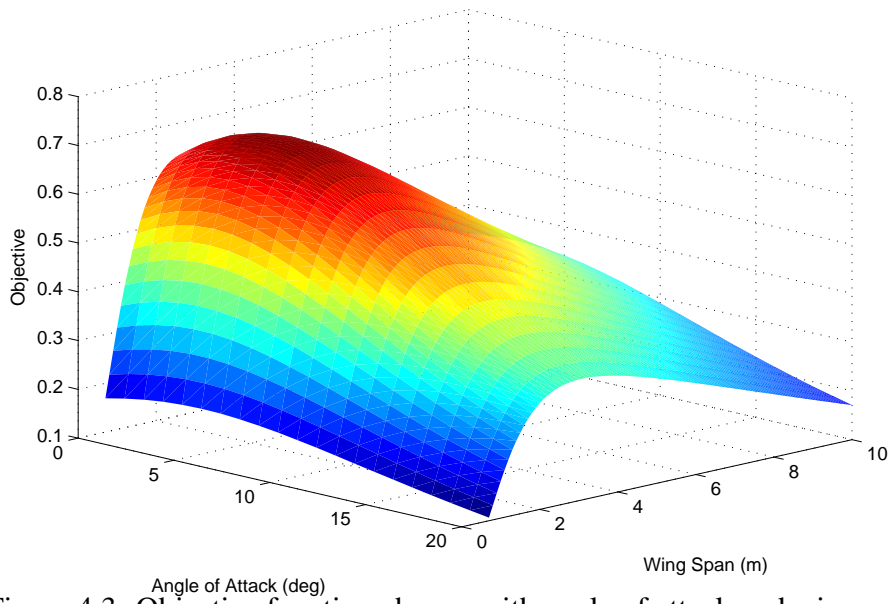


Figure 4.3: Objective function change with angle of attack and wing span

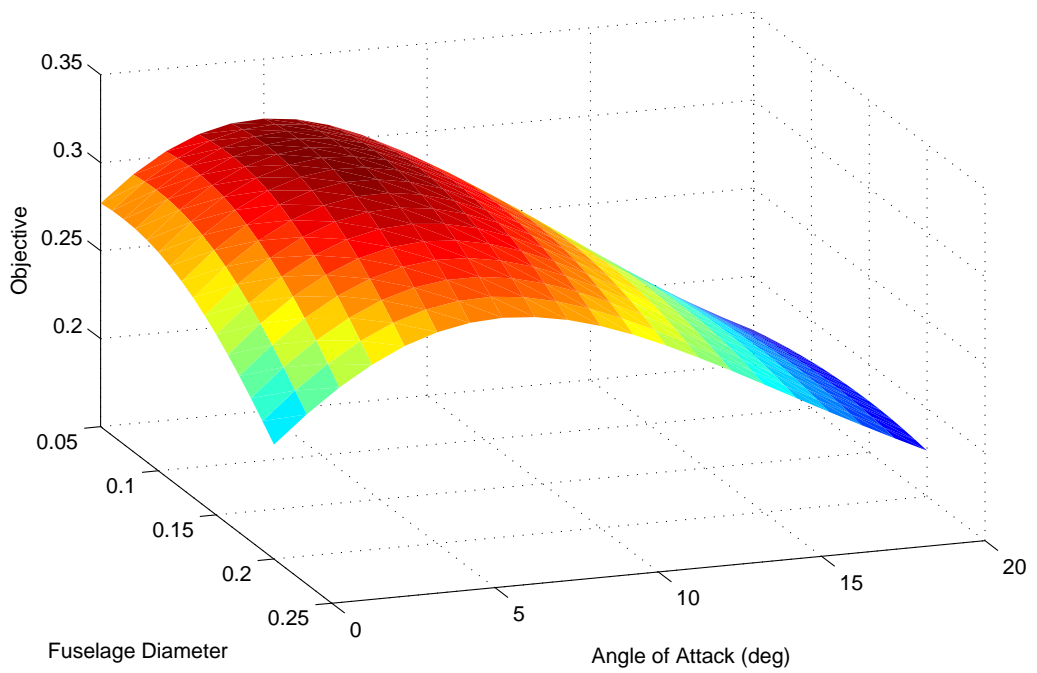


Figure 4.4: Objective function change with angle of attack and fuselage diameter

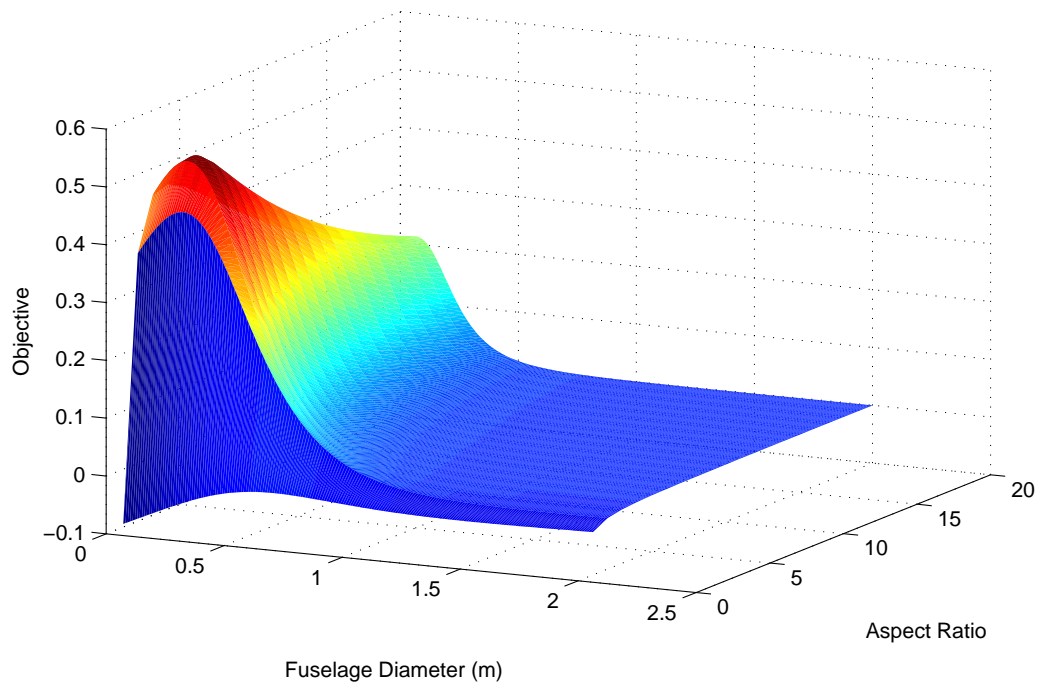


Figure 4.5: Objective function change with aspect ratio and fuselage diameter

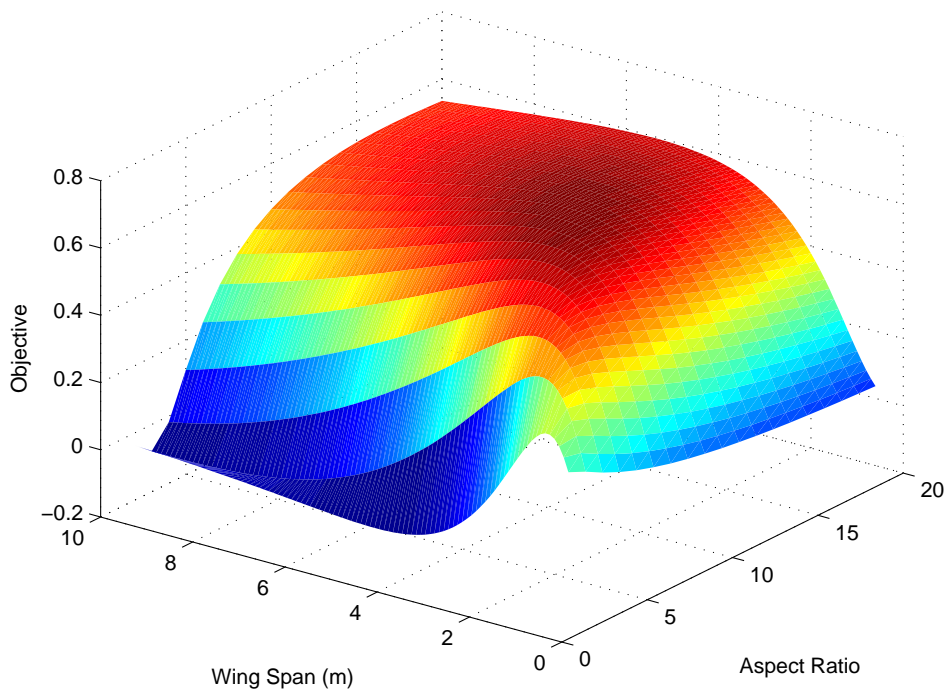


Figure 4.6: Objective function change with aspect ratio and wing span

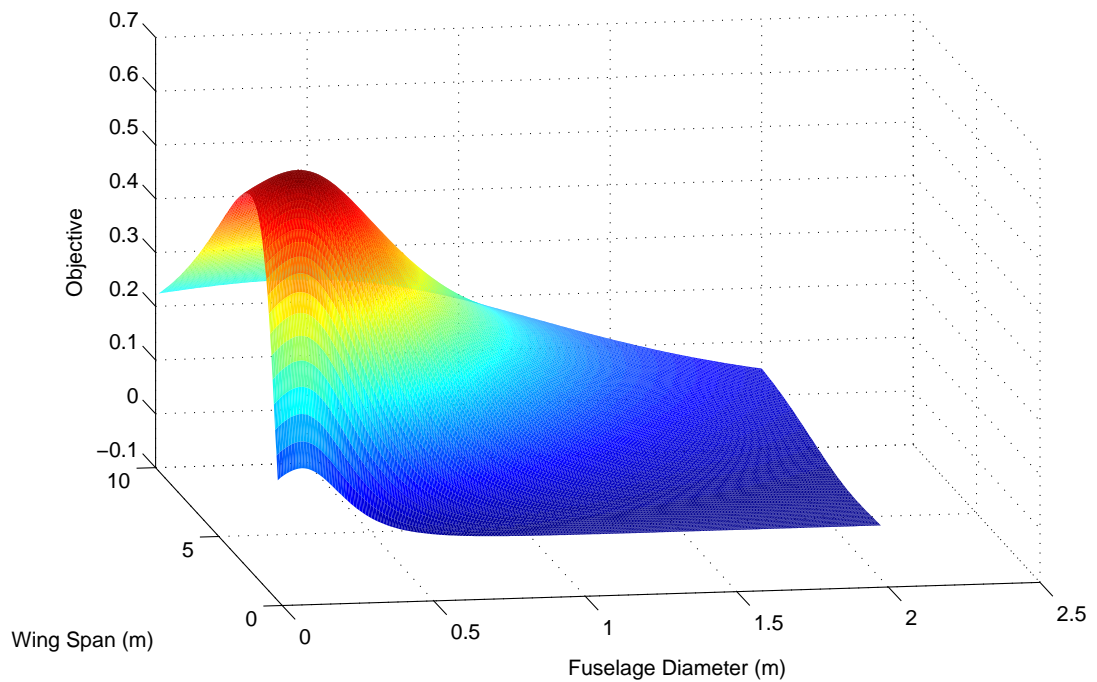


Figure 4.7: Objective function change with fuselage diameter and wing span

At the end of the selecting the moving variables, the upper and lower limits of these are determined according to the UAV class general specifications and general decided dimensions of the designed UAV. The values which are entered to the code are listed below.

- Angle of attack is limited between -5 degrees and 20 degrees increasing by 2 degrees,
- Horizontal tail volume ratio loop, which has increment value of 0.1, is from 0.1 to 0.6,
- Span is changed from 0.9 m to 1.4 m increasing by 0.1 m,
- Aspect ratio is selected among the numbers from 2 to 14,
- Fuselage diameter limits and increment are determined as 0.04 m, 0.12 m and 0.01 m.

At the end, all necessary input values are entered. Lastly, the code is run and the optimized parameters in terms of the objective function are computed.

- Wing span : 1.2 m
- Aspect ratio : 4
- Horizontal tail volume ratio : 0.3
- Angle of attack : -1 degrees
- Fuselage diameter : 0.08 m

4.8 DESIGN TOOL RESULTS

Entered input and calculated parameters form the aircraft in conceptual manner. The 3D views (Figure A.1 for isometric view, Figure A.2 for top view, Figure A.3 for side view, Figure A.4 for front view) and major dimensions (Figure A.5) of the UAV, which are prepared in CATIA program, can be seen in Appendix A. In addition to that, the equipments (Figure A.6), which are necessary for autonomous flight, practicing mission and landing, are placed (Figure A.7) in the fuselage by using CATIA. After that, the center of the gravity location is obtained (Figure A.8 and Figure A.9). In this manner, all component weights are implemented to the program and the center of gravity location is determined automatically. Centre of gravity location and again automatically calculated inertias by CATIA are entered to the code. Calculations are done according to these new values. After that, in the drawing, dimensions are updated according to the final results.

After the optimization is completed, code continues to compute all parameters related to the lift, drag, moment, weight, performance characteristic, stability and control derivatives and system matrix. Several parameter values of the designed mini UAV is concluded from the design tool. Initially, force and moment values are studied (Table 4.2). As it can be seen from the table, the difference between weight and lift forces is not grater than 1 N as desired. In addition to that, lift to drag ratio which is a vital parameter for an efficient aircraft is high enough compared with its competitors. This parameter affects several performance characteristics such as gliding performance.

Table 4.2: Force and moment values of the designed UAV

Forces-Moments			
c_L	0.675	L (N)	18.519
c_D	0.033	D (N)	0.910
c_M	-2.590	M (Nm)	-21.306
W/S (N/m ²)	49.100	L/D	20.361

Secondly, cruise, climb, maximum turn rate velocities are compared with the stall velocity since the aircraft is not to stall any segment of the flight mission. It is seen that, stall velocity is 8.9 m/s when cruise velocity is 12 m/s and maximum turn rate velocity is 13.6 m/s. After that, several performance properties (Table 4.3) are examined. In this manner, most important parameter for this UAV is mission time. At the end of the conceptual design, it can be seen that the mission time value satisfies the requirement which tells that the mission time will be 60 minutes. Moreover, it is 6 minutes more than the determined flight duration. Rate of climb and minimum turn radius values are within the acceptable interval. These parameter values supply the desired performance even if they can be developed.

Table 4.3: Some performance characteristic values

Performance Values	
MISSION TIME (min)	66.828
$\omega_{ins_{down}}$ (deg/s)	42.674
$\omega_{max_{ins}}$ (deg/s)	38.458
R_{min} (m)	8.231
RC_{max} (m/s)	4.072

Another investigation is done on the stability derivatives (Table 4.4). It is seen that the, whole stability derivatives are in the desired interval. One of the most important stability derivative is the pitching moment coefficient variation with angle of attack, which is the constraint parameter. For a stable aircraft, this derivative must be negative. This is satisfied in the designed UAV. As it can be seen from the Table 4.4, some parameters must be greater than zero and some of them must be less than zero (mentioned in Subsection 2.4 of Chapter 2). When these conditions are evaluated by

the data of the UAV, it can be seen that the UAV is stable.

Table 4.4: Stability derivatives of the designed UAV

Stability Derivatives					
$C_{D\alpha}$	0.598		$C_{m\dot{\alpha}}$	-1.131	
$C_{L\alpha}$	4.939		$C_{y\beta}$	-0.606	<0
$C_{m\alpha}$	-0.037	<0	$C_{l\beta}$	-0.141	<0
C_{D_u}	0.000		$C_{n\beta}$	0.084	
C_{L_u}	0.001		C_{y_p}	-0.042	
C_{m_u}	-0.009		C_{l_p}	-0.134	<0
C_{L_q}	3.981		C_{n_p}	-0.090	<0
C_{m_q}	-2.050	<0	C_{y_r}	0.178	>0
$C_{L\dot{\alpha}}$	1.768		C_{n_r}	-0.085	<0

After stability derivatives, control derivatives (Table 4.5) are also studied. There are some conditions for some of these derivatives mentioned in Subsection 2.4 of Chapter 2 as stability derivatives. As it can be seen from the Table 4.4, given conditions are satisfied by the designed UAV. In addition to them, how much flap, aileron and stabilizer incidence variations affect the aircraft's aerodynamical properties can be determined from the obtained data. The results are also beneficial for control loops design.

Table 4.5: Control derivatives of designed UAV

Control Derivatives		
$C_{L\delta_F}$	1.373	
$C_{L_{iht}}$	1.286	
$C_{m_{iht}}$	-1.385	
$C_{L\delta_E}$	0.383	
$C_{m\delta_E}$	-0.412	
$C_{l\delta_A}$	-0.151	<0
$C_{n\delta_A}$	0.027	>0
$C_{y\delta_R}$	0.153	>0
$C_{l\delta_R}$	0.009	>0
$C_{n\delta_R}$	-0.038	<0

UAV system matrices of two directions are occurred as below. By using these matri-

ces, a new controller can be designed. When the matrices are available, very important parameters for a control engineer such as characteristic equation, transfer function are very easy to found. Moreover, controllability and observability of the aircraft is checked. The designed UAV has full rank of controllable matrices of both longitudinal and lateral for whole input parameters. Therefore, the UAV is controllable. The same situation is valid for the observability of the UAV.

$$A_{longitudinal} = \begin{bmatrix} -0.0766 & 0.0100 & -2.0838 & -9.6610 \\ -0.1753 & -0.6407 & 11.7096 & -1.1290 \\ -1.3926 & 0.1369 & -42.1150 & 2.3371 \\ 0 & 0 & 1.0000 & 0 \end{bmatrix}$$

$$A_{lateral} = \begin{bmatrix} -0.0988 & 2.0699 & 11.8497 & 9.6610 & 1.7035 \\ -14.9933 & -12.0068 & -8.8926 & 0 & 0 \\ 9.9339 & -3.7084 & -0.8959 & 0 & 0 \\ 0 & 1.0000 & 0 & 0 & 0 \\ 0 & 0 & 1.0000 & 0 & 0 \end{bmatrix}$$

Last comments are related to the eigenvalues which are found from lateral and longitudinal A matrices. These values support a general information related to the aircraft's stability characteristics. In addition to that, they guide engineers how the aircraft can be controlled or what kind of controller should be designed and how the aircraft is made stable or which properties should be developed. When the obtained eigenvalues are investigated, it is seen that there are points which has real parts that are greater than zero. This means that there is an unstable situation in it. However, it can be fixed by a well-designed controller.

$$Eigenvalues_{longitudinal} = \begin{bmatrix} -42.2702 + 0.0000i \\ 0.5997 + 0.0000i \\ -0.5809 + 0.1285i \\ -0.5809 - 0.1285i \end{bmatrix}$$

$$Eigenvalues_{lateral} = \begin{bmatrix} 10.9121 + 0.0000i \\ -12.1498 + 3.8837i \\ -12.1498 - 3.8837i \\ 0.3860 + 0.0000i \\ 0.0000 + 0.0000i \end{bmatrix}$$

4.9 COMPARISON OPTIMIZED DESIGN with OTHER POSSIBLE DESIGNS

It is significant to observe that the conceptual design is really an successful design in given limitations. Therefore, chosen variables to be optimized are changed and results are compared with the data of the designed UAV. In this manner, span, angle of attack, aspect ratio, fuselage diameter and horizontal tail volume ratio are altered each by keeping the other ones constant.

Initially, when span is increased, it can be seen from the Table 4.6 and from the graph (Figure 4.8) that objective function which is constituted from the lift to drag ratio and wing loading increases. This increment continues to the span value of 2.7 m which is not included in the below table. As a peak value it is expected to select the 2.7 m of optimized span. However, due to the constraints, the span is selected by the code as 1.2 m which gives the highest objective function and supports constraints.

Table 4.6: Objective function and constraint parameters variation with span

Lift to Drag Ratio / Wing Loading	Lift - Weight (N)	$c_{m\alpha}$	Span (m)
0.159	-5.671	0.409	0.600
0.208	-4.754	0.231	0.700
0.256	-3.760	0.123	0.800
0.302	-2.696	0.055	0.900
0.344	-1.570	0.010	1.000
0.382	-0.388	-0.019	1.100
0.415	0.843	-0.037	1.200
0.443	2.114	-0.048	1.300
0.466	3.420	-0.054	1.400
0.486	4.753	-0.056	1.500

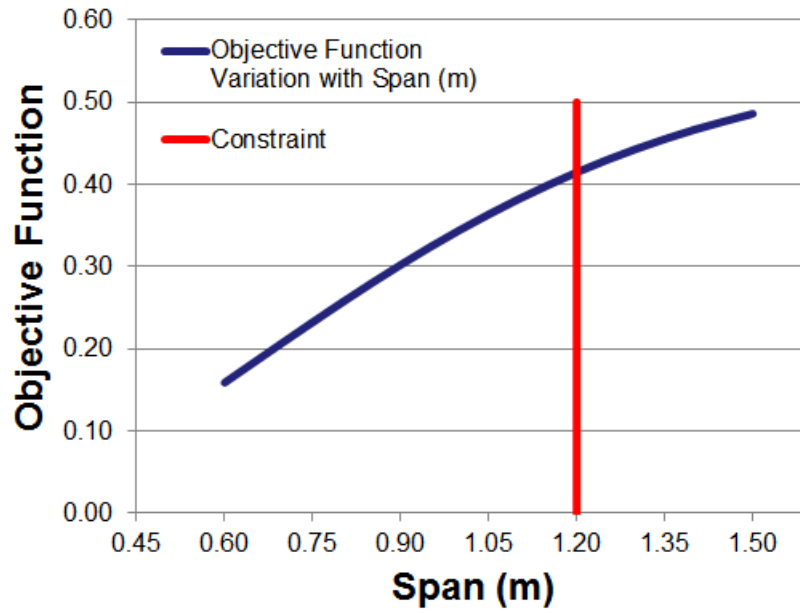


Figure 4.8: Graph of objective function variation with span and verification of constraints

Secondly, angle of attack change is studied. As it can be seen from the Table 4.7 and from the graph (Figure 4.9), 3 degrees of α gives the maximum objective function. However, due to the constraints, -1 degrees is selected as optimized value.

Table 4.7: Objective function and constraint parameters variation with angle of attack

Lift to Drag Ratio / Wing Loading	Lift - Weight (N)	$c_{m\alpha}$	Angle of Attack (deg)
0.228	-9.194	0.006	-5.000
0.344	-4.089	-0.016	-3.000
0.415	0.843	-0.037	-1.000
0.451	5.644	-0.057	1.000
0.466	10.576	-0.076	3.000
0.463	15.682	-0.093	5.000
0.444	20.959	-0.110	7.000
0.415	26.407	-0.125	9.000
0.381	32.021	-0.139	11.000
0.346	37.796	-0.151	13.000
0.312	43.728	-0.162	15.000
0.281	49.808	-0.171	17.000
0.253	56.028	-0.179	19.000

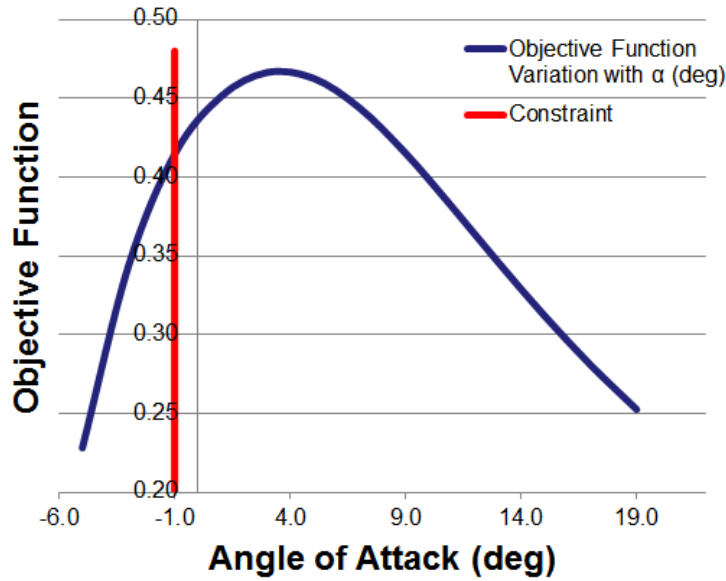


Figure 4.9: Graph of objective function variation with angle of attack and verification of constraints

Aspect ratio is another optimized parameter. When the Table 4.8 and the graph (Figure 4.10) is analysed, it is obvious that aspect ratio of 3 gives the highest ratio of lift to drag ratio and wing loading. However, to supply the constraint conditions aspect ratio of 4 is selected by the code.

Table 4.8: Objective function and constraint parameters variation with aspect ratio

Lift to Drag Ratio / Wing Loading	Lift - Weight (N)	$c_{m\alpha}$	Aspect Ratio
0.388	-1.283	0.309	2.000
0.422	1.144	0.037	3.000
0.415	0.843	-0.037	4.000
0.393	-0.055	-0.033	5.000
0.367	-1.019	0.013	6.000
0.340	-1.912	0.087	7.000
0.315	-2.703	0.180	8.000
0.292	-3.396	0.287	9.000
0.271	-4.000	0.405	10.000
0.251	-4.530	0.532	11.000
0.234	-4.996	0.666	12.000
0.218	-5.408	0.807	13.000
0.204	-5.775	0.953	14.000
0.191	-6.103	1.104	15.000

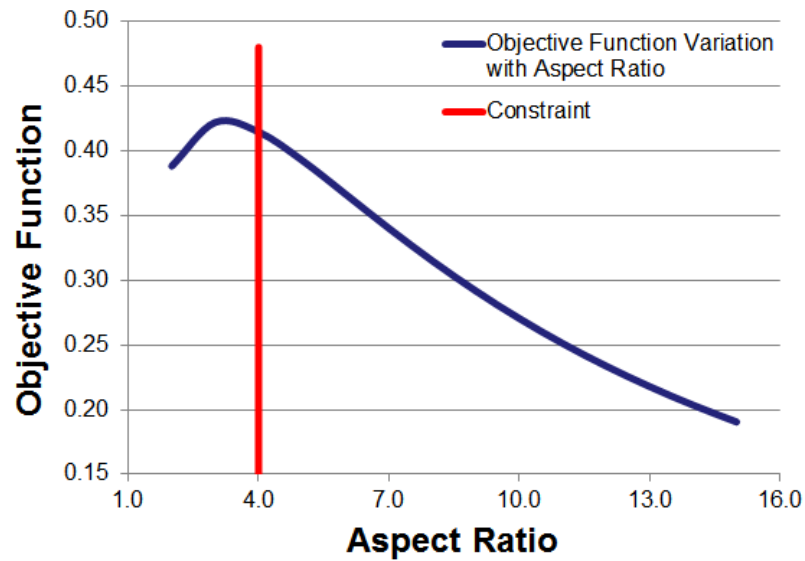


Figure 4.10: Graph of objective function variation with aspect ratio and verification of constraints

Fuselage diameter variation is examined. When the Table 4.9 and the graph (Figure 4.11) is looked, it is clear that maximum objective function can be supplied by the fuselage diameter of 0.12 m. Regarding the constraint parameters, 0.08 m is chosen as fuselage diameter since it gives the maximum objective function value which satisfies the constraints.

Table 4.9: Objective function and constraint parameters variation with fuselage diameter

Lift to Drag Ratio / Wing Loading	Lift - Weight (N)	c_{m_α}	Fuselage Diameter (m)
0.396	-0.107	-0.081	0.040
0.402	0.142	-0.072	0.050
0.407	0.384	-0.061	0.060
0.411	0.617	-0.050	0.070
0.415	0.843	-0.037	0.080
0.418	1.060	-0.023	0.090
0.420	1.269	-0.007	0.100
0.422	1.469	0.010	0.110
0.422	1.660	0.029	0.120
0.422	1.843	0.050	0.130
0.420	2.017	0.073	0.140

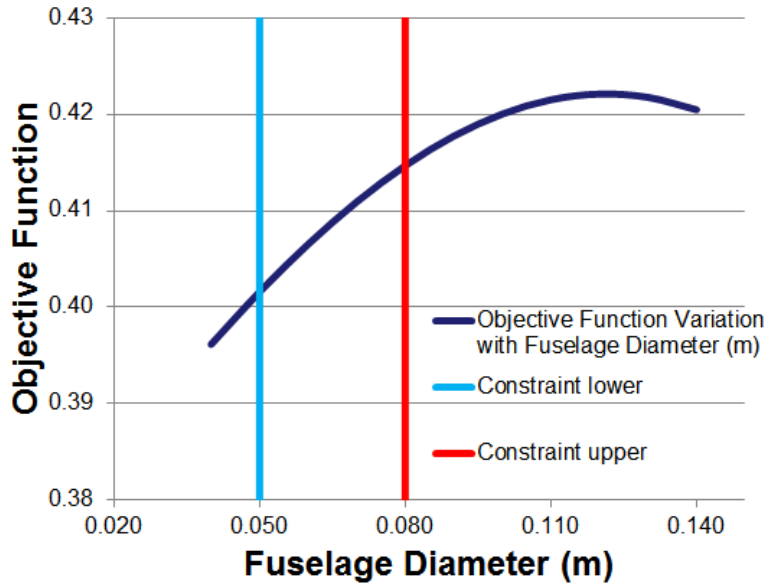


Figure 4.11: Graph of objective function variation with fuselage diameter and verification of constraints

Lastly, the variation of horizontal tail volume ratio is studied. As it can be seen from the Table 4.10 and from the graph (Figure 4.12), 0.3 is the value which meets all requirements.

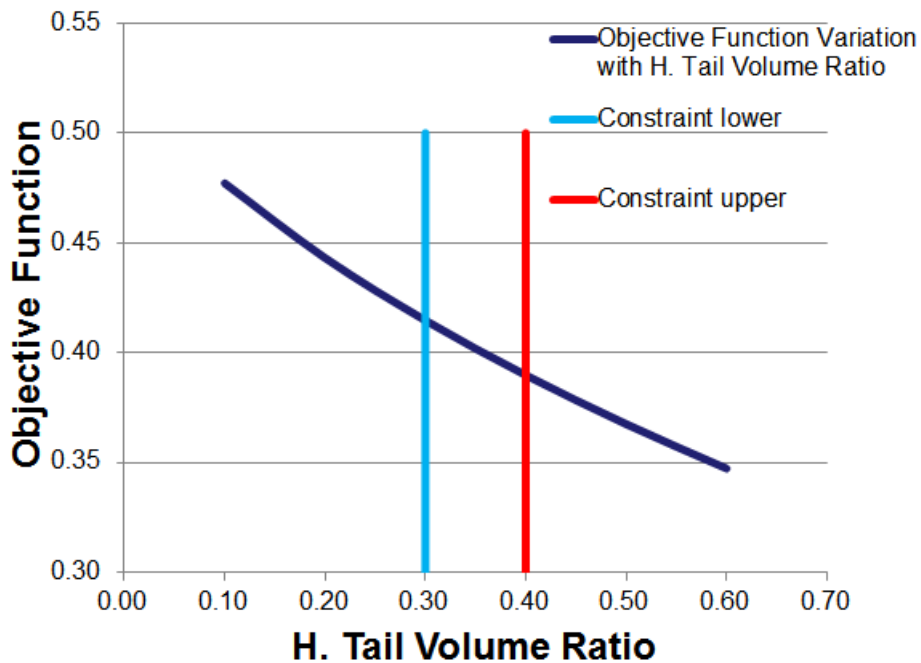


Figure 4.12: Graph of objective function variation with horizontal tail volume ratio and verification of constraints

Table 4.10: Objective function and constraint parameters variation with horizontal tail volume ratio

Lift to Drag Ratio / Wing Loading	Lift - Weight (N)	$c_{m\alpha}$	H. Tail Volume Ratio
0.477	2.045	0.267	0.100
0.443	1.406	0.115	0.200
0.415	0.843	-0.037	0.300
0.390	0.318	-0.189	0.400
0.367	-0.181	-0.340	0.500
0.347	-0.662	-0.492	0.600

When all these comparisons between different values of optimized parameters are taken in consideration, it can be seen that the optimization process of the code does its duty successfully. Therefore, the determined values of these five significant parameters for the optimized values of the designed UAV, will make the aircraft more efficient.

4.9.1 ADDITIONAL STUDY with SMALLER INCREMENT VALUES of MOVING VARIABLES

In addition to selecting the optimum values for determined input parameters, the accuracy of these values can be increased. In this manner, the code can be run again by choosing the moving variables' upper and lower limits closer to the calculated optimum values and by choosing sufficiently small increment values. At the end of all these computations, the following tables and graphs are obtained (from Table 4.11 to Table 4.15 and from Figure 4.13 to Figure 4.17). According to these tables and graphs, selected optimum values of moving variables can be modified as follows:

- Wing span : 1.21 m
- Aspect ratio : 3.8
- Horizontal tail volume ratio : 0.28
- Angle of attack : -1 degrees

- Fuselage diameter : 0.087 m

Table 4.11: Objective function and constraint parameters variation with span by smaller increment

Lift to Drag Ratio / Wing Loading	Lift - Weight (N)	$c_{m\alpha}$	Span (m)
0.392	-0.023	-0.025	1.130
0.396	0.099	-0.027	1.140
0.399	0.222	-0.029	1.150
0.402	0.345	-0.031	1.160
0.405	0.469	-0.032	1.170
0.408	0.593	-0.034	1.180
0.412	0.718	-0.035	1.190
0.415	0.843	-0.037	1.200
0.418	0.968	-0.038	1.210
0.421	1.094	-0.040	1.220
0.424	1.220	-0.041	1.230

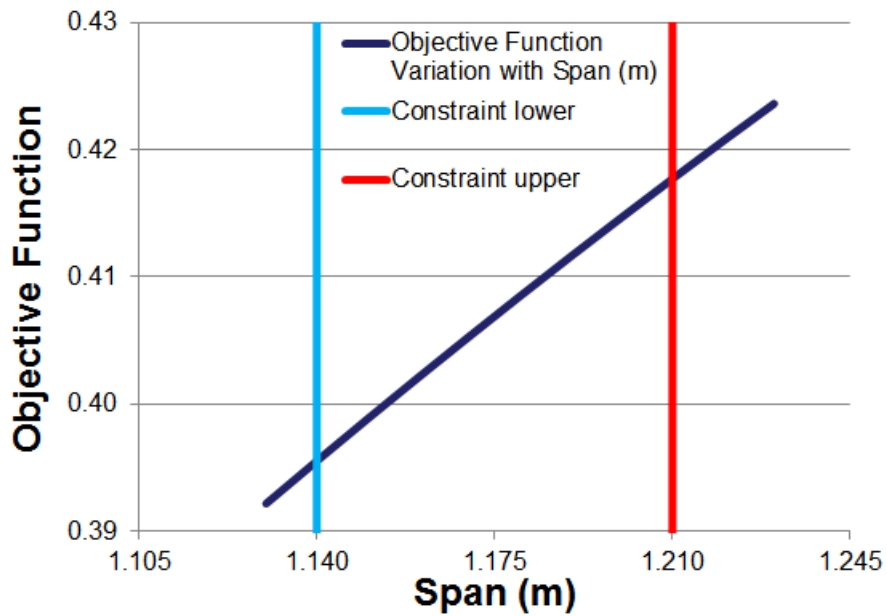


Figure 4.13: Graph of objective function variation with span and verification of constraints by smaller increment

Table 4.12: Objective function and constraint parameters variation with angle of attack by smaller increment

Lift to Drag Ratio / Wing Loading	Lift - Weight (N)	$c_{m\alpha}$	Angle of Attack (deg)
0.404	-0.13	-0.033	-1.4
0.407	0.114	-0.034	-1.3
0.409	0.357	-0.035	-1.2
0.412	0.6	-0.036	-1.1
0.415	0.843	-0.037	-1
0.417	1.085	-0.038	-0.9
0.42	1.326	-0.039	-0.8
0.422	1.567	-0.04	-0.7
0.424	1.808	-0.041	-0.6
0.426	2.049	-0.042	-0.5
0.428	2.288	-0.043	-0.4
0.43	2.528	-0.044	-0.3
0.432	2.767	-0.045	-0.2
0.434	3.005	-0.046	-0.1
0.436	3.243	-0.047	0
0.438	3.482	-0.048	0.1

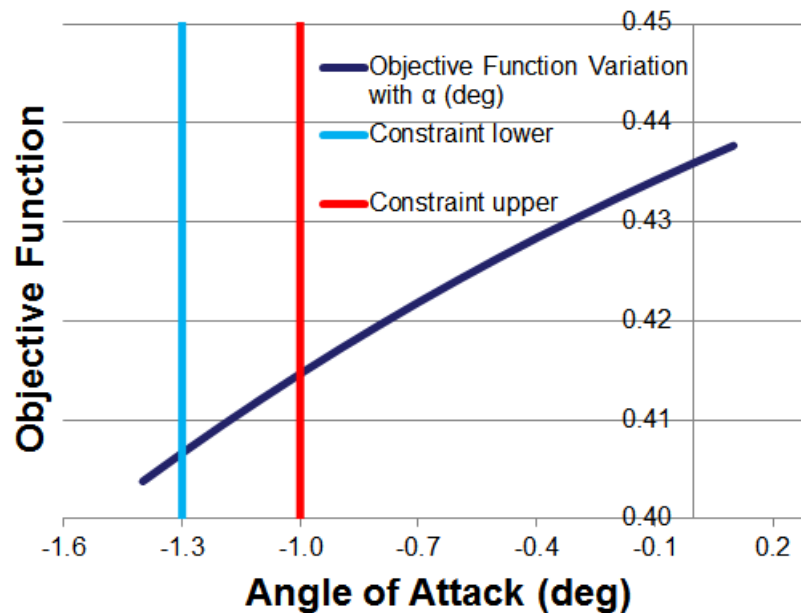


Figure 4.14: Graph of objective function variation with angle of attack and verification of constraints by smaller increment

Table 4.13: Objective function and constraint parameters variation with aspect ratio by smaller increment

Lift to Drag Ratio / Wing Loading	Lift - Weight (N)	$c_{m\alpha}$	Aspect Ratio
0.420	1.093	-0.020	3.600
0.419	1.041	-0.025	3.700
0.418	0.982	-0.030	3.800
0.416	0.915	-0.034	3.900
0.415	0.843	-0.037	4.000
0.413	0.765	-0.039	4.100
0.411	0.684	-0.041	4.200
0.409	0.599	-0.042	4.300
0.407	0.511	-0.042	4.400
0.405	0.420	-0.042	4.500
0.402	0.328	-0.041	4.600
0.400	0.234	-0.040	4.700
0.398	0.138	-0.038	4.800
0.395	0.042	-0.036	4.900
0.393	-0.055	-0.033	5.000
0.390	-0.152	-0.030	5.100

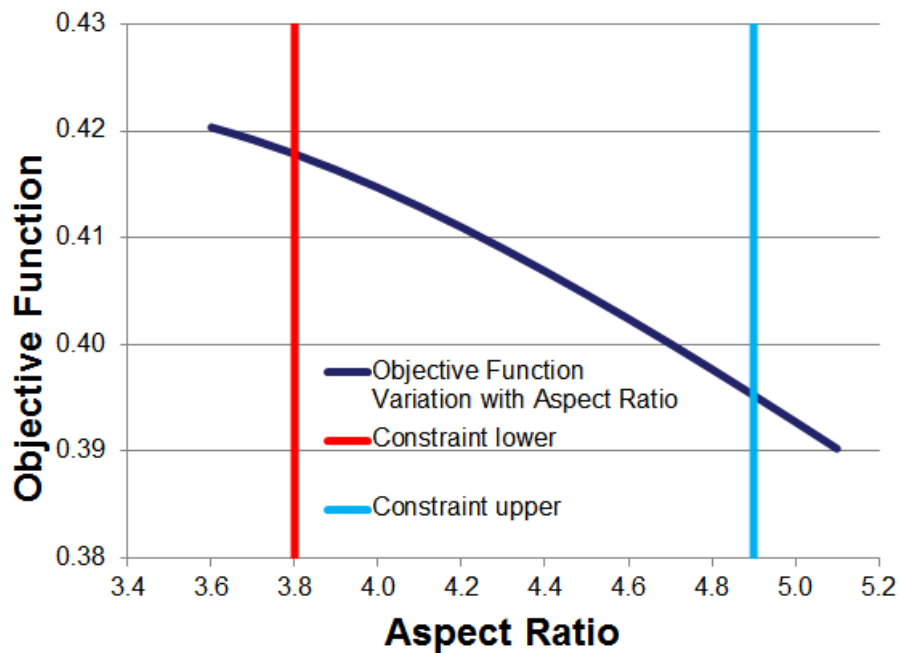


Figure 4.15: Graph of objective function variation with aspect ratio and verification of constraints by smaller increment

Table 4.14: Objective function and constraint parameters variation with fuselage diameter by smaller increment

Lift to Drag Ratio / Wing Loading	Lift - Weight (N)	$c_{m\alpha}$	Fuselage Diameter (m)
0.413	0.731	-0.044	0.075
0.413	0.754	-0.042	0.076
0.414	0.776	-0.041	0.077
0.414	0.798	-0.040	0.078
0.414	0.821	-0.038	0.079
0.415	0.843	-0.037	0.080
0.415	0.865	-0.036	0.081
0.415	0.887	-0.034	0.082
0.416	0.909	-0.033	0.083
0.416	0.931	-0.031	0.084
0.416	0.952	-0.030	0.085
0.417	0.974	-0.029	0.086
0.417	0.996	-0.027	0.087
0.417	1.017	-0.026	0.088
0.417	1.038	-0.024	0.089
0.418	1.060	-0.023	0.090

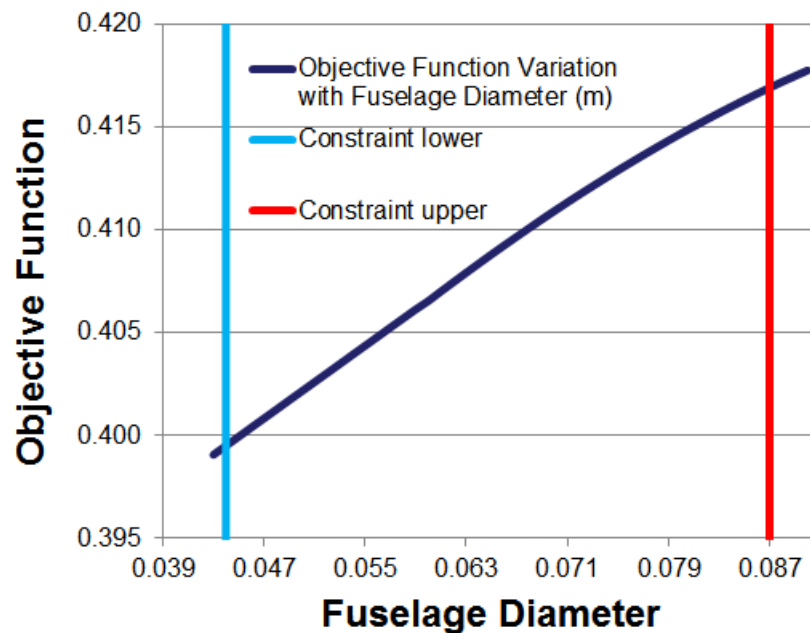


Figure 4.16: Graph of objective function variation with fuselage diameter and verification of constraints by smaller increment

Table 4.15: Objective function and constraint parameters variation with horizontal tail volume ratio by smaller increment

Lift to Drag Ratio / Wing Loading	Lift - Weight (N)	$C_{m\alpha}$	Horizontal Tail Volume Ratio
0.423	1.007	0.009	0.270
0.420	0.952	-0.007	0.280
0.417	0.897	-0.022	0.290
0.415	0.843	-0.037	0.300
0.412	0.789	-0.052	0.310
0.397	0.473	-0.143	0.370
0.395	0.421	-0.158	0.380
0.392	0.370	-0.174	0.390
0.390	0.318	-0.189	0.400
0.387	0.268	-0.204	0.410
0.385	0.217	-0.219	0.420
0.383	0.166	-0.234	0.430
0.381	0.116	-0.249	0.440
0.378	0.066	-0.265	0.450
0.376	0.016	-0.280	0.460
0.374	-0.033	-0.295	0.470
0.372	-0.083	-0.310	0.480

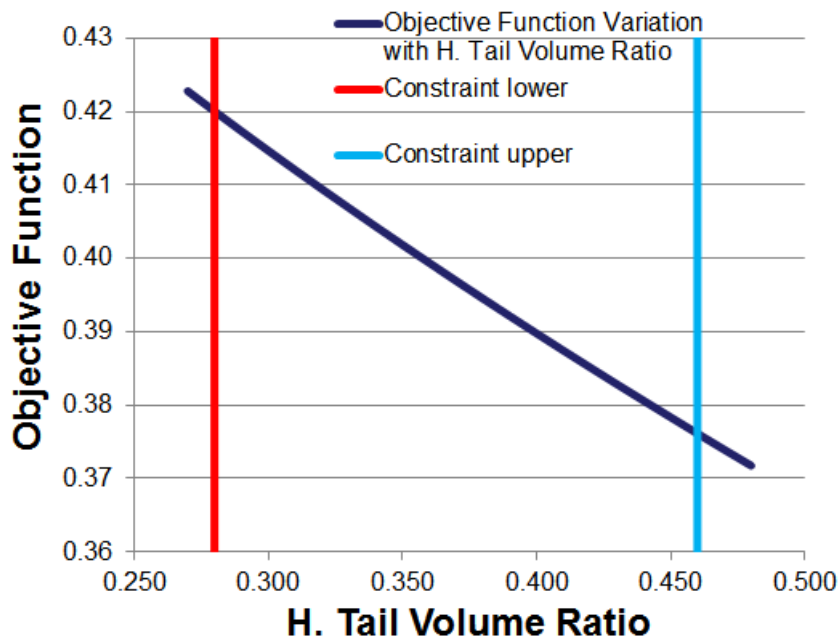


Figure 4.17: Graph of objective function variation with horizontal tail volume ratio and verification of constraints by smaller increment

CHAPTER 5

CONCLUSION

At the end of the thesis, a conceptual design tool in MATLAB environment is generated. This work includes the computations of lift and drag forces and pitching moment as well as the weight estimation of the composite structure of the designed aircraft. Moreover, the parameters which give information related to the performance characteristics of the designed UAV are computed. Stability and control derivatives and the state space representation are also discussed in the scope of the present thesis. Therefore, these values of the aircraft are also calculated in the code. In addition to determining these parameters optimization of the design is also done by the code. In this manner, maximum lift to drag ratios and minimum wing loading objectives are taken into account.

Conceptual design phase of a mini UAV is performed by running the design tool written in this thesis. The code written for this study is subject to several limitations as already mentioned in the previous chapters. These restrictions are basically related to the use of the code since the code is particularly designed for small mini class of UAVs powered by electrical motors and of limited range and endurance. These design characteristics are listed as:

- UAV is powered by an electric motor,
- UAV must be hand launched and land by parachute or deep stall,
- The flaps and other trailing edge controllers must be plain type,
- UAV is manufactured from composite materials and its weight is calculated accordingly using composite structures,

- The code is valid for subsonic flights, (not for compressible high speed flow aircraft)
- Horizontal and vertical tail airfoils should be the same type.

Regarding all these limitations and capabilities of the code, an indigenous mini UAV system previously designed, manufactured and currently undergoing autonomous flight testing is used to validate the design code realized in this thesis. This reference aircraft's properties are calculated and the results of this Mini UAV system built and flight tested are used to verify all the predictions of the design tool with those of the theoretical calculations, ground and flight tests results of the real system. In addition, the values are validated and corrected by some computer programmes such as ANSYS (CFD), DATCOM, CATIA (Inertia). In this manner, all the necessary input are provided and entered into the code. Since the aircraft is a designed and manufactured mini UAV, optimization process in the code is deactivated. Design tool is run only for the validation of the obtained results. In this manner, it is very important to observe that the computational time required to compute all of the values is very short. When the parameter values of the UAV taken from the generated design tool are compared with the real data of the product, it is seen that lift, drag and moment coefficients are very close to real ones, with a bias of about 1%. Stability derivatives are also close to data taken form CFD analysis. Endurance is also meaningful according to the test approximations.

When the design tool is used for designing an actual UAV system several advantages of this processes be understood better. Initially, most of the design books and existing tools are for fuel based propulsion systems. When an electrical motor is used for the propulsive system of an aircraft, further additional design features are needed, some modifications and some assumptions are needed for developing and incorporating these additional design capabilities into the code by using further formulation. This code gives the design steps needed for the design of the electrically driven propulsion system UAV. Power and thrust determinations are done by using electric motor data. In addition to that, performance parameters, especially mission time are computed by using motor current and battery capacity. To find the performance properties for each of the mission segment, some loops should be done in MATLAB, where these loops are very easily and successfully performed.

Secondly, in most of the available design codes estimation of weight is done by methods that are based on the fuel consumption and many of them are for larger aircraft and not suitable for the composite structure computations. On the other hand, this present code is for small mini class size aircraft with composite structures. In the recent years, hand launched mini UAVs are being very popular and are sought after. Therefore, in the code weight estimation is done for composite platforms. In this manner, the estimation of the weight is very close to the manufactured aircraft, since the experimental coefficients are used in the actual calculations.

Thirdly, the code includes selection of optimum values. This allows the user to choose several important parameters so that the design can offer the best solutions within the determined limits. In this manner, lift to drag ratio and wing loading parameters are preferred for the objectives of the optimization. In this way, most important properties (more power saving, efficient and manoeuvrable) for a small UAVs are mediated through the design tool.

Fourth advantage is being user-friendly. For example, if one variable was to be changed in the design phase, which is a very common situation especially for the conceptual design phase, the user has to change only that value. Other factors are recalculated again according to the new value automatically. The user does not have to worry about which parameter is affected from the change and what should the new value of the affected parameter be. This property of the code is supported by the equations which are obtained from the graphs. Therefore, during the whole conceptual design phase, the user does not require to read any data from graphs.

In conclusion, this code is a verified, user-friendly and time saving versatile design tool. It can be used for all conceptual designs of UAVs that meet the requirements.

REFERENCES

- [1] Lateral and longitudinal stability derivatives. <http://aerostudents.com/files/flightDynamics/lateralStabilityDerivatives.pdf>, last visited on August 2015.
- [2] John D. Anderson. *Aircraft Performance and Design*. McGraw-Hill, 1999.
- [3] Reg Austin. *Unmanned Aircraft Systems: UAVs Design, Development and Deployment*. Wiley, 2010.
- [4] Frank L. Lewis Brian L. Stevens. *Aircraft Control and Simulation*. John Wiley and Sons, 2003.
- [5] Vladimir Brusov and Vladimir Petrushik. Design approach for selection of wing airfoil with regard to micro-uavs. *Proceedings of the International Micro Air Vehicles Conference Summer Edition*, 2011.
- [6] David A. Caughey. Introduction to aircraft stability and control course notes for m&ae 5070. 2011.
- [7] Cadline Community. Autodesk labs - project falcon - wind tunnel simulation. <https://www.cadlinecommunity.co.uk/hc/en-us/articles/201694222-Autodesk-Labs-Project-Falcon-Wind-Tunnel-Simulation>.
- [8] M. V. Cook. *Flight Dynamics Principle*. Elsevier, 2007.
- [9] CFS Engineering. Ceasim. <http://www.ceasim.com/>.
- [10] Great OWL Publishing Engineering. Stability analysis module. <http://www.flightlevelengineering.com/downloads/stab.pdf>, last visited on August 2015.
- [11] AVID LLC. Avid acs. <http://www.avid aerospace.com/software/avid-accs/>.
- [12] Harold Youngren Mark Drela. Avl. <http://web.mit.edu/drela/Public/web/avl/>.
- [13] Harold Youngren Mark Drela. xfoil. <http://web.mit.edu/drela/Public/web/xfoil/>.
- [14] Kenneth Munson. *Jane's Unmanned Aerial Vehicles and Targets*. Jane's Information Group, 2002.
- [15] OAD. Ads, aircraft design software. <http://www.pca2000.com/en/index.php>.

- [16] Wolfgang Pointner and Gabriele Kotsis. Using formal methods to verify safe deep stall landing of a mav. *IEE*, 2011.
- [17] Daniel P. Raymer. *Aircraft Design: A Conceptual Approach*. AIAA, 2006.
- [18] Dr. Jan Roskam. *Part VI: Preliminary Calculation of Aerodynamic, Thrust and Power Characteristics*. DARcorporation, 2000.
- [19] Jan Roskam. *Methods for Estimating Stability and Control Derivatives of Conventional Subsonic Airplanes*. The University of Kansas, 1971.
- [20] Matthieu Scherrer. Miarex. <http://scherrer.pagesperso-orange.fr/matthieu/english/miarexe.html>.
- [21] Tornado stuff. Tornado. <http://tornado.redhammer.se/>.
- [22] Inc. WebFinance. Business dictionary. <http://www.businessdictionary.com/definition/optimization.html>, last visited on August 2015.
- [23] WindandWet. Airfoil tools. <http://airfoiltools.com/airfoil/details?airfoil=fx60100-il>, last visited on August 2015.
- [24] xflr5. xflr5. <http://www.xflr5.com/xflr5.htm>.

APPENDIX A

3D VIEWS AND DIMENSIONS OF UAV

3D views of the UAV can be found in below figures (from Figure A.1 to Figure A.4).

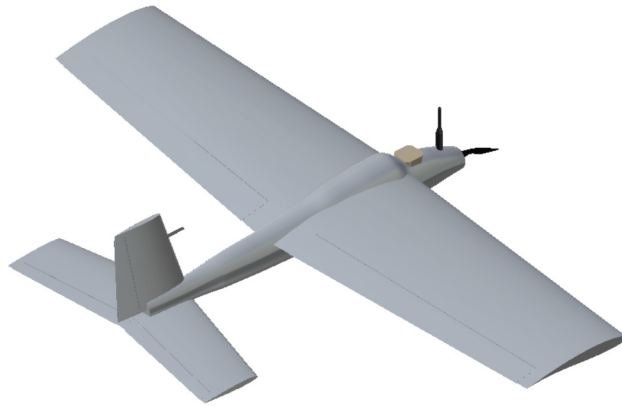


Figure A.1: Isometric 3D view of the UAV



Figure A.2: Top 3D view of the UAV

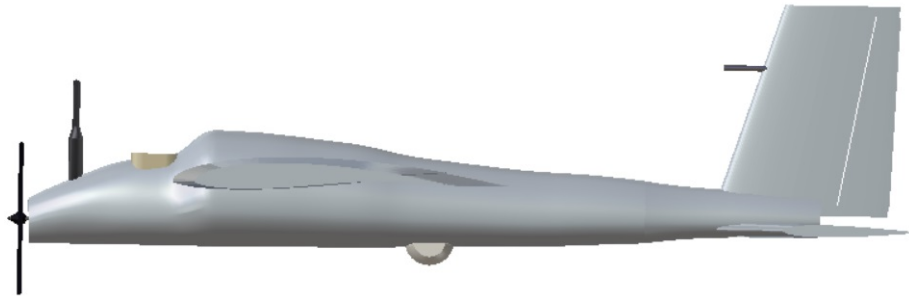


Figure A.3: Side 3D view of the UAV

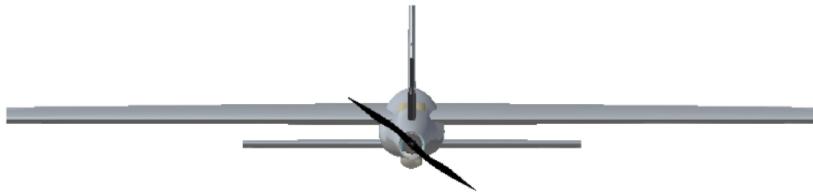


Figure A.4: Front 3D view of the UAV

Major dimensions of the UAV can be seen from the below Figure A.5.

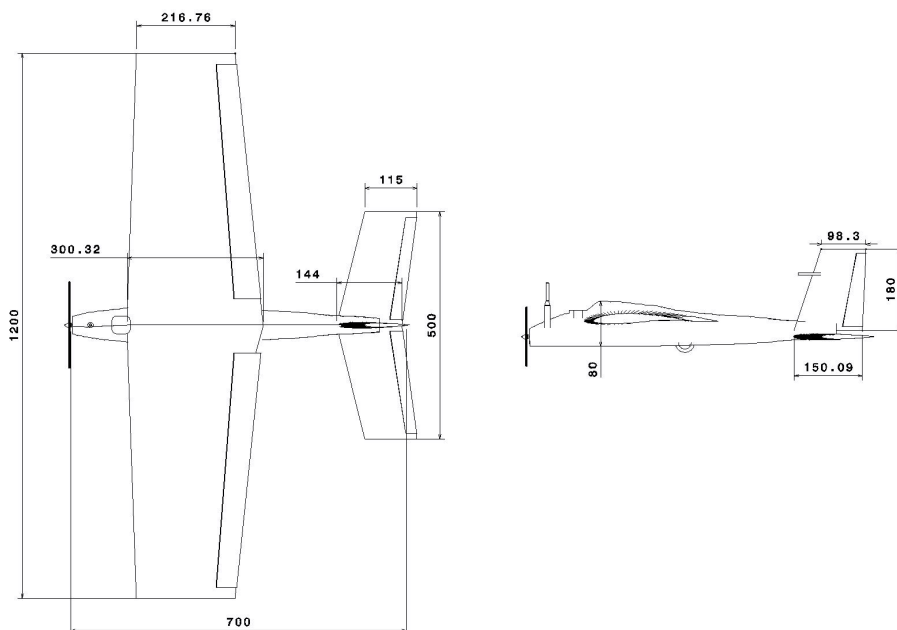


Figure A.5: Dimensions of the UAV

The equipments and their placement in the UAV is shown in below two Figures (Figure A.6 and Figure A.7).

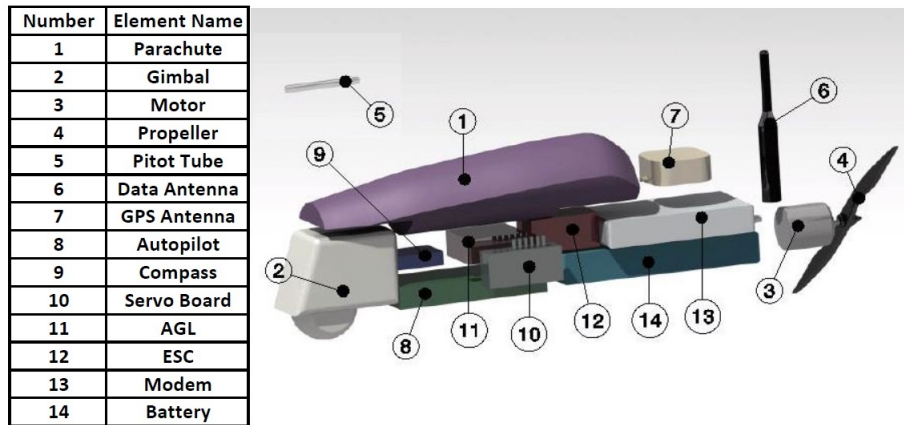


Figure A.6: Equipments of the UAV

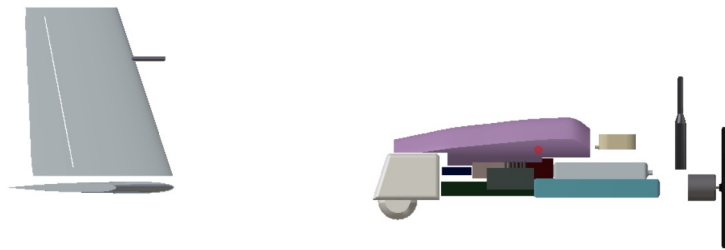


Figure A.7: Placement of equipments in the UAV

Lastly, centre of gravity location can be seen from the below Figure A.8 and Figure A.9.

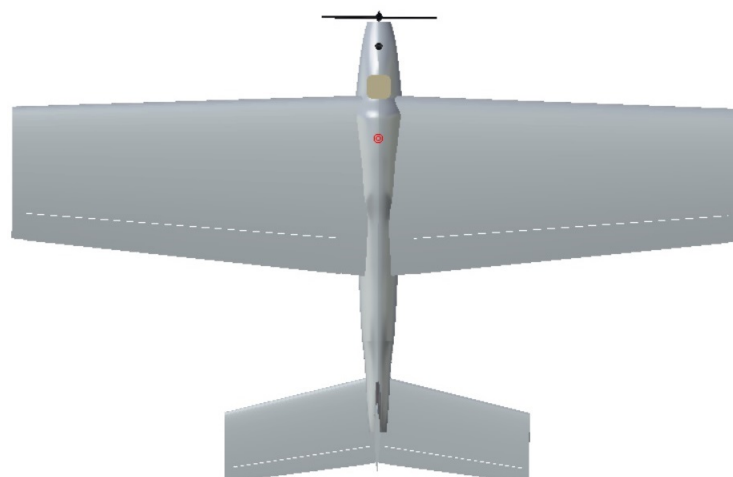


Figure A.8: Centre of gravity location of the UAV from the top view



Figure A.9: Centre of gravity location of the UAV from the side view

APPENDIX B

OPERATING MANUAL OF DESIGN TOOL

- Run the code.
- The user enters the values of intended parameters when the code starts to ask. First subject of the input parameters are optimization. Moving variable initial points, end points and increments are entered for the five parameters. In this manner, it is important to read the written notes such as "angles in degree and all other parameters in metric system". This note informs the user which units of parameters are required. Mean while, if a moving variable is selected as angle, this means that the entered value must be in degree; or if it belongs to a dimension, the value must be in meter.

Optimization Parameters Selection (angles in degree
and all other parameters in metric system (m,m²,m/s)

```
asked by code : moving variable 1  
optimization range initial value  
entered by user : 0.6  
mov1_start =  
    0.6000
```

```
asked by code : moving variable 2  
optimization range initial value  
entered by user : -5  
mov2_start =  
    -5
```

asked by code : moving variable 3
optimization range initial value
entered by user : 2
mov3_start =
2

asked by code : moving variable 4
optimization range initial value
entered by user : 0.04
mov4_start =
0.0400

asked by code : moving variable 5
optimization range initial value
entered by user : 0.1
mov5_start =
0.1000

asked by code : moving variable 1
optimization range end value
entered by user : 1.5
mov1_end =
1.5000

asked by code : moving variable 2
optimization range end value
entered by user : 19
mov2_end =
19

asked by code : moving variable 3
optimization range end value

entered by user : 15

mov3_end =

15

asked by code : moving variable 4

optimization range end value

entered by user : 0.14

mov4_end =

0.1400

asked by code : moving variable 5

optimization range end value

entered by user : 0.6

mov5_end =

0.6000

asked by code : moving variable 1

optimization increment value

entered by user : 0.1

mov1_inc =

0.1000

asked by code : moving variable 2

optimization increment value

entered by user : 2

mov2_inc =

2

asked by code : moving variable 3

optimization increment value

entered by user : 2

mov3_inc =

2

```
asked by code : moving variable 4
optimization increment value
entered by user : 0.01
mov4_inc =
    0.0100
```

```
asked by code : moving variable 5
optimization increment value
entered by user : 0.1
mov5_inc =
    0.1000
```

- Secondly, all general specifications of aircraft that can be categorized as 'Air Condition Input', 'Propulsion System Input', 'Airfoil Input for Wings and Tails', 'Geometry Input', 'Pitching Moment Input', 'Performance Input', 'Stability and Control Derivative Input', 'State Space Input' are entered to the code by user. This part of the code also includes a note (For selected moving variables, when their values are asked, enter "*mov#_sstart*" just as written). According to this note, for example it is assumed that the first selected moving variable is span. In this manner, when the code is asked to enter the value of the span, the user must write "*mov1_sstart*" to the command window.

For the selected moving variables; when their values are asked, enter *mov#_start* just as its written

```
ans =
Air Condition Input
```

```
asked by code : viscosity (Ns/m^2)
entered by user : 1.646*10^(-5)
mu_air =
    1.6460e-05
```

asked by code : cruise altitude (MSL) (m)
entered by user : 1500
alt_MSL =
1500

asked by code : angle of attack (deg)
entered by user : 'mov2_start'
aoa =
mov2_start

asked by code : cruise speed (m/s)
entered by user : 12
Vc =
12
...

ans =
Propulsion System Input

asked by code : battery volt (volt)
entered by user : 3.7
volt_batt =
3.7000
...

ans =
Airfoil Input for Wings and Tails

asked by code : thickness ratio
entered by user : 0.1
tc =
0.1000
asked by code : zero lift angle of attack

```

entered by user : -4
az1 =
    -4
...

ans =
Geometry Input

asked by code : fuselage length
entered by user : 0.05
fuse_leng =
    0.0500

asked by code : fuselage diameter
entered by user : 'mov4_start'
fuse_dia =
mov4_start

asked by code : fuselage average cross sectional
area
entered by user : 0.005
fuse_acrse =
    0.0050

asked by code : span (m)
entered by user : 'mov1_start'
b =
mov1_start
...

```

- As the third step the parameters which are chosen as moving variables are assigned to their numbered moving variable names by user. In this manner, it is very important to write the parameter names of moving variables in inverted

commas as the note is mentioned.

Equating moving variables to their selected parameters(Enter parameter name in inverted commas)

```
asked by code : moving variable 1
entered by user : 'b'
assign1 =
b
```

```
asked by code : moving variable 2
entered by user : 'aoa'
assign2 =
aoa
```

```
asked by code : moving variable 3
entered by user : 'AR'
assign3 =
AR
```

```
asked by code : moving variable 4
entered by user : 'fuse_dia'
assign4 =
fuse_dia
```

```
asked by code : moving variable 5
entered by user : 'Vr_ht'
assign5 =
Vr_ht
```

- Before the next step, the code does some computations and after that, user enters the last input parameters. These input variables are also related to the optimization. Constraint parameters are assigned and their limitation values are entered. Last two input belongs to the objective function; the parameter

which will be maximized and minimized are assigned. These objective function parameters and constraints (not the constrain limits) are also written in inverted commas just as the moving variables. This situation takes part as note.

Optimization Parameters Selection [Constraints(Enter parameter names in inverted commas) and their limits]

asked by code : constraint 1 (with upper limit)

entered by user : 'cM_alpha'

assign6 =

cM_alpha

asked by code : constraint 1 limit

entered by user : 0

Cons1_lim =

0

asked by code : constraint 2 (with lower limit)

entered by user : '5'

assign7 =

5

asked by code : constraint 2 limit

entered by user : 2

Cons2_lim =

2

asked by code : constraint 3 (with upper limit)

entered by user : '3'

assign8 =

3

asked by code : constraint 3 limit

entered by user : 6

Cons3_lim =

6

asked by code : constraint 4 (with lower limit)

entered by user : '6'

assign9 =

6

asked by code : constraint 4 limit

entered by user : 4

Cons4_lim =

4

asked by code : Objective Function Parameter that
will be maximized

entered by user : 'LifttoDrag'

assign10 =

LifttoDrag

asked by code : Objective Function Parameter that
will be minimized

entered by user : 'WingLoading'

assign11 =

Wing Loading

- After the all necessary input parameters are entered by user, the code starts calculations. At the end, all the computed values of the designed UAV can be achieved from the Matlab Workspace. In addition to that, the user can add a small script to write the data excel or other files.